

Some studies on open fires, shielded fires and heavy stoves

Citation for published version (APA):

Krishna Prasad, K. (1981). *Some studies on open fires, shielded fires and heavy stoves*. Eindhoven University of Technology.

Document status and date:

Published: 01/01/1981

Document Version:

Publisher's PDF, also known as Version of Record (includes final page, issue and volume numbers)

Please check the document version of this publication:

- A submitted manuscript is the version of the article upon submission and before peer-review. There can be important differences between the submitted version and the official published version of record. People interested in the research are advised to contact the author for the final version of the publication, or visit the DOI to the publisher's website.
- The final author version and the galley proof are versions of the publication after peer review.
- The final published version features the final layout of the paper including the volume, issue and page numbers.

[Link to publication](#)

General rights

Copyright and moral rights for the publications made accessible in the public portal are retained by the authors and/or other copyright owners and it is a condition of accessing publications that users recognise and abide by the legal requirements associated with these rights.

- Users may download and print one copy of any publication from the public portal for the purpose of private study or research.
- You may not further distribute the material or use it for any profit-making activity or commercial gain
- You may freely distribute the URL identifying the publication in the public portal.

If the publication is distributed under the terms of Article 25fa of the Dutch Copyright Act, indicated by the "Taverne" license above, please follow below link for the End User Agreement:

www.tue.nl/taverne

Take down policy

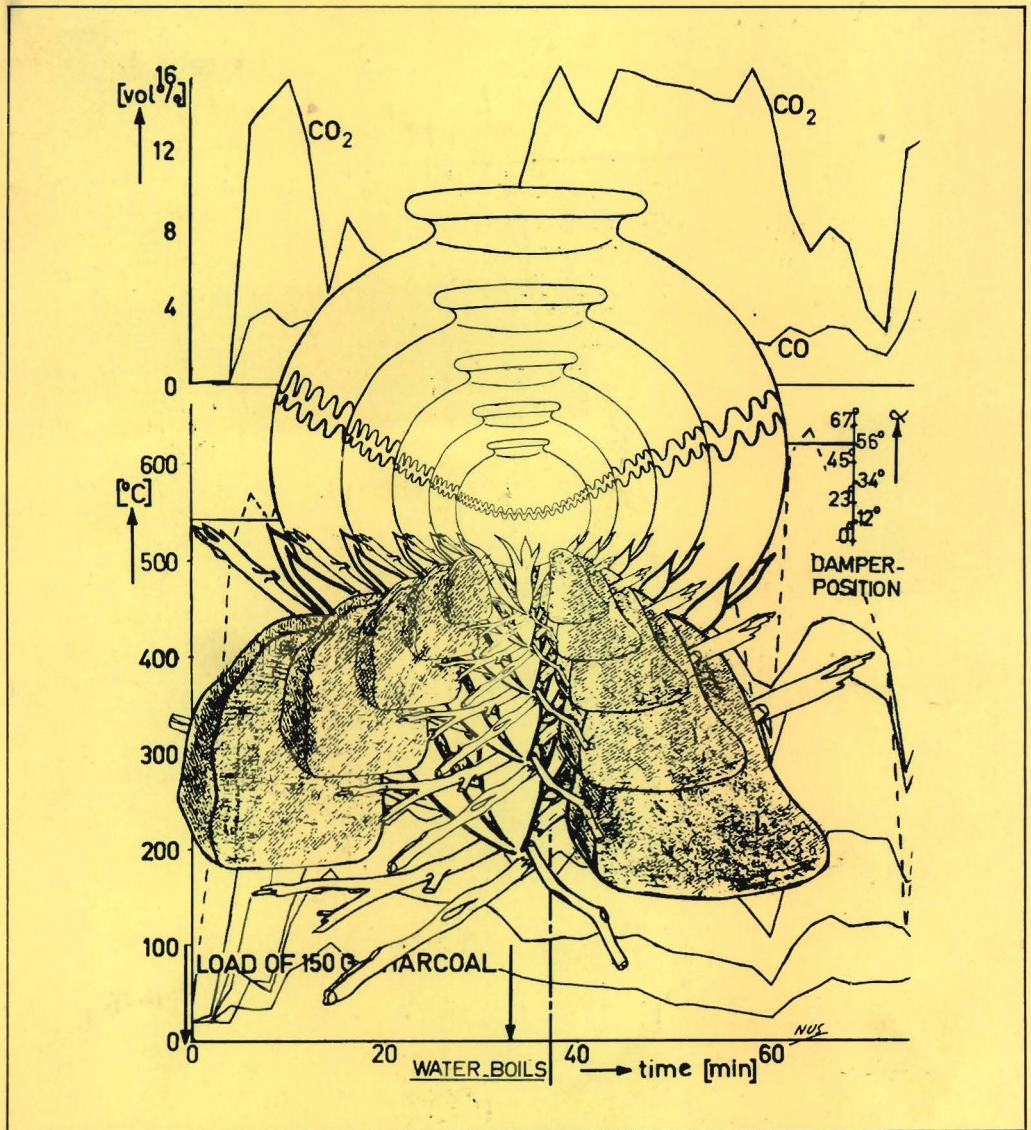
If you believe that this document breaches copyright please contact us at:

openaccess@tue.nl

providing details and we will investigate your claim.

Some studies on open fires, shielded fires and heavy stoves

Edited by
 K. Krishna Prasad
 Department of
 Applied Physics
 Eindhoven University
 of Technology
 Eindhoven,
 The Netherlands



A Report from
 The Woodburning Stove Group
 Departments of Applied Physics and Mechanical Engineering,
 Eindhoven University of Technology
 and
 Division of Technology for Society, TNO, Apeldoorn
 The Netherlands

Some studies on open fires, shielded fires and heavy stoves

Edited by
K. Krishna Prasad
Department of
Applied Physics
Eindhoven University
of Technology
Eindhoven,
The Netherlands

W. 145/1

DOCUMENTATIECENTRUM B.O.S. - T.H.E.	
class.	AA14-8104
dv.	
datum	

A Report from
The Woodburning Stove Group
Departments of Applied Physics and Mechanical Engineering,
Eindhoven University of Technology
and
Division of Technology for Society, TNO, Apeldoorn
The Netherlands

October 1981

CONTENTS

1	Introduction	1
2	Model predictions for open fires	3
	2.1 General	3
	2.2 Introduction	4
	2.3 The model	6
	2.4 Solution of the equations	10
	2.5 Model calculations and discussion	13
	- References	18
	- List of symbols	19
	- Appendix 2.1	20
3	Experiments on shielded fires	22
	3.1 Introduction	22
	3.2 First series of tests	22
	3.3 Second series of experiments	27
	3.4 Conclusion	33
	- Appendix 3.1	34
	- References	39
4	Some studies on the performance of cylindrical combustion chambers	40
	4.1 Introduction	40
	4.2 Design	41
	4.3 The experiments	44
	4.4 Results	47
	4.5 Two different efficiencies	52
	4.6 Radiation heat transfer	55
	4.7 Discussion and conclusions	59
	- References	60
	- Tables	61
	- Appendix 4.1	65
	- Appendix 4.2	69
5	Fuel bed behaviour	71
	5.1 Introduction	71
	5.2 Recording of the fuel bed weight loss	73
	5.3 Experimental results and discussion	75

	- References	77*
6	The performance of the nouna woodstove	79
	6.1 Introduction	79
	6.2 Design of the stove	80
	6.3 Experimental details	80
	6.4 Efficiency of the stove	82
	6.5 The combustion performance	84*
	6.6 The heat balance	87
	6.7 The effect of wood properties	89
	6.8 A comparison between the De Lepeleire/Van Daele wood stove and the Nouna wood stove	90
	6.9 Conclusions	91
	- References	93
	- Appendix	94
	- Tables	96
	- Figures	105
7	Some exploratory studies on an experimental heavy stove	130
	7.1 Introduction	130
	7.2 Design description	130
	7.3 Instrumentation	134
	7.4 Experimental programme	136
	7.5 General execution of the experiments	137
	7.6 Results and discussion	139
	7.7 Conclusions and recommendations	153
	- List of symbols	154
	- Table	155
8	Some implications of results	156
	- References	163

1. INTRODUCTION

by

K. Krishna Prasad

Eindhoven University of Technology,

Eindhoven, The Netherlands.

This is the third report from the wood-burning stove group in the Netherlands. The report divides itself into two parts.

The first part consisting of chapters 2 to 5 concentrates on different classes of open fires - open fires interpreted in a much broader sense than the conventional three stone fires. Paul Bussmann looks at the theory of open fires. The results at this moment show sufficient promise so that with a little more effort we should be in a position to have the ability to calculate the overall heat absorption behaviour of a 3-stone stove.

Piet Visser addresses himself to the question: what simple changes could one incorporate into the design of a simple open fire so that fuel economy improves? Adopting a purely empirical approach coupled with a conceptual model for the combustion of wood, he comes up with a design that is capable of producing efficiencies of the order of 50 %. The design holds great promise demanding further investigation than has been possible so far.

In the next chapter Jan Delsing examines the question of dimensioning a cylindrical combustion chamber and in the process shows the behaviour of radiant and convective heat transfer to pans in such systems. In the final chapter of this part Piet Visser and Paul Bussmann give some results indicating the behaviour of fuel beds in open fires with and without grates.

The second part consisting of chapters 6 and 7 presents work on two heavy stoves, with chimneys. Claus and his colleagues at TNO summarize the results of their labours for over six months on the Nouna Stove - a stove that is being introduced in Upper Volta. As in the previous report, TNO results provide a rather detailed picture of the stove behaviour under different operating conditions. A special feature of the study is the detailed attention paid to the heat absorption behaviour of the stove body; this happens to be the largest consumer of energy in such stoves.

In the next chapter, Marlies Knoll describes a heavy stove that was designed to provide considerable flexibility to study the effect of different design options on the stove performance. Some preliminary results on the stove show the possibilities of improving the performance of this class of stoves.

The final chapter provides a brief overall view of the foregoing results suggesting different possibilities for improving the fuel economy of wood burning stoves for cooking applications.

2. MODEL PREDICTIONS FOR OPEN FIRES

by

P. Bussmann

Eindhoven University of Technology,

Eindhoven, The Netherlands.

2.1. GENERAL

A part of the work done by the woodburning stove group, Eindhoven, aims at getting better theoretical understanding of the woodburning processes in open fires. This work until now is restricted to open fires because of the following three main reasons [Krishna Prasad 1980]. First of all it appears that the traditional stove of an overwhelming majority of the poor people of this world is a close relative of the open fire. Secondly laboratory tests in Eindhoven showed surprisingly high efficiencies, which lends a whole new perspective to the design of improved stoves and thirdly if we are able to understand an open fire it will provide very useful guidelines for designing more efficient stoves.

If the open fire is understood as a system in which different processes take place, then the most important system element is the heat source and the most important process is the combustion.

The study presented here gives a simple model by which it is possible to obtain the temperatures, velocities and mass flows in woodfires.

These characteristics can serve as a basis for evaluating heat transfer from the flames to different surfaces in a stove.

Insight into the behaviour of flame characteristics in wood fires is required for developing rules for dimensioning the combustion spaces in woodburning stoves.

Since in literature no experimental results were available on the small wood fires that are of interest in the present work, a series of experiments were performed to determine flame heights. The experimental results agree with the estimates derived from the model, for an excess air factor of 1.5 - 2.5.

2.2. INTRODUCTION

In order to model fires three regions in fires are distinguished from the bottom upwards:

(iii)

(ii)

(i)



Fig. 2.1. Wood fire divided into three regions.

(i) The region where the pyrolysis of wood takes place, charcoal is burnt and volatiles are released;

(ii) The region of the visible flame, where volatiles from the fuelbed react chemically with entrained air and hence heat is liberated; and

(iii) the region of rising hot gases where no combustion occurs, air is entrained and temperature drops rapidly with increasing height above the fuelbed.

This work aims at getting better understanding of the physical behaviour of processes in the second and third region, the column of hot rising gases with and without combustion.

In these regions the entrainment of ambient air plays an important role; it takes care of the oxygen supply. The origin of the entrainment is the following.



Fig. 2.2. Stream lines of entrained air

While the temperature of the gases above the fuelbed differs enormously from the ambient temperature, the total pressure is everywhere the same. Due to this, there will be a density difference and thus an upward force, the buoyancy force. The hot gases rise, first slowly but gradually, because of the buoyancy force faster and faster.

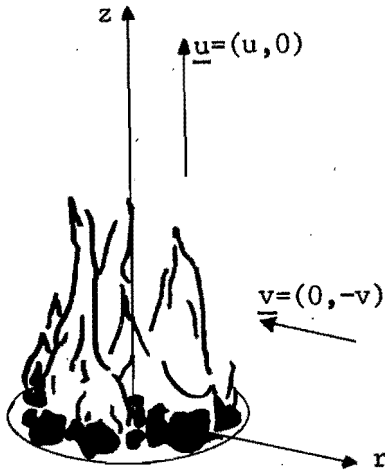
The velocity difference between the rising gases and the ambient gases at rest will cause friction; ambient fluid gets dragged along and will mix with the hot gases. This is called the entrainment process, which is also shown in fig. 2.2.

Making use of the so-called entrainment assumption, the model gives as a result the values of the temperature and the velocity attained in the flames. As will be shown, it is not needed therefore to get insight into the chemical processes. This would be a very complex task due to the many completely different hydrocarbons that are involved in the burning of wood. Thus the detailed knowledge of the combustion process is replaced by some gross estimations. The value of the charcoal-volatiles ratio and the specific heat of combustion are the only quantities that are needed. The fire problem thus reduces to the process of a rising gas column above a source in which initially heat is released.

The work of Lee and Emmons [Lee and Emmons, 1961] is taken as the starting-point for the construction of the present model. Lee and Emmons investigated a turbulent plume above a steady two-dimensional finite source of heated fluid in a uniform ambient fluid. By solving the fundamental equations of motion they got analytical expressions for plume width, buoyancy force and gas velocities as a function of the height above the source. A similar model was developed by Steward [Steward, 1970] for circular fires taking into account the liberation of heat by combustion in the first part of the hot gas column. This was done by introducing a source term in the energy equation. By solving the problem Steward rewrote the continuity equation in such a way that his model gave only as a result the height above the fuelbed at which a given amount of air was entrained. However, Steward's model explained trends in experimental flame height data. It was found that a numerical evaluation of his model gave close agreement with the flame height data with all points falling near a curve which represents 400 % excess air. That is why a model of the type of Steward is believed to give the best theoretical results for different classes of fires [Cox and Chitty, 1980].

Due to the interest in woodstoves the results of Steward's model is considered inadequate. The main difference between the present model and the work of Steward lies in the manner in which the continuity equation is implemented. The straight forward approach of Lee and Emmons is chosen for the purpose.

2.3. THE MODEL



The problem of the rising gas column above the fuelbed is considered to be a turbulent free convection problem. The fundamental equations of mass, momentum and energy make up the basis of the model. (see fig. 2.3. for the geometry)

Fig. 2.3. Wood fire geometry

In arriving at these equations the following assumptions are made.

1. The volatiles leaving the fuelbed and the air that is entrained in the convection column behave like ideal gases; the gas properties of volatiles and air are the same.
2. The convection column has reached a steady state.
3. The driving force is the buoyancy; pressure gradients are neglected.

The pressure differences in vertical direction, due to the hydrodynamic pressure gradient is of no significance for this situation. The radial pressure difference is neglected because the transverse accelerations are small relative to those in vertical direction;

4. Turbulent flow is fully developed and thus molecular transfer mechanisms are neglected relative to turbulent processes.
5. Turbulent temperature and density variations are small relative to turbulent velocity variations.
6. Radiant heat losses from the flames need not be taken into account.

Under the foregoing assumptions the fundamental equations reduce to the continuity equation.

$$\frac{\partial}{\partial z} \rho u - \frac{1}{r} \frac{\partial}{\partial r} r \rho v = 0 \quad (1)$$

The momentum equation for the z-direction.

$$\frac{\partial}{\partial z} \rho u^2 - \frac{1}{r} \frac{\partial}{\partial r} r \rho v = (\rho_a - \rho)g - \frac{\partial}{\partial z} \overline{\rho u_f^2} - \frac{1}{r} \frac{\partial}{\partial r} r \overline{\rho u_f v_f} \quad (2)$$

The energy equation

$$\frac{\partial}{\partial z} \rho u c_p T - \frac{1}{r} \frac{\partial}{\partial r} r \rho v c_p T = \dot{w} \quad (3)$$

Where ρ , u , v , T give the time averaged values of the density, the axial velocity, the radial velocity and the temperature. While u_f and v_f give the turbulent fluctuation of the velocities.

The quantity \dot{w} , the source term in the energy equation, denotes the heat release per volume per second by combustion. \dot{w} becomes zero at that height where no further combustion takes place.

The first term on the right hand side of the momentum equation represents the buoyancy force, while the other two terms give the contribution of turbulence to the momentum transfer. The term $\frac{\partial}{\partial z} \overline{\rho u_f^2}$ can be neglected because it is of smaller order of magnitude than the last term, representing the Reynolds stress gradient [Eckert and Drake 1972].

Because the flow is axisymmetric : $v = 0$ at $r = 0$. Using this and intergrating the continuity equation with respect to r , we get

$$\frac{d}{dz} \int_0^{\infty} \rho u r dr = r \rho v |_{(z, \alpha)} \quad (4)$$

The equation states that the increase in the ascending mass flow is due to the entrainment of ambient air.

Using the same arguments as for integrating the continuity relation and noting that the Renolds stress is zero for both $r = 0$ and $r = \infty$, integration of the momentum equation with respect to r gives:

$$\frac{d}{dz} \int_0^{\infty} \rho u^2 r dr = \int_0^{\infty} g (\rho_a - \rho) r dr \quad (5)$$

Which states that the increase of vertical momentum in the hot gas column is due to the buoyancy force.

Finally integrating the energy equation with respect to r gives:

$$\frac{d}{dz} \int_0^{\infty} \rho u c_p T r dr = \rho_0 v c_p T \Big|_{(z, \infty)} + \int_0^{\infty} \dot{w} r dr. \quad (6)$$

Which states that the increase in energy flux over the convection column is caused by the energy content of entrained air plus the combustion heat released.

Before the integrated equations lead to solutions, some more assumptions have to be made. They concern firstly the shape of the velocity and temperature profile, secondly the way in which air is entrained and thirdly the way in which heat is liberated in the flames.

2.3.1 The velocity and temperature profiles

In the analysis of the buoyant plume without combustion most workers have assumed a Gaussian-profile of temperature and velocity at each horizontal position.

Measurements do not confirm this completely [Cox and Chitty 1980], but experimental results relating to the behaviour of the convection plume agree closely with theoretical predictions when these profiles are used [Lee and Emmons 1961].

However, in the analysis of the buoyant plume with combustion considered here, top-hat profiles are assumed. This is done because of the rather big temperature and velocity gradients near the edge of the plume.

Thus if b represents the plume radius then for a first approximation

$$\begin{aligned} r < b &\rightarrow T = T(z) , u = u(z) \\ r > b &\rightarrow T = T_a , u = 0 \end{aligned} \quad (7)$$

2.3.2 The entrainment assumption

In order to solve the set of equations of motion, also the momentum equation in radial direction is needed. However, this second momentum equation is replaced by the entrainment assumption.

The entrainment assumption relates the flow of entraining air to the flow of ascending gases. In the weakly buoyant plume where the Boussinesq approximation can be applied, the entrainment assumption for circular plumes is:

$$rv|_{(z, \infty)} = \alpha ub$$

Where α is the entrainment constant. There is a lot of confusion about the precise value of the entrainment constant. List and Imberger [List and Imberger 1973] showed that this is because there just is no unique entrainment coefficient. Dimensional reasoning coupled with published experimental results shows that for round, weakly buoyant jets there is a transition in the entrainment coefficient from $\alpha = 0.057$ (for round jets near the source) to $\alpha = 0.082$ (for round plumes far from the source). The entrainment assumption has been extended to strongly buoyant plumes. This has led to the following modification:

$$rv|_{(z, \infty)} = \alpha \left(\frac{\rho}{\rho_a}\right)^{\frac{1}{2}} ub \quad (8)$$

In the model calculations this modified assumption is used together with $\alpha = 0.08$, the entrainment coefficient value for round plumes. This value of α differs from the value used by Steward of 0.057 which is the entrainment constant for round jets.

2.3.3 The combustion

To get an expression for the source term in the energy equation, \dot{w} , the following two assumptions are made. Firstly, as long as there are volatiles available, they will burn instantaneously with entrained air. The quantity needed is the stoichiometric amount plus the excess amount; so the heat liberated at height z above the fuelbed is proportional to the entrained air flow. Secondly it is assumed that combustion occurs homogeneously over a cross-section of the flame. This assumption is not strictly true, but is consistent with the top-hat temperature profile.

The source term at height z above the fuelbed is then given by

$$\underbrace{\rho_a 2\pi b dz \alpha \left(\frac{\rho}{\rho_a}\right)^{\frac{1}{2}} u}_{\text{entrained air flow}} * \underbrace{\frac{1}{n_s \lambda}}_{\text{fuel to air ratio}} * Q_v * \underbrace{\frac{1}{\pi b^2 dz}}_{\text{reciprocal volume}} \quad (9)$$

Where n_s is the stoichiometric air to fuel ratio and λ is the excess air factor.

2.4. SOLUTION OF THE EQUATIONS

With the assumptions (7, 8, 9) it is possible to carry out the integrations in equation 4-6. Written in a dimensionless form they become:

continuity equation:
$$\frac{d}{dz} \rho' u' b'^2 = \sqrt{\rho' u' b'}$$
 (10)

momentum equation (z-direction):
$$\frac{d}{dz} \rho' u'^2 b'^2 = (1 - \rho') b'^2$$
 (11)

energy equation

for distances smaller than the flame height:

$$\frac{d}{dz} u' b'^2 = (1 + V) \sqrt{\rho' u' b'}$$
 (12a)

for distance larger than the flame height:

$$\frac{d}{dz} u' b'^2 = \sqrt{\rho' u' b'}$$
 (12b)

Where

$$z' = 2 \alpha \frac{z}{b_0}, \quad b' = \frac{b}{b_0}, \quad u' = F \frac{u}{u_0}, \quad \rho' = \frac{\rho}{\rho_a}$$

and

$$F = \sqrt{2\alpha} \frac{u_0}{\sqrt{g b_0}}, \quad V = \frac{Q_v}{n_s \lambda c_p T_a}$$

b_0 is the radius of the fuel bed m

u_0 is the velocity of the gases leaving the fuelbed $m \cdot s^{-1}$

T_a is the ambient temperature K

Q_v is the specific heat of the volatiles

$$= \frac{Q_{\text{wood}} - (1 - U) Q_{\text{charcoal}}}{U} \quad \text{J} \cdot \text{kg}^{-1}$$

U = the mass fraction volatiles

The method of solution is given in appendix 2.1.

The results for distances above the fuelbed smaller than the flame height, are summarized here:

the dimensionless mass flow rate $\phi_m (= \rho' u' b'^2)$ is taken as the independent variable.

The dimensionless momentum flow rate in z-direction $\phi_p (= \rho' u'^2 b'^2)$ is:

$$\phi_p = \left[\frac{5}{6} V \phi_m^3 - \frac{5}{4} C_1 \phi_m^2 - C_2 \right]^{\frac{2}{5}}$$

The dimensionless density or reciprocal temperature is:

$$\rho' = \frac{1}{T'} = \frac{\phi_m}{\phi_m (V + 1) - C_1}$$

The dimensionless velocity is:

$$u' = \frac{\phi_p}{\phi_m} \tag{13}$$

The squared dimensionless plume radius is:

$$b'^2 = \frac{\phi_m [\phi_m (V + 1) - C_1]}{\phi_p}$$

and the height above the fuelbed is given by

$$z' = \int \frac{\phi_m}{\rho_0' F} \frac{d\phi_m}{\sqrt{\phi_p}}$$

Where

$$C_1 = \rho_0' F \left[V - \frac{1 - \rho_0'}{\rho_0} \right] \text{ and } C_2 = [\rho_0' F^2]^{\frac{5}{2}} - \frac{5}{6} V [\rho_0' F]^3 - \frac{5}{4} C_1 [\rho_0' F]^2$$

For distances above the flame height V becomes zero but, except this, the solution stays the same. The problem is completely governed by ρ_0' , V and F.

To relate these results to combustion practise, the Froude number is rewritten in such a way that u_0 , the velocity of gases leaving the fuelbed, is eliminated.

The mass flow of the gases from the fuelbed is equal to the production of volatiles $U \frac{P}{Q_w}$ kg.s⁻¹ plus the charcoal combustion products

$$(n_s + 1)(1 - U) \frac{P}{Q_w} \text{ kg.s}^{-1}.$$

The initial velocity is then given by:

$$u_0 = \frac{1}{\rho_0 \pi b_0^2} [n_s (1 - U) + 1] \frac{P}{Q_w} \text{ m.s}^{-1}$$

and the Froude number becomes equal to

$$F = \sqrt{2\alpha} \frac{1}{\sqrt{g b_0}} \frac{[n_s (1 - U) + 1] \frac{P}{Q_w}}{\rho_0 \pi b_0^2}$$

2.5. MODEL CALCULATIONS AND DISCUSSION

Figure 2.4 presents some of the more significant results obtained through computation from the model. The temperature, width of the flame/plume, and the velocity have been plotted as a function of height measured from the fuel bed. The power output of the fire (really burning rate of the fuel), excess air factor and percentage volatiles have been varied parametrically.

Before going into the discussion of these results, a few other observations are in order. The Froude number for small wood fires is of the order of 10^{-2} . Calculations show that the plume diameter first decreases until the local Froude number is larger than one. This fact explains the characteristic neck observed in flame photographs. Far from the fuel bed the Froude number becomes one with a balance between entrained air flux and buoyancy, which maintains the velocity constant [Lee and Emmons, 1961]. The consequence of the small initial Froude number is that the fire conditions at the fuel bed are not of much importance. Calculations performed with different fuel bed temperatures and diameters show that they have marginal influence on the flame heights, flame temperatures, plume diameters and gas velocities. Of course the fuel bed diameters and temperatures are of significant importance in stoves as they determine the radiant heat transfer to the pans.

Turning now to the results, the temperature and diameter profiles of the flame show a sharp discontinuity. This is really a consequence of the fact that the source term in the energy equation is set to zero abruptly when the air entrained by the flame reaches a predetermined value (determined by the excess air factor) signifying the end of combustion.

Fig. 2.4.a. shows that the power output of the fire does not influence the maximum temperature in the system. It influences only the flame height which increases according to $P^{2/5}$.

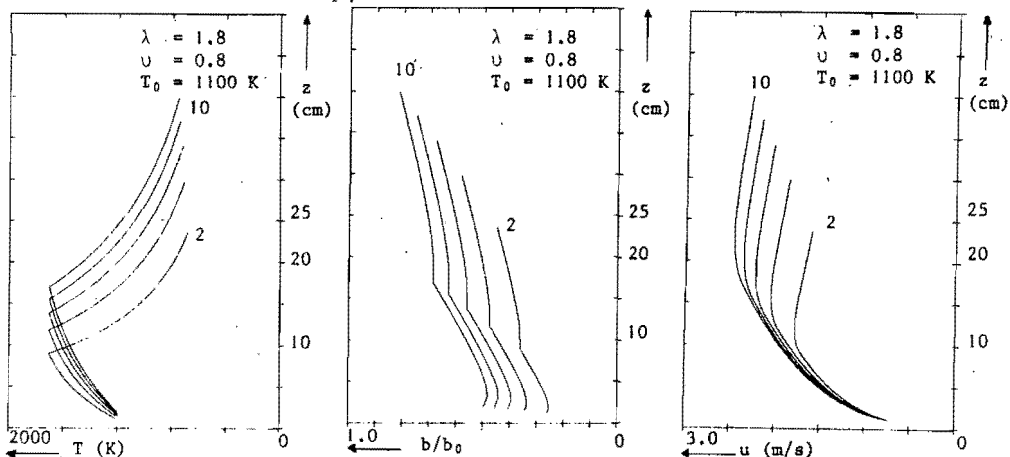


Fig. 2.4.a. Temperature; plume width-fuel bed diameter ratio and velocity as function of the height with varied power output ($P = 2, 4, 6, 8, 10$)

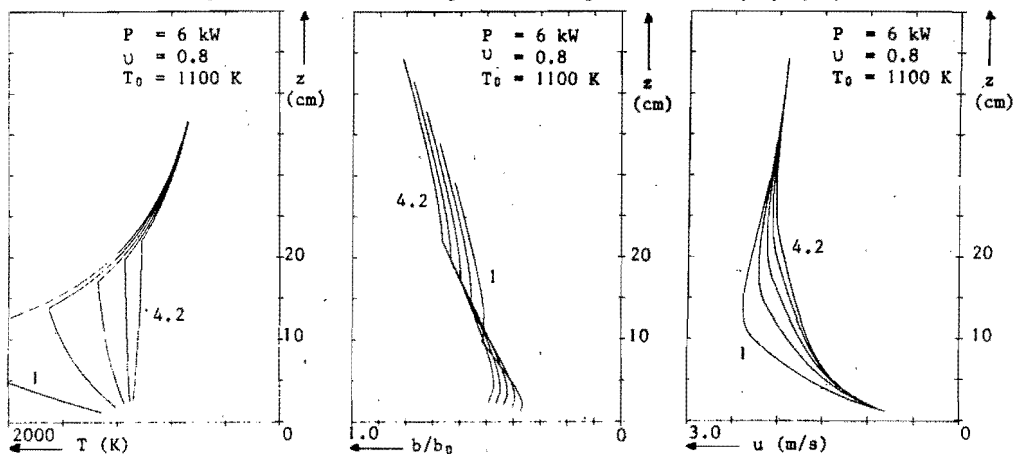


Fig. 2.4.b. Temperature; plume width-fuel bed diameter ratio and velocity as function of the height with varied excess air factor ($\lambda = 1, 1.8, 2.6, 3.4, 4.2$)

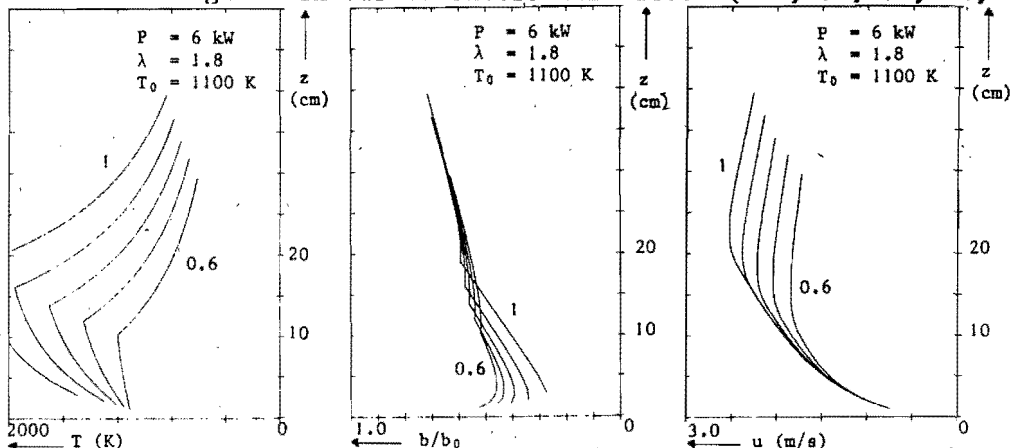


Fig. 2.4.c. Temperature; plume width-fuel bed diameter ratio and velocity as function of the height with varied volatiles ratio ($U = 0.6, 0.7, 0.8, 0.9, 1$)

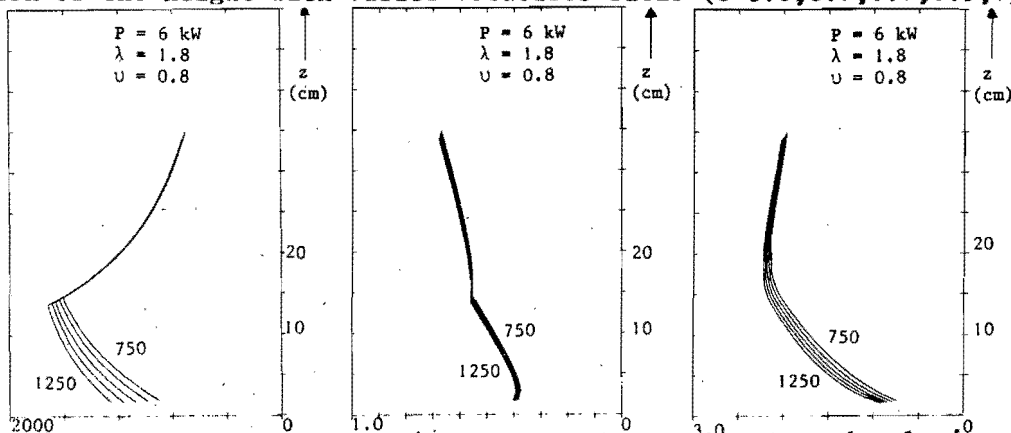


Fig. 2.4.d. Temperature; plume width-fuel bed diameter ratio and velocity as function of the height with varied fuel bed temp. ($T_0 = 750, 850, 950, 1050$)

This agrees with the finding of Steward [Steward, 1970] using a simpler model. This would serve as a first approximation for a scaling law for the design of combustion volumes in stoves.

The maximum velocity attained in the system also increases with the power output of the fire. The fire diameter profiles clearly show the characteristic neck near the fuel bed (as pointed out earlier).

In the present model the excess air factor is taken as a parameter. The actual value needs to be picked from experimental results. As is to be expected increase in excess air factor reduces the maximum temperatures, increases flame heights and reduces maximum velocities (fig. 2.4.b). The mass fraction of volatiles leaving the fuel bed is not exactly known but will vary around 0.8 [Brame and King, 1967]. The question is whether all of it will burn. Emmons [Emmons, 1980] points out that flaming combustion burns only limited fractions of the volatiles. For example polystyrene foamed plastic burns only 50 % of the mass pyrolyzed; the remainder appears as a dense cloud of soot, unburned and partially burned volatiles. The experiments on open wood fires (see later) do not suggest this level of unburned volatiles. However this possibility is included in the analysis by letting the mass fraction vary parametrically. The results shown in fig. 2.4.c. show simply the expected behaviour due to incomplete combustion.

Because of lack of experimental results on small wood fires it is difficult to check the validity of the model. Therefore a series of experiments were performed to compare experimentally determined flame heights with those predicted by the model. In each experiment the power output of the fire was held constant by adding predetermined quantities of oven-dry wood at known intervals of time. After the charcoal bed had built up, there ensued a steady state period for the burning as could be determined by the fuel bed thickness and flame heights. The flames were photographed roughly 20 times over a period of 15 minutes.

The power output could be varied by varying the fuel bed diameter. The flame height corresponding to a certain power output was taken as the distance between the top of the fuel bed and the visible flame tip on the photographs averaged over the twenty photographs. The results are shown in fig. 2.5.

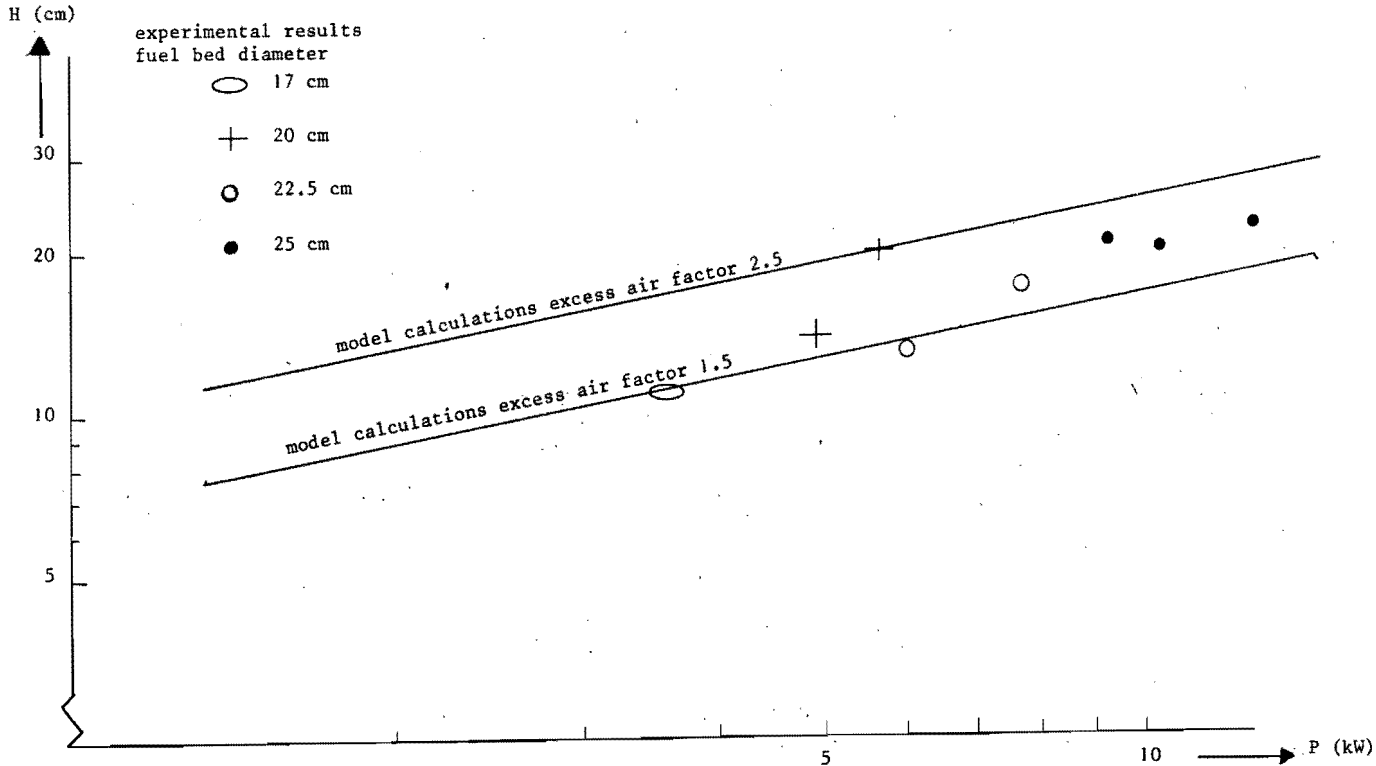


Fig. 2.5. Flame height as function of the power output.

The model calculations first of all explain the experimentally observed trends in flame heights for the wood fires tested. As stated before the flame height is proportional to $P^{2/5}$. The excess air factor required for a quantitative agreement with the experiments lies between 1.5 and 2.5. A value of 2 adequately represents the data. The fact that Steward required an excess air factor of 4 for agreement with experiments is attributed to the rather low value of entrainment factor he used. A value of 0.08 represent the conditions in the fire better. [List and Imberger, 1973]

The present experiments did not measure the velocities and the temperatures. In order to evaluate these results from the model, the experimental results of Cox and Chitty [Cox and Chitty, 1980] were used. These experiments were on simulated fire plumes produced by burning natural gas as a diffusion flame on a porous refractory burner. The axial velocity at the flame height level in their experiments correlated according to

$$U_0 = C P^{\frac{1}{5}}.$$

the $\frac{1}{5}$ th power law is consistent with the height-power output correlation mentioned earlier. The constant C was found to be 1.867.

In the present model C depends strongly on the heating value of the fuel, Stoichiometric air-fuel ratio and excess air factor. Using an excess air factor of 2, as determined in the present work (Cox and Chitty did not report this quantity), the programme was rerun for natural gas. C from the calculations was found to be 1.633.

The measured temperatures were only 1250 K.

If we note that the present model employs top hat profiles and the measurements were at the axis of the fire, the discrepancy in velocity could be considered modest. The overprediction of the temperature should be attributed to several reasons. Firstly, the measurements did not correct for radiation errors. The error was estimated to be about 20 % at 1250 K. This will bring the actual temperature up to 1500 K. Secondly the model does not include radiation losses and the possibility of incomplete combustion. Considering the crudeness of the model, the agreement between experiment and the model should be judged reasonable.

The problem with the model is that it underpredicts velocity, but over-predicts the temperature. This requires further investigation.

REFERENCES

Brame, J.S.S. and King, J.G., (1967)

"Fuel". Arnold, London.

Cox, G. and Chitty, R., (1980)

"A study of the deterministic properties of unbounded fire plumes" in "combustion and Flame", 39, pp 191.

Eckert, E.R.G. and Drake, R.M., (1972)

"Analysis of Heat and Mass Transfer", pp 356, Mc Graw-Hill, Tokyo.

Emmons, H.W., (1980)

"Scientific Progress on Fire" in "Annual Review of Fluid Mechanics", 12, Annual Reviews Inc., Palo Alto.

Krishna Prasad, K., (1980)

Lecture "On the modelling of wood-burning stoves" University of Technology, Eindhoven.

Lee, Shao-Lin and Emmons, H.W., (1961)

"A study of natural convection above a line fire", in "Journal of Fluid Mechanics", 11, pp 353.

List, E.J. and Imberger, J., (1973)

"Turbulent Entrainment in Buoyant Jets and Plumes", in "Journal of the Hydrantics Division", HY9, pp 1461

Steward, F.R., (1970)

"Prediction of the height of turbulent diffusion buoyant flames", in "Combustion Science and Technology", 2, pp 203.

LIST OF SYMBOLS

z	coordinate in axial direction	(m)
r	coordinate in radial direction	(m)
b	plume width	(m)
u	velocity axial direction	(m/s)
v	velocity in radial direction	(m/s)
ρ	density	(kg/m ³)
T	temperature	(K)
c_p	specific heat of air and volatiles	(J/(kg K))
Q_v	specific combustion heat of volatiles	(J/kg)
Q_w	specific combustion heat of wood	(J/kg)
Q_c	specific combustion heat of charcoal	(J/kg)
\dot{w}	source term in the energy equation	(J/(m s))
P	power output of the fire	(J/s)
α	entrainment constant	(-)
n_s	Stoichiometric air to fuel ratio	(-)
λ	excess air factor	(-)
F	Froude number	(-)
V	combustion number	(-)
U	volatiles ratio	(-)
ϕ_m	dimensionless mass flux	(-)
ϕ_p	dimensionless momentum flux	(-)

indices

a	ambient
σ	fuel bed
f	turbulent fluctuation

APPENDIX 2.1.

Comparison of the equations with and without combustion (equation 10^a and 10^b) shows that they have the same character. Therefore only the solution is given of the set equations for the flame region.

Calling the dimensionless mass flow rate $\phi_m = \rho' u' b'^2$

and the dimensionless momentum flow rate $\phi_p = \rho' u'^2 b'^2$

and using the relations

$$b'^2 = \frac{\phi_m^2}{\rho' \phi_p}$$

the equations 10, 11, 12 transform into:

the continuity equation

$$\frac{d}{dz'} \phi_m = \phi_p^{\frac{1}{2}} \tag{15}$$

the momentum equation in z' direction

$$\frac{d}{dz'} \phi_p = \frac{(1 - \rho')}{\rho'} \frac{\phi_m^2}{\phi_p} \tag{16}$$

the energy equation

$$\frac{d}{dz'} \frac{\phi_m}{\rho'} = (1 + V) \phi_p^{\frac{1}{2}}$$

Eliminating ϕ_p from equation 15 and 16 gives:

$$\frac{d}{dz'} \left[V - \frac{1 - \rho'}{\rho'} \right] \phi_m = 0 \quad \text{and thus}$$

$$\phi_m \left[V - \frac{1 - \rho'}{\rho'} \right] = C_1 \quad \text{or} \quad \rho_1 = \frac{\phi_m}{\phi_m (V + 1) - C_1}$$

Using the boundary conditions for $z = 0$, the expression for C_1 becomes:

$$C_1 = \rho_0' F \left[V - \frac{1 - \rho_0'}{\rho_0'} \right]$$

It is now possible to eliminate ρ' from equation 16 doing so and dividing the momentum equation by the continuity equation, we get:

$$\frac{d \phi_m}{d \phi_p} = [V \phi_m^2 - C_1 \phi_m] * \frac{1}{\phi_p^{\frac{3}{2}}} \quad \text{and thus}$$

$$\phi_p^{\frac{5}{2}} = \frac{5}{6} V \phi_m^3 - \frac{5}{4} C_1 \phi_m^2 - C_2 \quad (17)$$

Using the boundary condition for $z' = 0$ again

$$C_2 = (\rho_0' F^2)^{\frac{5}{2}} - \frac{5}{6} V (\rho_0' F)^3 - \frac{5}{4} C_1 (\rho_0' F)^2$$

Finally making use of the continuity equation

$$z' = \int_{\rho_0' F}^{\phi_m} \frac{d \phi_m}{\phi_p^{\frac{1}{2}}}$$

Because of relation 17, the density, plume width, velocity and position above the fuelbed are given as function of ϕ_m only. Taking ϕ_m as independent variable the problem is solved.

3. EXPERIMENTS ON SHIELDED FIRES

by

P. Visser.

Eindhoven University of Technology,

Eindhoven, The Netherlands.

3.1. INTRODUCTION

The experiments on the three stone open fire as published in one of our earlier reports (Krishna Prasad 1980) have had no follow up for some time for several reasons.

The main one was the publication of the woodstove compendium. (De Lepeleire et al 1981).

However, while working on the compendium, every now and then I have done some tests on open fires, which were more or less shielded. This paper will give a discription of these tests and the results.

The first series of tests concern an open fire on a grate, shielded with rings in a number of different configurations. The results do not point to an obvious conclusion, only that there is some improvement compared to the non-shielded fire.

The second series of tests concern a shielded fire on a grate, with controllable primary and secondary air entrance holes, and a shield around the pan too. This showed a substantial improvement compared to the non-shielded fire, in terms of waterboiling efficiencies.

3.2. FIRST SERIES OF TESTS

3.2.1 Experiments

We were looking for a simple change in the configuration of an open fire on a grate that would improve the performance. Out of a paper from (Modak, 1977) we picked up the idea of putting a ring around the grate.

This would reduce radiation losses and concentrate gases on the bottom of the pan. Further ideas concerned the preheating of the combustion air and divide the combustion air into primary and secondary air streams. These we tried to realize by putting a second ring around the first one and a small ring in the middle on the grate.

With these features we tested a number of possible configurations, using a small and a large grate. Each test was only done once or twice, but with our present routine in testing we believe the results to be reliable; in others words repeating the test will give an efficiency within 2 percentage points of the first figure. Experimental conditions that were constant over the tests were:

- An aluminium pan, diameter 28 cm, height 24 cm, containing 5 l of water, covered with a lid.
- Fuelwood in blocks of 15 * 15 * 50 mm, oven-dry, white fir.
- Total amount of wood 1000 g.
- Initial water temperature about 20°C.
- Windfree conditions.
- Recharging when the flames of the previous charge had almost disappeared.

The results of these tests will be presented in the next section, by giving a schematic picture of the configuration and experimental data. We have tried to group together experiments with only a single change in configuration as much as possible.

The efficiency was calculated according to the usual formula

$$\eta = \frac{m_w * C(T_b - T_i) + m_v * R}{m_f * B} * 100\%$$

where η = efficiency

m_w = initial amount of water

m_v = amount of water evaporated during the experiment

m_f = amount of fuel burnt

C = specific heat of water

T_b = temperature of boiling of water

T_i = initial temperature of water in the pan

R = heat of evaporation of water at atmospheric pressure and 100°C

B = combustion value of wood used.

Values for the various quantities used were:

$$C = 4.2 \quad \text{kJ/kg. K.}$$

$$R = 2256.9 \quad \text{kJ/kg}$$

$$B = 18.730 \quad \text{kJ/kg}$$

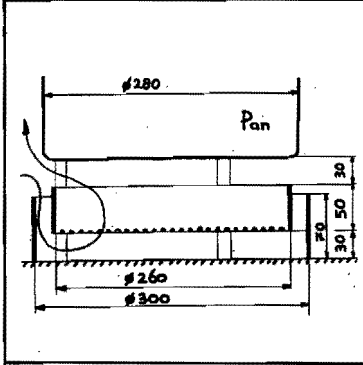
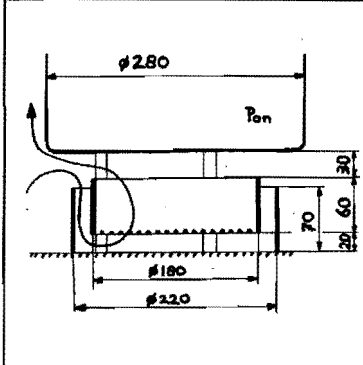
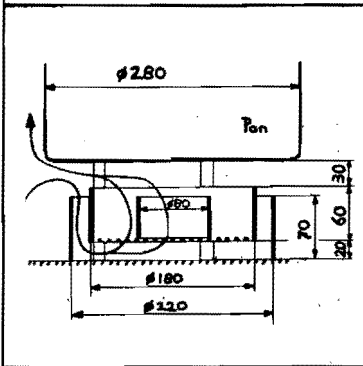
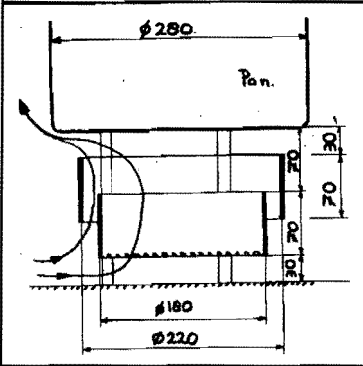
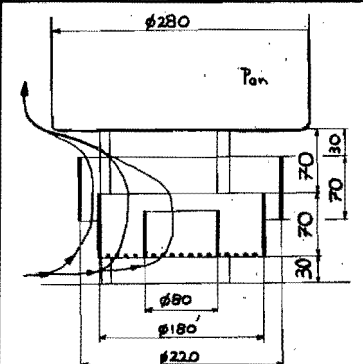

Power is calculated in terms of wood fed into the fire per unit time. It is calculated as an average over all the charges except the last one, because the burning time of the last charge is much longer, being the time from the moment that the wood is fed to the fire until the moment that the water stops boiling.

The behaviour of the fire is characterized by some remarks, concerning the way of burning and if there was a build up of a charcoal bed during the experiment. A fire is a good fire when it is characterized as good or fiercely burning. In this case the fire can entrain enough air from the surroundings for the combustion. When the charcoal bed is building up then there is not enough air coming under the grate to burn the charcoal or, approaching the problem from the other side: there is more wood fed to the system than it can handle.

3.2.2 Results

The outcome of these experiments does not lead to any obvious conclusion. There is however a trend visible that good burning fires, that do not build up a charcoal bed, give the higher efficiencies. But this is also a matter of the amount of wood fed to the fire. A configuration that functions badly at one power can give high efficiencies at a lower power with smaller charges. So it is not possible to say that one configuration is superior to all the others.

The only conclusion that can be drawn is that shielding the fire with some kind of ring does improve the performance of an open fire on a grate, compared to the one without any shielding, which under the same experimental conditions, gave a maximum efficiency of 26%. (Krishna Prasad, 1980) (Visser, 1981).

	η	P (kW)	Charge (g)	Remarks
	33.8	6.3	100	<ul style="list-style-type: none"> - fierce burning fire - no building up of charcoaled
	25.5	4.7	100	<ul style="list-style-type: none"> - building up of charcoaled
	34	3.5	50	<ul style="list-style-type: none"> - quiet burning fire - no building up of charcoaled
	28.5	4.3	100	<ul style="list-style-type: none"> - building up of charcoaled - a bit smoldering fire
	26.6	6.8	100	<ul style="list-style-type: none"> - fierce burning fire - no building up charcoaled
	23.4	7.1	100	<ul style="list-style-type: none"> - fierce burning fire - little building up of charcoaled

	η	P (kW)	Charge (g)	Remarks
	27.9	5.6	100	- building up charcoalbed - smoldering fire
	26.9	6.2	100	- quiet burning fire - little building up of charcoalbed
	26.1	6	100	- good burning fire - little building up of charcoalbed
	29.2	7.4	100	- fierce burning fire - no building up of charcoalbed
	30.6	3.5	50	- good burning fire - no building up of charcoalbed
	23.8	6.7	100	- good burning fire - no building up of charcoalbed

3.3. SECOND SERIES OF EXPERIMENTS

We were convinced on the basis of the foregoing experiments that it is important to divide the combustion air into primary and secondary air. This is based on the following model of the burning of wood.

We can divide the woodfuel into two parts: the volatiles, which escape from the wood when it is heated and which burn with the well-known yellow flames; and the carbon, which burns with a blue flame. The model says that the volatiles burn above the fuelbed and get their oxygen from the environment and that the carbon burns in the fuelbed (actually the carbon is the fuelbed) and it gets its oxygen through the grate.*

At the same time, when the primary air flow is decreased, and as a result of this there are less volatiles to burn, the amount of secondary air must also decrease, so that just enough air is coming to the volatiles to burn completely. More air is useless and cools down the gases with a negative effect on the efficiency.

If we want to put these ideas into practice, we must shield the fire, and make adjustable holes in the shield. One set of holes under the grate for primary air and one set of holes above the grate for secondary air are to be provided.

3.3.1 The stove

A stove that satisfies these requirements is depicted in fig.3.1 We have used the same grate from the previous experiments, with a diameter of 18 cm. Built of steel bars ϕ 4 mm with meshes of 1 * 1 cm. The shield is a cylinder of steel sheet, 1 mm thick. There are 24 holes for primary and 24 holes for secondary air, all of them ϕ 8.5 mm.

To be able to control the airflow, there is a ring around the airholes which has the same number of holes, of the same diameter in it. By sliding this ring the airholes can be fully open, fully closed or any position in between.

* For a more elaborate discussion on this subject, see chapter 5.

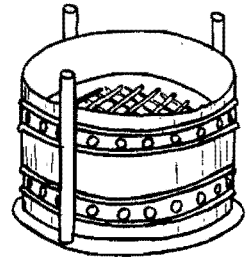
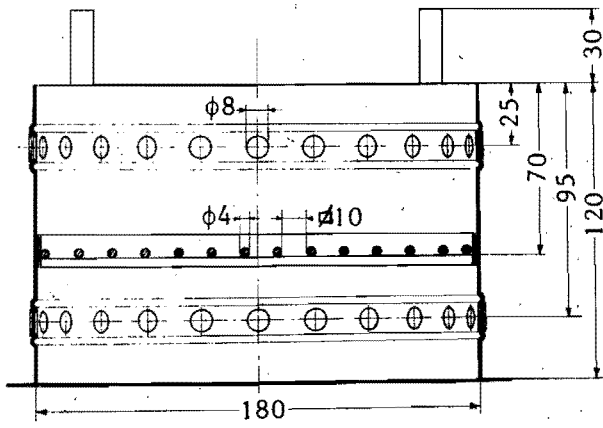


Fig. 3.1. Shielded fire.

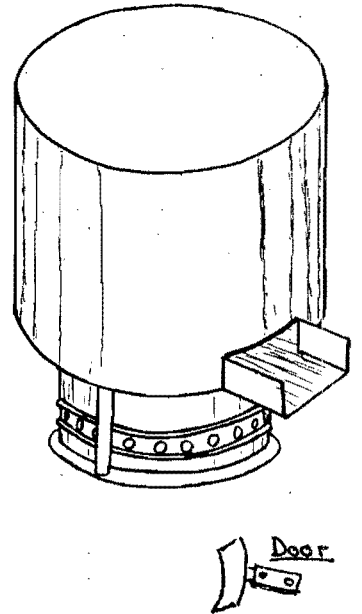
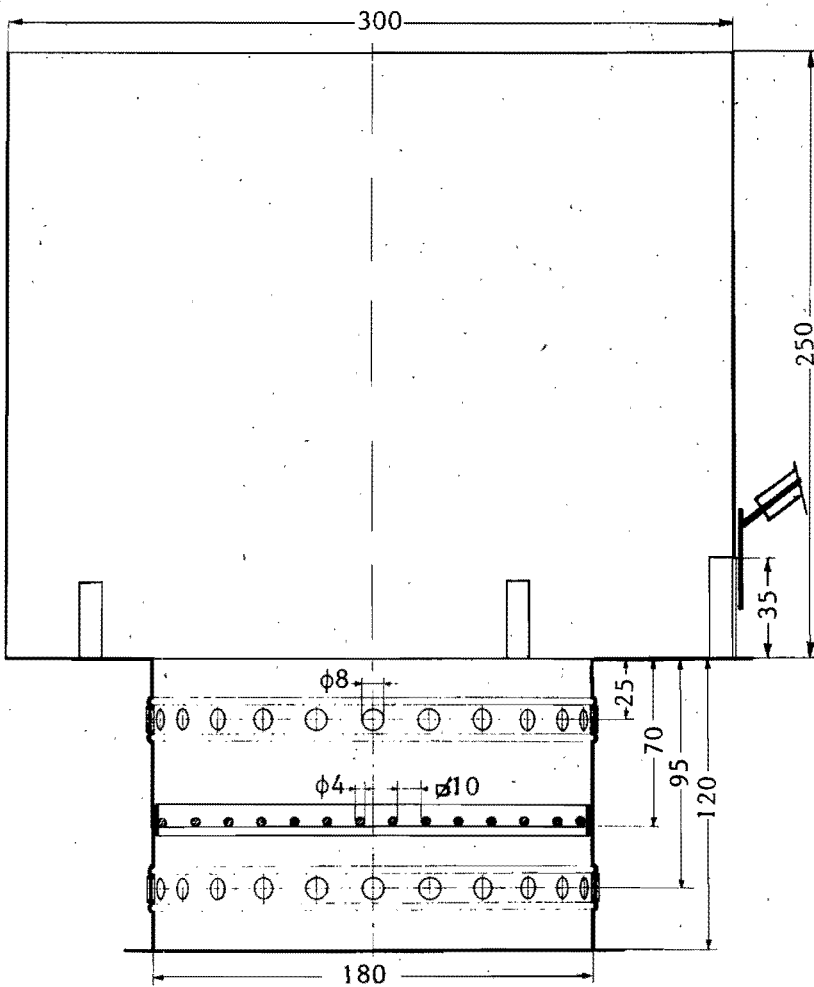


Fig. 3.2. Shielded fire with shielded pan.

The pan is supported by three legs attached to the shield. Later the stove was extended with a shield around the pan, as shown in fig. 3.2. This was done to force the hot gases through the narrow annular space between the shield and the pan in order to increase the heat exchange between the gases and the pan.

Considerations and calculations that have determined the dimensions of this stove are grouped together in appendix 3.1.

3.3.2 Experimental conditions

The experimental conditions were mostly the same as in the previous experiments, the differences were:

- Fuelwood in blocks of 15 * 15 * 50 and 30 * 30 * 100 mm oven-dry, white fir.
- Fire driven at a chosen power, to say every x minutes, y g. of wood was fed to the fire, independent of the condition of the fire.

3.3.3 Results

First one experiment was done with the stove without the shield around the pan. With woodblocks of 15 * 15 * 50 mm we got 33 % efficiency at a power of 4,8 kW. The primary and secondary air holes were fully open.

This was again an improvement of some percentage points to the previous experiments, but a quick and simple experiment with an old paint can as a shield around the pan had shown that we could gain more. So we built a shield around the pan and repeated the experiment, using different sizes of wood, because the little blocks gave a very fierce burning fire. The results are gathered in table 3.1.

Table 3.1. Influence of the size of the wood used.

Airholes		Size of woodblocks	Power	Efficiency
prim	sec			
open	open	15 * 15 * 50	6.1	41.7 %
open	open	19 * 12 * 50*	5.2	42.3 %
open	open	25 * 25 * 83	4.7	48 %
open	open	25 * 23 * 83	4.7	49 %
open	open	30 * 30 * 100	5.2	49 %

* We have changed our standard woodsize from 15 * 15 * 50 mm to 19 * 12 * 50 mm, because these can be more economically made at the carpentry-shop. Comparalise tests did not show any difference in results.

Table 3.2. Influence of the change in flow passage and power output.

η [%]	5.5 kW	3.6 kW	2.8 kW
	105 g. in 6 min.	105 g. in 9 min.	105 g. in 12 min.
Both open	51.4	45.8	42.3
prim. closed sec. open	31.6	41.5	41.6
sec. closed prim. open	37.5	41.7	43

From this table we can clearly see that at a constant power of ± 5 kW and all air holes open, the size of the woodblocks makes a big difference in the efficiency. This probably due to the fact that the big pieces evolve their volatiles at a lower and more constant rate than the small woodpieces. We could not use even bigger blocks because the dimensions of the woodcharging opening. To investigate the influence of the change in flowpassage area for the primary and secondary air we did experiments with the holes fully open, the primary airholes closed and secondary airholes open and the other way around. We did this at three different power levels. These three powerlevels were obtained by increasing the time between two charges of 100 gr. In practice this came to a charge of 3 blocks of wood, with a weight of ± 105 g/charge. The results are shown in table 3.2. and plotted in a graph, fig. 3.3. From these the following conclusions can be drawn.

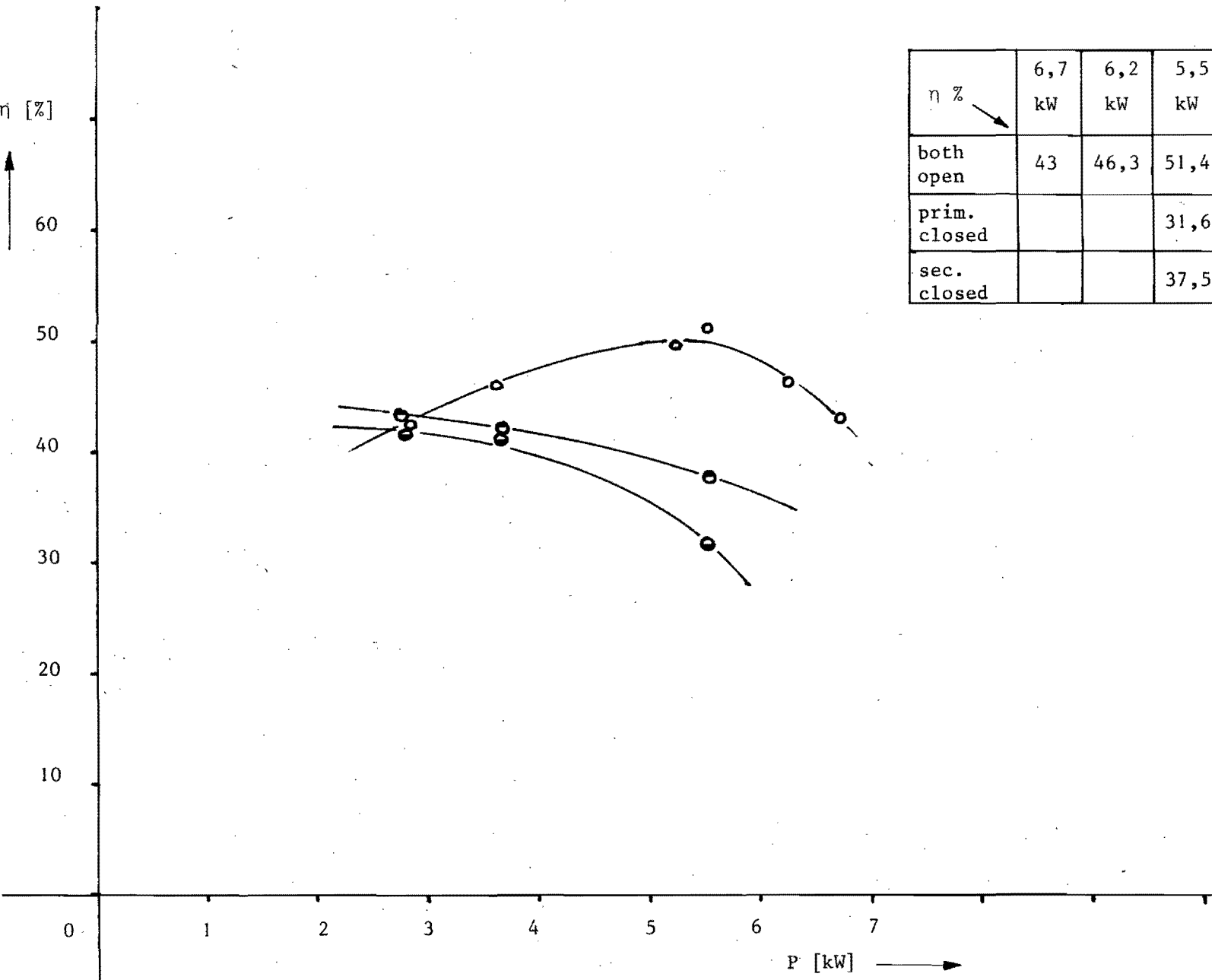
Closing the airholes has a great influence on the performance of the fire, especially with the high powers. At low power the three lines come together on the 40 % level. It is clear that the closure of the primary airholes has a greater influence than the closure of the secondary airholes.

We can try to explain this behaviour from our model.

With primary and secondary airholes open, the efficiency increases with power. This means that, at the highest power rate the charcoal and volatiles get enough air to burn, because there is no tendency that the curve is bending down at still higher powers. To verify this, we have done two more experiments with both holes open, at a power of 6.2 and 6.7 kW.

Then the efficiency drops quickly. The fire becomes more smoky. At the power of 6.7 kW, there is a built-up of the charcoal bed. Apparently the fire suffers from a lack of oxygen. The negative slope of the curve with lower powers can be explained by the amount of excess air that is drawn in through the holes and cool down the combustion gases.

Closing down the secondary airholes makes the fire suffer from a lack of oxygen, which has the greater negative effect at higher power. At lower powers the air that is not used for the combustion of the carbon on the grate is used to burn the volatiles, resulting in higher efficiencies.



η %	6,7 kW	6,2 kW	5,5 kW	5,2 kW	3,6 kW	2,8 kW
both open	43	46,3	51,4	49,5	45,8	42,3
prim. closed			31,6		41,5	41,6
sec. closed			37,5		41,7	43

Fig. 3.3. Efficiency as function of power.

Closing the primary airholes is the worst thing to do. Practically this is the same situation as a fire without grate. The oxygen for the burning of the carbon must flow downward, or even diffuse down to reach the carbon, which makes charcoal and volatiles suffer from a lack of oxygen, specially at the power of 5.5 kW. Visual observations confirm this. There was a heavy build-up of the charcoal bed, that even made it difficult to add new charges to the fire, and at the end of the experiment the pan was covered with a shining layer of tar instead of soot.

At the power of 2.8 kW lack of oxygen does no longer obstruct the fire and it burns normally with a reasonable efficiency.

3.4. CONCLUSION

The general conclusion can be, that this kind of stove is a promising way of improving the performance of a wood fire for cooking. It shows high efficiencies over a range of power from 2.8 to 6.7 kW, with a maximum efficiency of 51 % at 5.5 kW.

Because the fire is shielded it probably will not be very sensitive to wind, but its behaviour was not tested in windy conditions.

All tests concerned the boiling of water, with the pan filled for about one third and on the outside completely shielded to the top.

For the cooking of food this configuration may cause trouble. Because the gases between the shield and the pan are hot, about 200 °C, the pan wall at and above the level of the food will obtain temperatures far over 100 °C. This may cause burning of the food, especially when it is of a thick consistency. Solution for this is, of course, to sink the pan into the shield just up to the foodlevel, or make a lower shield, conserving the optimal distance between pan and grate, but both these solutions will consequently cause a loss of efficiency.

APPENDIX 3.1

CONSIDERATIONS AND CALCULATIONS TO THE DIMENSIONS OF THE STOVE

Diameter. From our previous experiments we had the grate of 18 cm diameter, which had proven to be suitable for this size of pan. So the diameter became 18 cm.

Height of the pan above the grate. Here we took the optimal height from our open fire experiments, being between 7 and 11 cm. To have more space to put the wood in we choose a height of 10 cm.

Height of the pan above the rim of the fire chamber. Shadow-graphs taken of the open fire showed that naturally there is a layer of hot gases at the bottom of the pan of about 3 cm. So we decided to take this for a start.

Height of the space under the grate is not so critical. It must be enough so that the incoming air can spread over the hole grate. We took 5 cm.

Number and size of the airholes. Therefore we first have to know the amount of air needed. If we design our stove for a power of 5 kW, we can make the following calculations:

5 kW = 5 kJ/sec.

Combustion value of wood 18730 kJ/kg.

Though mass flow of wood: $\phi_w = \frac{5}{18730} = 0.26$ g/sec.

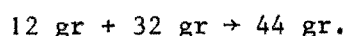
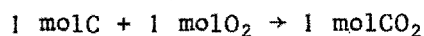
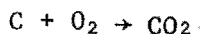
Assuming that 80 % of the wood burns as volatiles and 20 % as charcoal (Brame & King 1967) gives:

$$0.26 * 0.2 = 0.052 \text{ g/sec charcoal}$$

$$0.26 * 0.8 = 0.208 \text{ g/sec volatiles.}$$

First the amount of primary air.

We want complete combustion so the reaction can be put as:



So the amount of oxygen needed:

$$\phi_{O_2} = \frac{32}{12} * 0.052 = 0.14 \text{ g/sec.}$$

which means a volume flow at 20 °C of:

$$1 \text{ mol } O_2 = 22.4 \text{ l.}$$

$$\phi_{VO_2} = \frac{0.14}{32} * \frac{273 + 20}{273} * 22.4 = 0.105 \text{ l/sec.}$$

With 21 % of oxygen in air, the air flow becomes:

$$\phi_{VA} = \frac{100}{21} * 0.105 = 0.5 \text{ l/sec.}$$

Secondly the amount of secondary air.

Composition of white fir (Brame & King 1967)

Carbon	: 50.4 %	
Hydrogen	: 5.9 %	
Oxygen	: 43.4 %	
Ashes	: 0.3 %	by weight

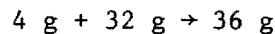
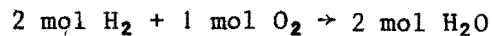
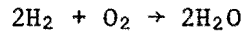
Because 20 % of the wood burns as charcoal, in the volatiles is left $50.4 - 20 = 30.4$ % carbon, so the mass flow of volatiles becomes:

$$\text{Carbon} : 0.26 * 0.304 = 0.079 \text{ g/sec}$$

$$\text{Hydrogen} : 0.26 * 0.059 = 0.015 \text{ g/sec}$$

$$\text{Oxygen} : 0.26 * 0.434 = 0.113 \text{ g/sec.}$$

The hydrogen is assumed to combine with the oxygen to form H₂O:



This reaction consumes:

$$\frac{4}{32} * 0.113 = 0.014 \text{ g/sec } H_2$$

So there is $0.015 - 0.014 = 0.001$ g/sec H₂ left, which uses:

$$\frac{32}{4} * 0.001 = 0.008 \text{ g/sec } O_2$$

The carbon will need:

$$\frac{32}{12} * 0.079 = 0.211 \text{ g/sec } O_2$$

$$\text{Total} \quad 0.008 + 0.211 = 0.219 \text{ g/sec } O_2.$$

This means a volume flow of:

$$\phi_{VO_2} = \frac{0.219}{32} * \frac{273 + 20}{273} * 22.4 = 0.164 \text{ l/sec.}$$

The required airflow then becomes:

$$\phi_{VA} = \frac{100}{21} * 0.164 = 0.78 \text{ l/sec.}$$

So now we have got; for a fire of 5 kW:

Primary air : $\phi_{VAP} = 0.5 \text{ l/sec} = 0.5 * 10^{-3} \text{ m}^3/\text{sec.}$

Secondary air : $\phi_{VAS} = 0.78 \text{ l/sec} = 0.78 * 10^{-3} \text{ m}^3/\text{sec.}$

Assuming an air velocity through the holes of 0.5 m/sec we need an area of:

$$\frac{0.5 * 10^{-3}}{0.5} = 1 * 10^{-3} \text{ m}^2 \text{ for primary air and}$$

$$\frac{0.76 * 10^{-3}}{0.5} = 1.56 * 10^{-3} \text{ m}^2 \text{ for secondary air.}$$

Now for ease of construction we want to make number and size of primary and secondary airholes the same, which seems reasonable because the estimates of the required air flows are not too far apart. We take the average needed area to be:

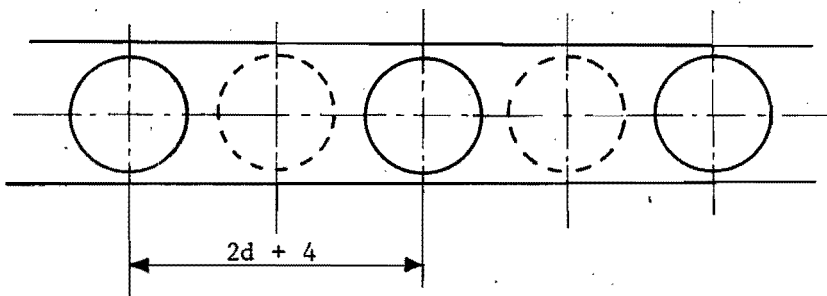
$$\frac{1000 + 1560}{2} = 1280 \text{ mm}^2$$

The circumference of the fire chamber is:

$$\pi * 180 = 565 \text{ mm.}$$

Number of holes n, diameter of holes d, then

$$\left. \begin{aligned} (2d + 4) * n &= 565 \\ n * \frac{n}{4} d^2 &= 1280 \end{aligned} \right\} \begin{aligned} \frac{565}{2d+4} * \frac{n}{4} * d^2 &= 1280 \\ d &= 8.5 \text{ mm} \end{aligned}$$

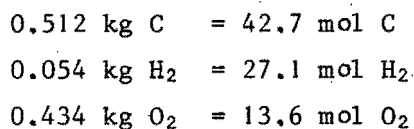


With an access air factor λ of 1, 2, 3 we get diameters of 8.5; 17; 25.5 mm. For these experiments the diameter of the holes was 8.5 mm.

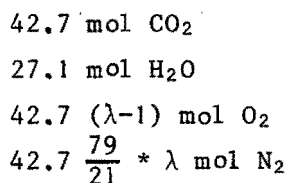
Dimensions of the shield around the pan. According to a paper of Prof. De Lepeleire, presented at the 5 th. woodstove-day at Apeldoorn, april 1981, (De Lepeleire, 1981) in which he presented some theoretical models in heat transfer, concerning woodstoves, the gap between pan and shield is taken to be 1 cm. So the outside diameter of the shield becomes 30 cm. The height of the shield is so that it covers the pan as much as possible, concerning the grips of the pan, and is 25 cm.

Estimate of the gas velocity in the anular space between the pan and the shield.

Per kg wood there is:



Burning this wood, assuming complete combustion and an air access factor λ , gives an amount of flue gas of:



total. $27.1 + 203.3 \lambda$ mol flue gas of standard conditions

Here by is assumed that the H₂ consumes all the O₂ in the wood and that air is composed of 21 % O₂ and 79 % N₂

This gives a volume flow of:

$$(27.1 + 203.3 \lambda) * 22.4 * 10^{-3} = (607 + 4554 \lambda) * 10^{-3} \text{ m}^3$$

If we take λ to be 1, 2, 3 we get volume flows of:

$$\begin{aligned}\lambda = 1 & \quad \phi_{V1} = 5.16 \text{ m}^3 & \text{ at } 273 \text{ }^\circ\text{K} \\ \lambda = 2 & \quad \phi_{V2} = 9.72 \text{ m}^3 & \text{ for 1 kg of wood} \\ \lambda = 3 & \quad \phi_{V3} = 14.27 \text{ m}^3\end{aligned}$$

Assuming an average flue gas temperature of 300 $^\circ\text{C}$ we find:

$$\begin{aligned}\phi_{V1} &= 10.83 \text{ m}^3/\text{kg} \\ \phi_{V2} &= 20.4 \text{ m}^3/\text{kg} \\ \phi_{V3} &= 29.95 \text{ m}^3/\text{kg}\end{aligned}$$

The flow area is $\frac{\pi}{4} (0.30^2 - 0.28^2) = 9.1 * 10^{-3} \text{ m}^2$

For power we take 5 kW which gives:

$$\frac{5}{18730} = 0.267 * 10^{-3} \text{ kg/sec}$$

in which 18730 kJ/kg is the combustion value of the wood.

With this, the estimated velocities become

$$\begin{aligned}V_1 &= \frac{10.83 * 0.267 * 10^{-3}}{9.1 * 10^{-3}} = 0.32 \text{ m/sec} \\ V_2 &= & = 0.6 \text{ m/sec} \\ V_3 &= & = 0.88 \text{ m/sec}.\end{aligned}$$

In the paper of Prof. De Leppeleire (1981) mentioned before he predicts a gain of 50% to the non shielded situation for a shield like the one of this stove and flue gas velocities in this range. This prediction matches with our experimental results. Without a shield the efficiency was about 30 % and with a shield we find an efficiency of about 45 %, which is indeed a gain of 50 % to the original 30 % efficiency.

REFERENCES

Brame, J.S.S., and King, J.G., (1967)

"Fuel". Arnold, London.

Modak, A.T., (1977)

"Thermal radiation from pool fires". In

"Combustion and Flame", 29, 1977. pp. 177-192.

Krishna Prasad, K., (ed) (1980)

"Some performance tests on open fires and the family cooker". pp. 50. Eindhoven University of Technology, Eindhoven, and T.N.O., Division of Technology for Society, Apeldoorn.

De Leppeleire, G., Krishna Prasad, K.,

Verhaart, P., Visser, P., (1981).

"A woodstove compendium" pp. 379. Eindhoven University of Technology, Eindhoven.

De Leppeleire, G. (1981)

"Theoretical Models in Heat Transfer". pp. 13.

K.U. Leuven, Louvain.

Visser, P. (1981)

"Het open vuur, verslag van een inleidend onderzoek".

pp. 43. Eindhoven University of Technology, Eindhoven.

4. SOME STUDIES ON THE PERFORMANCE OF CYLINDRICAL COMBUSTION CHAMBERS*

by

J. Delsing

Eindhoven University of Technology,

Eindhoven, The Netherlands.

4.1. INTRODUCTION

Experience with earlier designs of woodstoves such as the family cooker showed that combustion was far from complete in these designs [see for example Sielcken & Nieuwvelt, 1981]. One of the major problems with the family cooker was that it was unable to operate with sufficiently deep fuel beds. This was a severe limitation not only on the power output of the stove but also on the operational convenience since the stove required frequent refuelling.

In order to study the problem of combustion of wood in fuel beds in greater detail, a cylindrical combustion chamber was designed by Verhaart (1980). In particular the intention of the design was to investigate the possible influence of secondary air on combustion. The first stage of the present investigation concentrated on looking at the power output of the stove. Experiments showed that the design required modifications and a grate was included in later experiments.

* The work reported here was done as part of the curricular requirement towards the Ingenieur degree in the Department of Applied Physics at the Eindhoven University of Technology.

4.2. DESIGN

The design of the stove is shown in fig. 4.1.

The stove consists of two tubes: one inner and one outer made of 4 mm thick steel sheet. The bottom of the inner tube is closed except for some holes which provide the primary air. The secondary air holes are made in the upper half of the tube. The outer tube serves to pre-heat the secondary air. The three most important aspects on which the design was based will be discussed below.

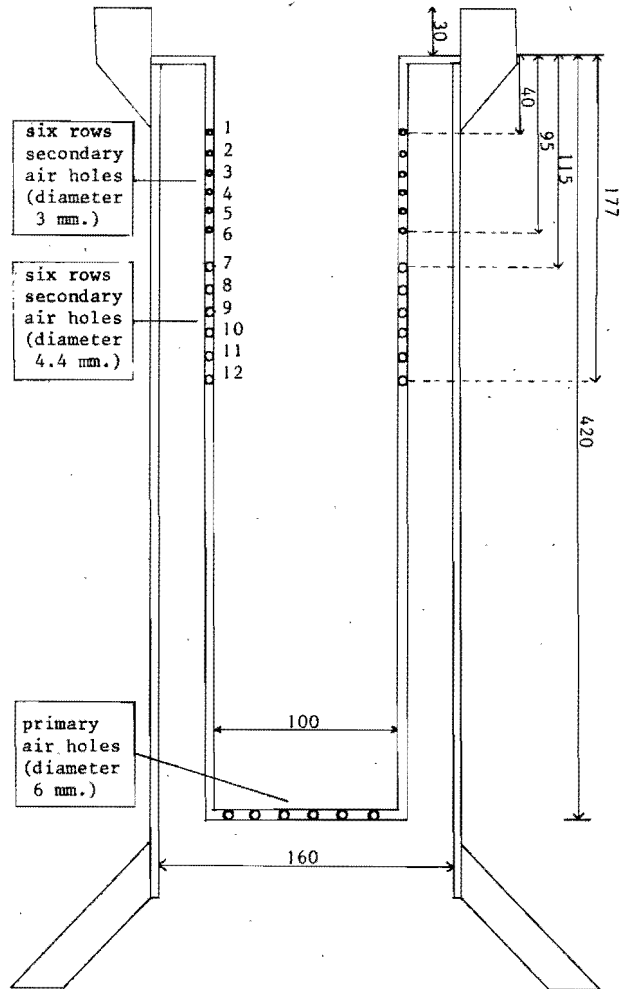


Fig. 4.1. Design of the stove

4.2.1 Power output

The stove was designed to perform at a power output of 3 kW. This power output of the fire is defined as the ratio of the amount of wood burnt in one charge multiplied by the combustion value of the wood and the time interval between two charges.

Thus

$$P = \frac{\Delta m_f B}{\Delta t}$$

where

- P = power output of the fire (W)
 Δm_f = amount of wood burnt in one charge (kg)
B = combustion value of the wood (J/kg)
 Δt = time interval between two charges (s)

4.2.2 Required wood storing capacity

It was intended that the stove should operate with charges of 250 g. Such a charge results in a height of wood of 200 mm from the bottom of the inner tube (diameter 100 mm), using wood blocks of $12 * 19 * 50 \text{ mm}^3$.

This explains why it was necessary for the tube to be so high (420 mm).

4.2.3 Primary and secondary air holes

The combustion process can be split roughly into two phases. First the release and combustion of the volatiles, and second the combustion of the charcoal. It is the intention that the charcoal is burnt by the primary air and the volatiles by the secondary air. If the amount of charcoal (20 % of the wood) and volatiles (80 %) [Brame and King 1967], is known, one can calculate how much primary and secondary air is needed to burn a certain quantity of wood.

When we next take a power output at which the stove should operate (3 kW for this stove) we know how much air is needed per unit of time.

By making some gas temperature estimates, and by means of the buoyancy force, the velocity of the air that is drawn into the stove can be calculated. If the air velocity and the amount of air needed per unit of time is known, then the total area of the primary and secondary holes can be calculated. The amount of air required found above is the stoichiometric amount of air times the excess air factor. In the calculations an excess air factor of 1.4 has been used.

Finally one finds the following values:

$344 * 10^{-6} \text{ m}^2$ for the primary air holes

$549 * 10^{-6} \text{ m}^2$ for the secondary air holes

In the original design the secondary air was drawn into the stove through small tubes, so that the air came into the center of the stove. This was done to get a better mixing of air and volatiles. Since this did not work the idea was discarded and the tubes were removed. The holes were closed and new ones were made. The experiments which followed were not very successful and the stove still smoked very badly. Therefore some more secondary air holes were made at the place where the small tubes were located. With these extra holes the stove performed better. All these experiments were done before starting on the series of experiments described in this report. Finally the stove had the following holes:

19 primary air holes with a diameter of 6.0 mm and a total area of $537 * 10^{-6} \text{ m}^2$.

72 secondary air holes with a diameter of 4.4 mm and a total area of $1095 * 10^{-6} \text{ m}^2$.

120 secondary air holes with a diameter of 3.0 mm and a total area of $848 * 10^{-6} \text{ m}^2$.

We can see that the total area of the primary air holes is slightly greater than the calculated value, but the total area of the secondary air holes is even more than 3 times the calculated value. (for detailed information see appendix 4.1.).

This was the starting point of the experiments described in the next section.

4.3. THE EXPERIMENTS

A stove is characterised not only by its efficiency numbers but also by the power range over which it can operate and the size of the charges it can work with. That is why the goal of the first experiments was to establish, the power output and charge size the stove could manage.

This was done by varying:

- charge size
- time interval between two charges
- number of secondary air holes opened.

thereafter the power output and the variables mentioned above were kept constant. The second series of experiments aimed at establishing the influence of secondary air on the combustion efficiency. This was done by varying the distance between fuel bed and pan by means of a movable grate. The reason for this will be explained in the next section.

4.3.1 General

In every experiment an aluminium pan with a diameter of 28 cm, and a height of 24 cm (wallthickness 1 mm) was used. The pan was covered with an aluminium lid which was provided with a hole for a termocouple to measure the water temperature. The pan was filled with 5 kg of water. In all experiments oven-dry white fir wood was used. During an experiment 1 kg of wood was added to the fire in small charges. In all experiments, except two, wood blocks with dimensions 12 * 19 * 50 mm³ were used. At every instance of recharging the pan was lifted from the stove to put the wood into the stove. An experiment was terminated when the last charge of fuel got completely burnt. In every instance, at that moment the water in the pan had just ceased boiling. After every test the pan with the left over water was weighed on a balance (Berhel, type piccolo), to see how much water had evaporated during the test.

4.3.2 Variables

Between the different tests some variables were altered. The size of the charges was varied from 25 to 50 g. The time interval between two charges varied from 3 to 5 minutes. Finally the number of secondary air holes which were open, were altered by covering some rows of secondary air holes with a thin aluminium sheet.

4.3.3 Efficiency calculations

After each experiment the efficiency was calculated according to the definition given by THE - Eindhoven and TNO - Apeldoorn (see paragraph 3.2.1).

4.3.4 Observations

The performance of a stove is not only characterised by its efficiency numbers, but also by the way it performs from a visual viewpoint. The colour of the flames, the time in which the volatiles are completely burnt and the height of the charcoal fuel bed give important information about the performance of the stove, especially about the combustion properties of the stove. Therefore observation formed an important part of the experimental work. From these observations it appeared that the fire sometimes had to be helped by blowing into the stove or shaking it.

4.3.5 Temperatures

The temperature of the water, the flue gases and of the stove-wall were measured every minute. This was done by means of shielded chromel-alumel thermocouples (type: Tgo-HL-AK-gC). The measuring points are indicated in fig. 4.2.

The thermocouples were connected to a central multichannel data logger (Deric, Digitrend 220), which was connected with a terminal (Burroughs 390) producing punched paper-tape. Later a computer was fed with these paper-tapes to make graphs of the temperatures.

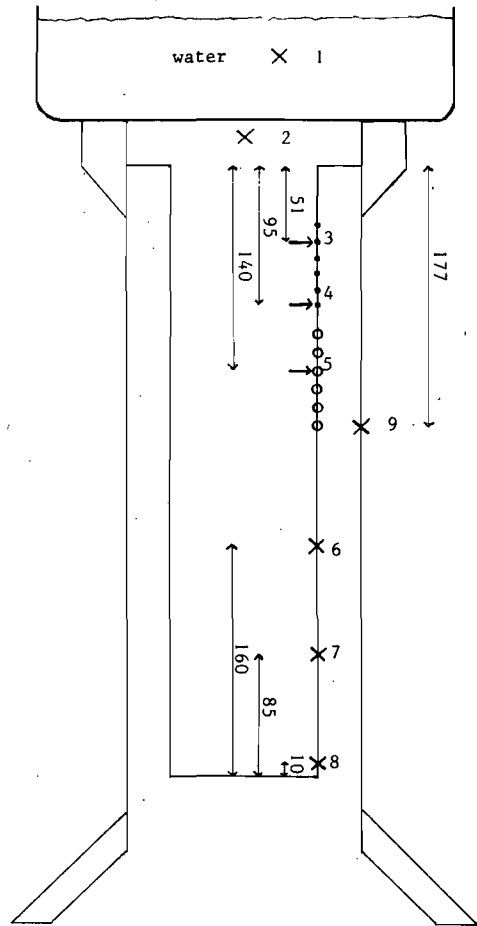


Fig. 4.2. Measuring points of the temperatures

4.4. RESULTS

4.4.1 First series of experiments

As stated before, the first series of experiments were meant to establish the charge sizes and power outputs the stove could manage.

Charge size

It was already known that charges of 250 g, for which the stove was designed, were far too large for this stove. But it also appeared that even with charges of 50 g the stove failed to burn independently of the recharge time. Only with very small charges of 30 g or less the stove burned to some degree. As a consequence of the small charges, the distance between fuel bed and secondary air holes became too large. The volatiles had to bridge over a long distance before they arrived at the secondary air holes and probably were too cold to burn. As a result the stove smoked very badly. Opening more secondary air holes did not help. Moreover to know how to apply secondary air in stove designs for developing countries, such small charges of 50 g or less were not admissible.

Power output

It appeared that the stove only worked within a small range of power outputs. A power output of 2 kW was too low; the stove performed very badly which can be seen (table 4.1.) from the efficiency numbers we got. On the other hand a power output of 3 kW was too high. The stove did not work in a steady state; the charcoal fuel bed kept on building up. Not enough primary air was available for the charcoal combustion. This problem was also due to the ashes that clogged the primary air holes. To sum up we were faced with the following problems:

- The stove could only work with small charges
- The ignition of volatiles was bad
- The stove worked only within a small range of power outputs
- There was excessive build up of the charcoal fuel bed

These problems meant that very often we had to help the stove along by blowing some extra air into the fire, shaking it and even sometimes by lighting it again.

To solve these problems the application of a grate was considered. Operating the stove with a grate would first decrease the distance between the fuel bed and secondary air holes, and secondly would decrease the clogging of the primary air holes with ashes.

The grate was hung into the stove by three steel wires. As expected, experiments showed that, with the grate, the stove performed better.

The ignition of the volatiles mostly happened directly after the recharging. It also became possible to work with greater charges (50 g). These improvements can also be seen from the higher efficiencies which were reached (22.7 %; 18.7 %; 18.5 %; 25.9 %; 23.4 %; see table 4.1). Operating the stove with bigger wood blocks (20 * 20 * 67 mm³) resulted in a reasonable performance (efficiency 23,6 %). Using even larger wood blocks did not work; after 3 charges the fuel bed rose above the stove. The application of the grate did not solve however the problem of the building up of the charcoal fuel bed.

To solve this problem 11 extra primary air holes with a diameter of 6 mm were made in the bottom of the stove. The total number of primary holes was now 30. This change caused the expected effect. We noticed that the combustion process of charcoal was speeded up, so that the charcoal fuel bed did not become as thick as in the earlier experiments, making it easier to reach a steady state. The results of this first series of experiments are given in table 4.1.

4.4.2 Second series of experiments

Because of the importance of the distance between fuel bed and secondary air holes it was decided to perform a series of experiments in which only the height of the grate was varied. In these tests small wood blocks (12 * 19 * 50 mm³) were used in charges of 50 g each added after 5 minutes. All the secondary air holes were left open except for the three lowest rows.

The previous experiments suggested that with this configuration the highest efficiencies were obtained (25.9 % and 23.4 %). The results are given in table 4.2. The experiments show that the efficiency increases when the distance between the grate and the pan becomes smaller.

In the last two experiments the grate was placed at such a height that there were even open secondary air holes beneath the grate. During these two tests the stove smoked very badly. This indicates that the combustion of the volatiles was far from complete. This may have been due to the fact that a part of the secondary air functions as primary air. So it is obvious that more secondary air is needed.

In spite of this, these two experiments showed the highest efficiencies (31.6 % and 31.8 %). This may be a consequence of the fact that the fuel bed was closer to the pan, so that more radiation heat was absorbed by the pan. Regarding this radiation heat some calculations have been made by using a simple model. These calculations are discussed in section 4.6.

The efficiencies of the series of these experiments have also been set into a graph as a function of the distance between the grate and the pan (see fig. 4.3).

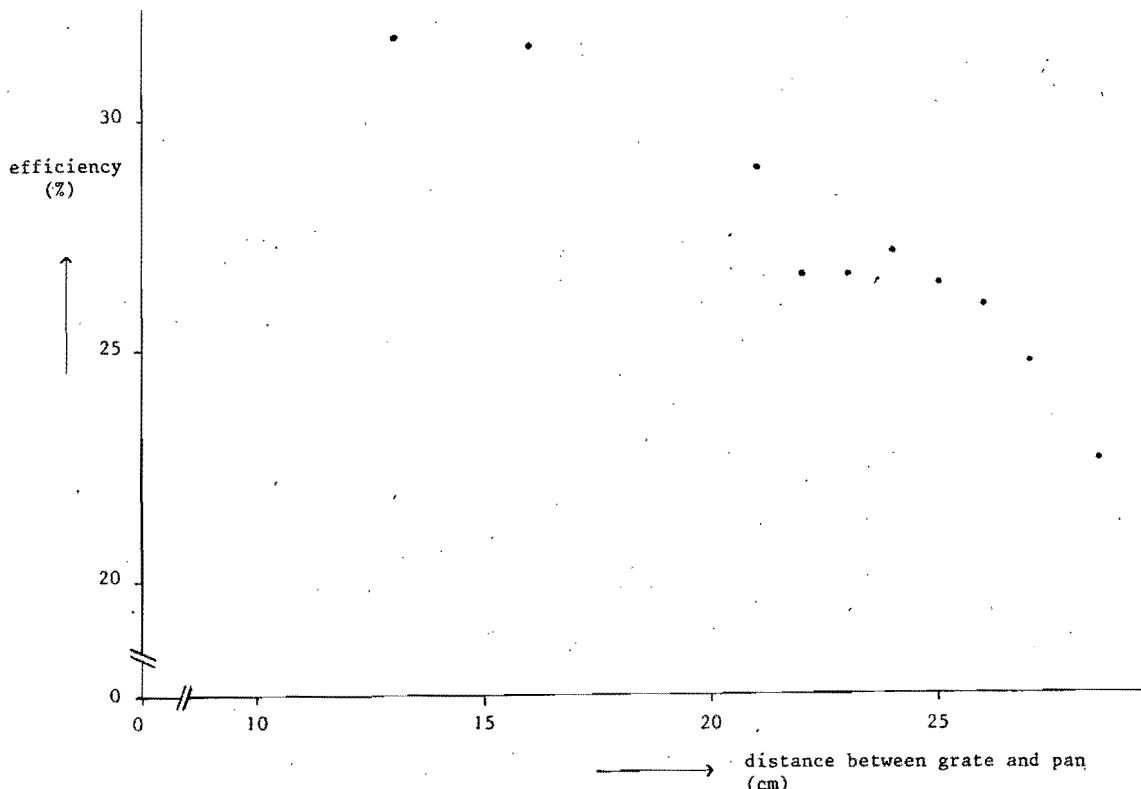


Fig. 4.3. Efficiency as a function of distance between grate and pan.

Note:

Before experiment nr.16 was started the pan was carefully cleaned. In this experiment a much higher efficiency was obtained than in the previous two experiments. However, the only difference between these tests was that the grate was brought about 1.5 cm higher. We could therefore conclude that the difference was most probably caused by the absence of the soot layer beneath the pan which works as an insulation.

From this point the pan was cleaned before each experiment. This is also the reason why only the results of tests from experiment nr. 16 onwards are included in fig. 4.3.

4.4.3 Combustion of the volatiles

In all experiments there often was a certain time (about 2 minutes) before the recharging where there were no flames anymore. At that point all the volatiles were burnt and the fire was only coaling. During the time that the flames were still there, the pan was sometimes lifted for a moment from the stove to look at the fire. No blue flames were seen, only yellow flames coming out of the secondary air holes. These yellow flames which are an indication of incomplete combustion might be a consequence of the fact that the volatiles were released too fast after the recharging. So at that point there was not enough secondary air to burn the volatiles completely. This can also be seen from the fact that these yellow flames were usually accompanied by some smoking of the stove.

If the volatiles could be released more continuously this might be an improvement for the combustion and would also result in higher efficiencies. It may therefore be worthwhile to make a system in which the release of the volatiles is controlled.

4.4.4 Temperature graphs

It was expected that the measured temperatures, especially the wall temperatures of the stove, could give some information about the performance of the stove.

However, there is not much difference between them in different tests. What can indeed be seen in these graphs are the moments where rechargings took place. One can also get an approximation of the time taken to reach a steady state.

The water temperatures and some of the wall temperatures are used to obtain some calculations. The water temperatures were used to calculate the efficiency differences between the period prior to the water boiling and the period over which the water boils. The wall temperatures were used for the radiation heat transfer calculations. Some of the temperature graphs are included in Appendix 4.2.

4.5. TWO DIFFERENT EFFICIENCIES

As stated earlier some calculations concerning the difference between the efficiency of the heating-up period and the efficiency of the boiling period have been made.

These calculations have been carried out as an experimental contribution for finding a good definition for the efficiency of wood burning cooking stoves (Krishna Prasad 1981).

Every experiment is divided into two periods. The first is the heating-up period and the second, the boiling period (see fig.4.4).

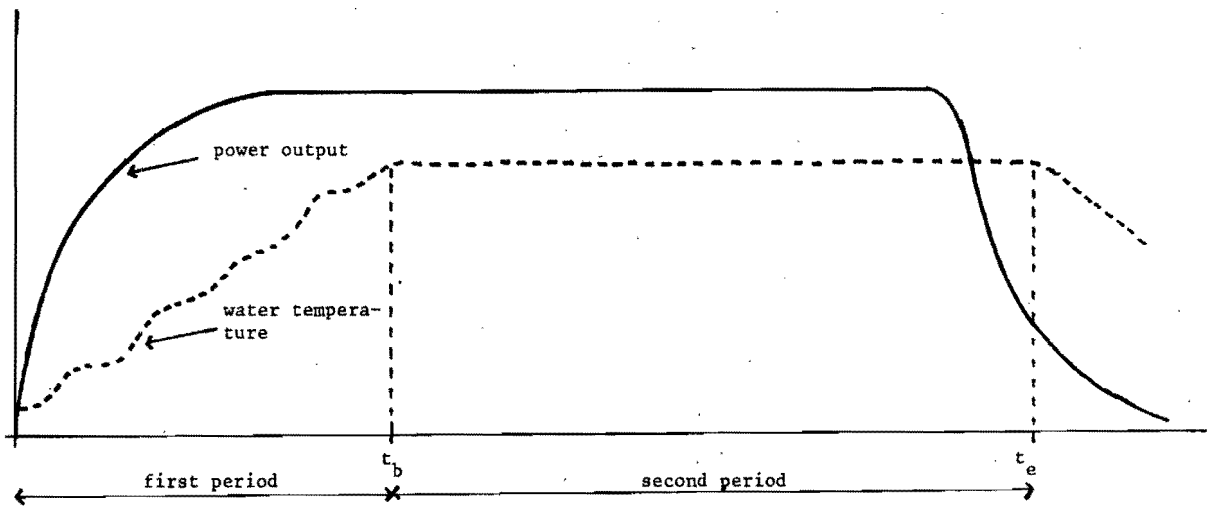


Fig. 4.4. Power output from fire and water temperature as a function of the time

To see if there is a difference between the efficiencies in the two periods, the calculated expected loss of evaporated water in the second period is compared with the real mass-loss measured.

The expected loss of evaporated water is calculated as follows:

First the net power input into the water in the first period is averaged. This mean power input is calculated using the formula

$$P_{in,1} = \frac{m_w * C_p * (T_b - T_i)}{t_b}$$

where

- $P_{in,1}$ = average power input of first period (W)
- m_w = initial amount of water in the pan (kg)
- C_p = specific heat of water at constant pressure (J/kg.K)
- T_b = temperature of boiling water ($^{\circ}$ C)
- T_i = initial temperature of the water in the pan ($^{\circ}$ C)
- t_b = time the water starts boiling (s)

It is assumed that there is no evaporation of water in this period.

Using this power input, an expected loss of evaporated water in the boiling phase can be calculated.

$$\Delta m_v = \frac{P_{in,1} * (t_e - t_b)}{R}$$

where

- Δm_v = expected loss of evaporated water during second period (kg)
- R = specific latent heat of evaporation of water at atmospheric pressure and 100° C (J/kg)
- t_e = time the water stops boiling (s)

The ratio of the expected loss of evaporated water to the real loss is equal to the efficiency ratio in the first and second phases if the mean power output in the first and second period is the same.

if

$$P_{out,1} = \frac{\int_0^{t_b} P_{out}(t) dt}{t_b}$$

and

$$P_{out,2} = \frac{\int_{t_b}^t P_{out}(t) dt}{t_e - t_b}$$

where

$$P_{out,1} = \text{mean power output in first period} \quad (W)$$

$$P_{out,2} = \text{mean power output in second period} \quad (W)$$

$$P_{out}(t) = \text{time dependent power output} \quad (W)$$

then

$$P_{in,1} = \eta_1 P_{out,1} \quad , \quad P_{in,2} = \eta_2 P_{out,2}$$

where

$$\eta_{1,2} = \text{efficiency in first or second period}$$

and

$$(\Delta m_v)_{\text{expected}} = \frac{P_{in,1} * (t_e - t_b)}{R}$$

$$(\Delta m_v)_{\text{real}} = \frac{P_{in,2} * (t_e - t_b)}{R}$$

thus

$$\frac{(\Delta m_v)_{\text{expected}}}{(\Delta m_v)_{\text{real}}} = \frac{P_{in,1}}{P_{in,2}} = \frac{\eta_1}{\eta_2} = \frac{P_{out,1}}{P_{out,2}}$$

is equal to

$$\frac{\eta_1}{\eta_2} \text{ if } P_{out,1} = P_{out,2}$$

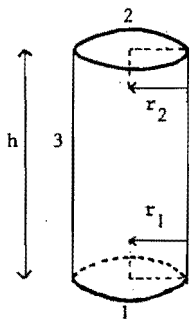
In fact this constant mean power output assumption is not justified (see fig. 4.4).

In the beginning the charcoal bed is built up and as a consequence the power will increase in time. At the end of the experiment the reverse situation occurs. But as long as the slopes of the power output curve are steep, the results are correct to the first approximation.

The results show that in general the expected mass-losses are greater than the real mass-losses of water. So the efficiencies in the heating-up periods are greater than the efficiencies in the boiling periods, if one supposes that the assumption of the same average power output in these two periods is rather good. (for detailed results see table 4.3).

4.6. RADIATION HEAT TRANSFER

In order to get an idea of the radiant heat absorbed by the pan, some calculations were made concerning radiant heat transfer. These calculations are based on a model in which the stove with the pan is represented as an enclosure of three surfaces (see fig. 4.5)



- Surfaces
- 1 - top of the fuelbed
 - 2 - part of bottom of the pan that receives radiation heat
 - 3 - wall of the stove between fuelbed and pan.

Fig. 4.5. Model of the stove

The following assumptions are made:

- the surfaces are black
- there is no direct radiation heat transfer to surroundings
- the fuelbed thickness is 4 cm, so h becomes the distance between grate and bottom of the pan minus 4 cm.
- $r_1 = r_2 = 5$ cm

With this model the following equation holds for all the surfaces [Sparrow and Cess, 1970]:

$$P_i = \sigma A_i T_i^4 - \sum_{j=1}^3 T A_j T_j^4 F_{A_j-A_i} \quad (1)$$

where:

- P_i : net rate of heat loss from surface i (W)
- T : Stefan-Boltzmann constant ($Wm^{-2}K^{-4}$)
- A_i : area of surface i (m^2)
- T_i : temperature of surface i (K)
- $F_{A_j-A_i}$: view factor which gives the fraction of radiation heat leaving surface j that arrives at surface i.

The view factors $F_{A_j-A_i}$ depend on the geometric shape of the surfaces concerned, and obey the following rules:

$$A_j F_{A_j-A_i} = A_i F_{A_i-A_j} \quad (2)$$

$$\sum_{j=1}^3 F_{A_i-A_j} = 1 \quad (3)$$

The last rule is evident, because in an enclosure the heat leaving any surface must be absorbed by the other surfaces of the enclosure. Substituting equation (2) into equation (1) one finds:

$$P_i/A_i = \sigma T_i^4 - \sum_{j=1}^3 \sigma T_j^4 F_{A_i-A_j} \quad (1a)$$

The view factor $F_{A_1-A_2}$ is given by:

$$F_{A_1-A_2} = \frac{1}{2} (Z - \sqrt{Z^2 - 4X^2Y^2})$$

where

$$X = r_2/h ; \quad Y = h/r_1 ; \quad Z = 1 - (1 - X^2)Y^2$$

Using equation (2) and (3) together with the assumption that $A_1 = A_2$, the view factors become a function of $F_{A_1-A_2}$, A_1 and A_3 only.

Because surface 1 and 2 are flat,

$$F_{A_1-A_1} = F_{A_2-A_2} = 0$$

Further:

$$F_{A_1-A_3} = 1 - F_{A_1-A_2}$$

$$F_{A_2-A_1} = F_{A_1-A_2}$$

$$F_{A_2-A_3} = 1 - F_{A_2-A_1} = 1 - F_{A_1-A_2}$$

$$F_{A_3-A_1} = A_1 F_{A_1-A_3} / A_3 = A_1/A_3 (1 - F_{A_1-A_2})$$

$$F_{A_3-A_2} = A_2 F_{A_2-A_3} / A_3 = A_1/A_3 (1 - F_{A_1-A_2})$$

$$F_{A_3-A_3} = 1 - F_{A_3-A_1} - F_{A_3-A_2} = 1 - 2 A_1/A_3 (1 - F_{A_1-A_2})$$

Thus, knowing $F_{A_1-A_2}$, all the other view factors can be calculated.

In the calculations of the different radiant heat fluxes, the following procedure is followed:

It is assumed that a third of the heat produced by the fire is radiation heat.

The temperatures of the bottom of the pan (T_2) and the wall of the stove (T_3) are assumed to be the steady-state temperatures. So $T_2 = 373$ K and T_3 is the average temperature value measured.

With equation (1a) for $i = 1$, the temperature of the fuel bed is calculated. Next the amount of radiation heat absorbed by the pan (P_r) and the stove ($P_{r,1}$) can be calculated. By multiplying the power output with the efficiency we can calculate the total heat absorbed by the water in the pan. The difference between the total heat and the radiation heat absorbed by the pan gives us a measure for the convection heat absorbed by the pan.

These calculations are done for the series of experiments in which only the height of the grate was varied. The results are shown in Table 4.4.

The radiation and convection heat absorbed by the pan as a function of the distance between the top of the fuel bed and bottom of the pan are given in fig. 4.6.

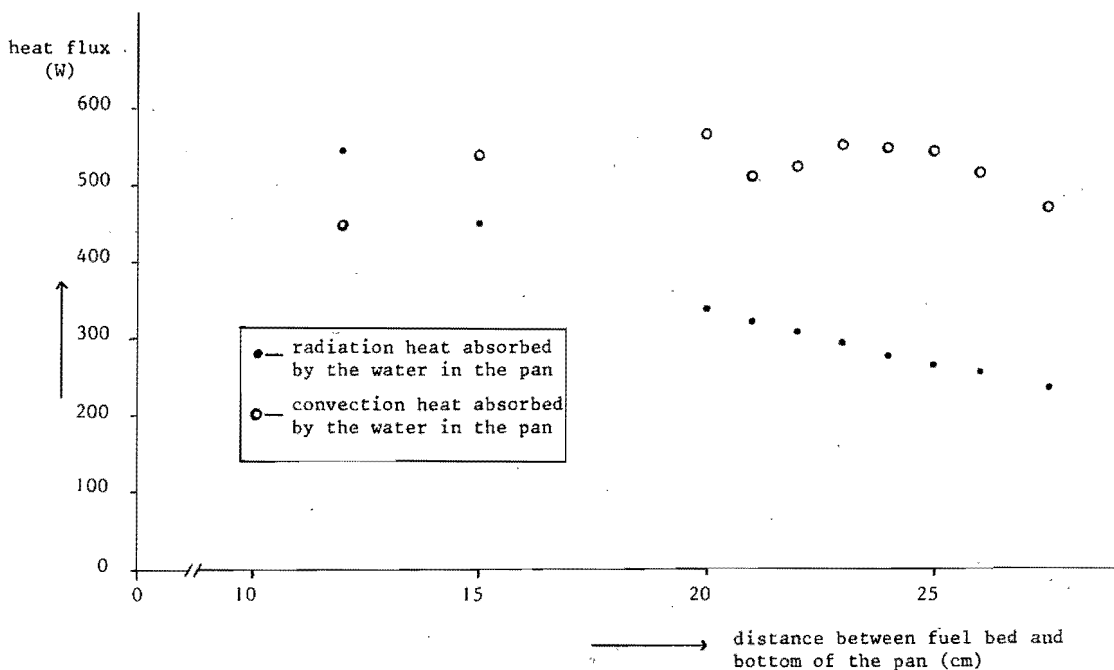


Fig. 4.6. Radiation and convection heat absorbed by the water in the pan as a function of the distance between fuel bed and bottom of the pan.

The radiation heat absorbed by the pan increases when h (distance fuel bed - bottom of pan) becomes smaller. It also appears that the convection heat is rather constant in a certain range for h (12 - 22 cm). For $h = 17$ cm the convection heat absorbed by the pan is the highest (564.6 W). The two experiments where h is even smaller (12 cm and 9 cm), especially the experiment where $h = 9$ cm, show a much smaller convection heat. But because the radiation heat absorbed by the pan in these two experiments is greater, this results in a higher efficiency in these two experiments.

At least one remark must be made regarding these calculations. For the fuel bed temperature value between 1260 K and 1270 K have been found.

These values are much too high. They should be around 1100 K, but not as high as 1260 K. The reason for this value is due to the rather high proportion of the heating value assumed to be radiated by the fuel bed. If this is reduced the relative proportion of radiative and convective heat transfer will change. However, more investigation is required to clarify this problem.

4.7. DISCUSSION AND CONCLUSIONS

It will be clear that we had to solve some problems before a reasonable performance of the stove was obtained.

Without a grate it seemed very difficult to get the stove working reasonably. The fuel bed kept rising, charges had to be small (about 30 g) and the ignition of the volatiles after a recharging was bad.

With the grate the ignition became much better and it also became possible to work with greater charges (50 g). More primary air holes decreased the rising of the fuel bed. It also appeared that the stove only worked within a small range of power outputs.

Finally, and quite tentatively I would like to offer some guidelines for the design of other stoves working with secondary air.

- The cross-sectional area of the stove must not be too small. With a greater cross-sectional area first greater charges can be used and secondly the combustion of the charcoal might go faster.
- The distance between fuel bed and secondary air holes should not be too great (less than 20 cm).

REFERENCES

Krishna Prasad, K. (1980)

Some performances tests on open fires and the family cooker. Wood burning Stove Group, Technical University of Eindhoven.

Krishna Prasad, K. (1981)

A study on the performance of two metal stoves. Woodburning Stove Group, Technical University of Eindhoven.

Sparrow, E.M. and Cess, R.D. (1970)

Radiation Heat Transfer, Wadsworth Publishing company.

Table 4.1 Efficiencies of the first series of experiments

Size of the woodblocks : 12 * 19 * 50 mm

Initial amount of water : 5 kg

Experiment number	opened sec. air holes (rows)	distance bottom pan-grate (cm)	fuel charge (g)	time interval between charges (min)	heat or power output (kW)	total amount of wood (kg)	initial temp of water (°C)	time to boil (min)	evaporated water (kg)	efficiency (%)
1	1-12	-	25	4	1.95	1	17.2	112	0.215	11.9
2	1-12	-	30	3	3.12	1.5	20	54	0.708	11.6
3	7-12	-	30	3	3.12	1.02	18	50	0.895	20.1
4	7-12	-	30	4	2.34	0.99	18	79	0.730	18.2
5	9-12	-	25	4	1.95	1	19	106	0.115	10.5
6	9-12	35	30	3	3.12	1.02	18	36	1.158	22.7
7	1-12	35	30	3	3.12	1.02	19	47	0.833	18.7
8	1-7	28	25	3	2.6	1	19.4	53	0.790	18.5
9	1-9	31.5	30	3	3.12	1.02	21	34	1.460	25.9
*10	1-9	31.5	±100	7.5	4.16	1	21	31	1.225	23.6
**11	1-9	31.5	±100	10	-	0.3	19.5	-	-	-
12	1-9	31.5	50	5	3.12	1	20	37	1.202	23.4

* Size of the woodblocks : 20 * 20 * 67 mm

** Size of the woodblocks : 30 * 30 * 100 mm
after 3 charges raise the fuel above the stove

Table 4.2 Efficiencies of the second series of experiments

size of the woodblocks : 12 * 19 * 50 mm
 initial amount of water : 5 kg
 opened secondary air holes : row 1-9
 fuel charge : 50 g
 time interval between charges : 5 min.
 heat or power output : 3.12 kW
 total amount of wood : 1 kg

experiment number	distance bottom pan-grate (cm)	initial temp. of water (°C)	time to boil (min)	evaporated water (kg)	efficiency (%)
* 13	31.5	20	41	0.893	19.7
14	31.5	20	49	0.670	17.0
15	30	20.5	53	0.552	15.5
** 16	28.5	20	36	1.130	22.6
17	27	26.5	31	1.367	24.7
18	26	20	31	1.410	25.9
19	25	21.5	31	1.463	26.4
20	24	20.5	29	1.515	27.1
21	23	22.5	29	1.490	26.6
22	22	21	32	1.475	26.6
23	21	19	29	1.648	28.9
24	16	20	27	1.876	31.6
25	13	21	29	1.900	31.8

* fuel charge : 30 g
 time interval between charges : 3 min.

** from this experiment the pan was cleaned before each experiment.

Table 4.3 Difference between the efficiency in the heating-up period and the efficiency in the boiling period.

experiment number	time to boil (min)	water stops boiling (min)	$(\Delta m_v)_r$ (kg)	$(\Delta m_v)_e$ (kg)	η_1/η_2	experiment number	time to boil (min)	water stops boiling (min)	$(\Delta m_v)_r$ (kg)	$(\Delta m_v)_e$ (kg)	η_1/η_2
1	112	165	0.215	0.364	1.69	13	41	115	0.893	1.340	1.50
2	54	164	0.708	1.513	2.14	14	49	109	0.670	0.909	1.36
3	50	125	0.895	1.142	1.28	15	53	107	0.552	0.752	1.36
4	79	143	0.730	0.617	0.85	16	36	112	1.130	1.567	1.39
5	106	164	0.115	0.411	3.57	17	31	110	1.367	1.739	1.27
6	36	111	1.158	1.586	1.37	18	31	107	1.410	1.821	1.29
7	47	114	0.833	1.672	1.29	19	31	-	1.463	-	-
8	53	128	0.790	1.059	1.34	20	29	116	1.515	2.214	1.46
9	34	110	1.460	1.639	1.12	21	29	112	1.490	2.059	1.38
10	31	91	1.225	1.419	1.16	22	32	114	1.975	1.879	1.27
11	-	-	-	-	-	23	29	115	1.648	2.230	1.35
12	37	105	1.202	1.365	1.14	24	27	111	1.876	2.310	1.23
						25	29	112	1.900	2.099	1.10

Table 4.4 Radiation heat transfer

experiment number		(bottom of pan) (K)	(wall of stove) (K)	(fuel-bed) (K)	(efficiency) (%)	(radiation heat abs. by pan) (W)	(convection heat abs. by pan) (W)	(lost radiation heat to the walls of stove) (W)
16	0.127	373	713	1265	22.6	236.6	468.5	803.4
17	0.140	373	723	1267	24.7	256.6	514.0	783.4
18	0.149	373	723	1266	25.9	265.3	542.8	774.4
19	0.160	373	723	1266	26.4	276.5	547.2	763.5
20	0.172	373	733	1267	27.1	295.1	550.4	744.9
21	0.184	373	733	1267	26.6	307.3	522.6	732.7
22	0.198	373	733	1266	26.6	320.9	509.0	719.1
23	0.214	373	733	1266	28.9	337.1	564.6	702.9
24	0.321	373	743	1274	31.6	448.3	537.6	591.7
25	0.418	373	753	1261	31.8	545.2	447.0	494.8

APPENDIX 4.1.

Calculations concerning primary and secondary air holes.

Required power output = 3 kW

Flow of wood consumed : $\phi_w = \frac{P}{B}$ (kg/s)

where B = combustion value of the wood

We assume a combustion value $B = 18.73 * 10^6$ J/kg

which gives a wood consumption of:

$$\phi_w = \frac{3 * 10^3}{18.73 * 10^6} \text{ kg/s} = 160 * 10^{-6} \text{ kg/s}$$

Primary air holes

Part of the wood burning as charcoal?

Assuming 20 % of the mass of wood burns as charcoal
means a charcoal consumption

$$\phi_c = 0.20 * \phi_w = 0.20 * 160 * 10^{-6} \text{ kg/s} = 32 * 10^{-6} \text{ kg/s}$$

For complete combustion ($C + O_2 \rightarrow CO_2$) this needs a supply
of oxygen

$$\phi_o = \frac{32}{12} * \phi_c = 85.3 * 10^{-6} \text{ kg/s}$$

which means a volume flow (at 50°C)

$$\phi_{v,o} = \frac{\phi_o}{32} * \frac{273 + 50}{273} * 22.4 \text{ m}^3/\text{s} = 70.67 * 10^{-6} \text{ m}^3/\text{s}$$

The required air flow then becomes (21 % O₂ in air)

$$\phi_{v,A} = \frac{100}{21} * \phi_{v,o} = 336.5 * 10^{-6} \text{ m}^3/\text{s} = 337 \text{ ml/s}$$

Now we assume that the air is drawn into the stove by the column
of hot air in the wood space and above it.

Assume total height h of column 250 mm.

Mean temperature we take to be 250°C.

By means of the law of Bernoulli $\Delta p = \frac{1}{2} \rho v^2$, we can calculate the
velocity of the air drawing into the stove.

If we assume that the draught is used entirely to draw air of 50°C through the holes we get:

$$\Delta P = gh (\rho_{50} - \rho_{250})$$

Density of air at a temperature T

$$\rho_T = \frac{273}{273 + T} * \rho_0$$

so:

$$v = \sqrt{\frac{2\Delta P}{\rho_{50}}} = \sqrt{\frac{2 * g * 0.25 * (\rho_{50} - \rho_{250})}{\rho_{50}}} =$$

$$\sqrt{2 * 0.25 * 9.81 * \left(1 - \frac{\rho_{250}}{\rho_{50}}\right)} = \sqrt{2 * 0.25 * 9.81 * \frac{200}{273 + 250}} =$$

$$1.37 \text{ m/s}$$

So at a velocity of 1.37 m/s the total cross area of the holes A must be such that the required flow of air will pass through.

$$v * A = \phi_{vA} \rightarrow A * \phi_{vA/v} = 337/1.37 * 10^{-6} \text{ m}^2 = 246.6 * 10^{-6} \text{ m}^2$$

$$40 \% \text{ excess air} \rightarrow A = 344 * 10^{-6} \text{ m}^2$$

Secondary holes

Assuming that 20 % of the mass of wood burns as charcoal then 80 % burns as volatiles on secondary air.

The composition of the used fir wood is according to Brame and King by weight:

carbon : 50.4 %

hydrogen : 5.9 %

oxygen : 43.4 %

ashes : 0.3 %

So far the volatiles we have left per 100 g of wood

carbon : 50.4 - 20 = 30.4 g

hydrogen : 5.9 g

oxygen : 43.4 g

ashes : 0.3 g

which gives in mol (we neglect the ash)

$$\text{carbon} : 30.4/12 = 2.5333 \text{ mol C}$$

$$\text{hydrogen} : 5.9/2 = 2.95 \text{ mol H}_2$$

$$\text{oxygen} : 43.4/32 = 1.3563 \text{ mol O}_2$$

The hydrogen is assumed to combine with the oxygen according to $2\text{H}_2 + \text{O}_2 \rightarrow 2\text{H}_2\text{O}$ so that all oxygen disappears, having some hydrogen left.

$$2.95 - 2 * 1.3563 = 0.2375 \text{ mol H}_2$$

which will need $0.2375/2$ mol O_2

The carbon needs 1 mol O_2 /mol C to form CO_2 , so that the oxygen demand in the secondary air or 100 g wood is:

$$2.53 + 0.1188 = 2.6521 \text{ mol O}_2$$

which gives:

$$2.6521 * \frac{T + 273}{273} * 22.4 * 10^{-3} \text{ m}^3 \text{ O}_2$$

so:

$$\frac{100}{21} * 2.6521 * \frac{T + 273}{273} * 22.4 * 10^{-3} \text{ m}^3 \text{ air/100 g wood is needed.}$$

Thus the secondary air flow becomes:

$$\phi_{vA_5} = \phi_w * 10 * \frac{100}{21} * 2.6521 * \frac{T + 273}{273} * 22.4 * 10^{-3} \text{ m}^3/\text{s}$$

Assuming the temperature of the incoming air to be 200°C (is preheated in the space between inner and outer tube) we get:

$$\phi_{vA_5} = 160 * 10^{-6} * 10 * \frac{100}{21} * 2.6521 * \frac{200 + 273}{273} * 22.4 * 10^{-3} \text{ m}^3/\text{s}$$

$$\phi_{vA_5} = 784.22 * 10^{-6} \text{ m}^3/\text{s} \approx 784 \text{ ml/s}$$

Minimum height of entrance of the secondary air $h_s = 0.34$ m.

Draught at that height in an environment at 22°C is:

$$\Delta p = gh_s (\rho_{22} - \rho_{200})$$

so that:

$$v_s = \sqrt{\frac{2\Delta p}{\rho_{200}}} = \sqrt{2 * g * h_s * \frac{(\rho_{22} - \rho_{200})}{\rho_{200}}}$$

or:

$$v_s = \sqrt{2 * g * 9.81 * 0.34 * \frac{273 + 200 - 273 - 22}{273 + 22}} = 2.0063 \text{ m/s}$$

$$v_s = 2 \text{ m/s}$$

area needed:

$$\phi_{vA_s}/v_s = \frac{612 * 10^{-6}}{2} \text{ m}^2 = 306 * 10^{-6} \text{ m}^2$$

$$40 \% \text{ excess air} \rightarrow A_s = 549.0 * 10^{-6} \text{ m}^2$$

APPENDIX 4.2. Temperature graphs of some experiments

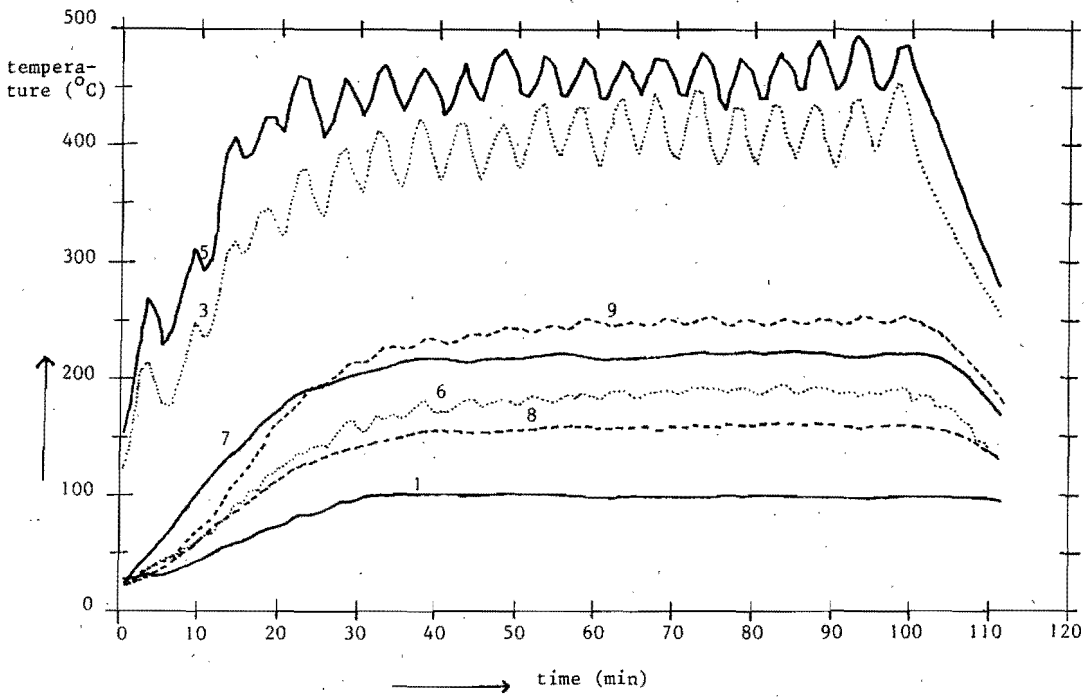


Fig. A.4.1. Temperature graph of experiment number 18

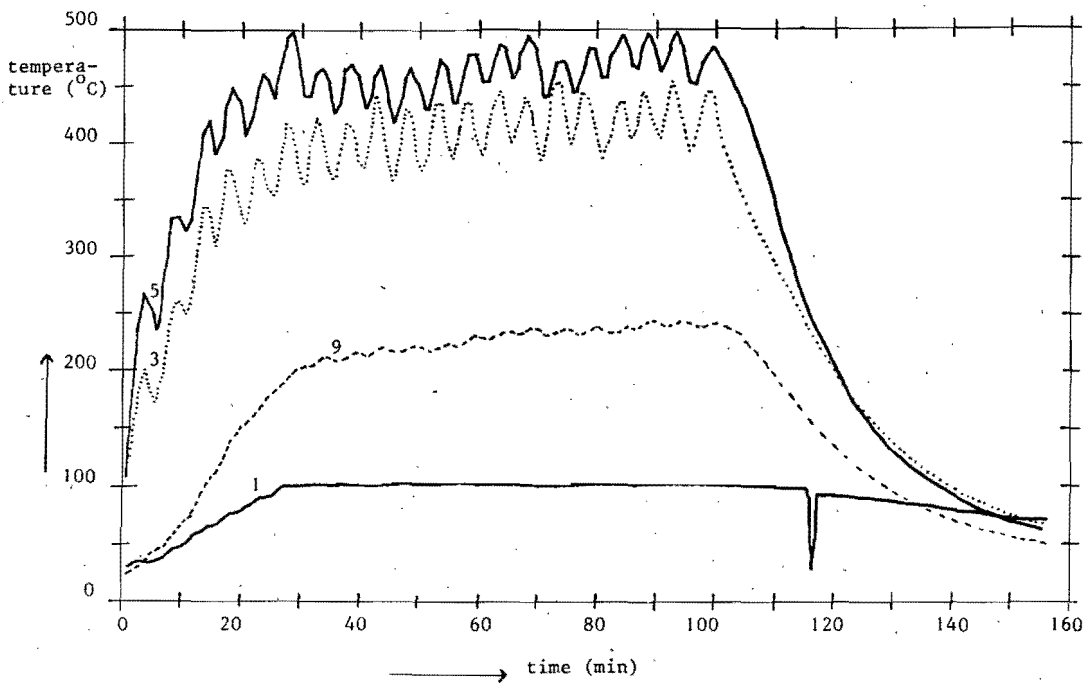


Fig. A.4.2. Temperature graph of experiment number 21

The number in the temperature graphs correspond with the measuring points of the temperatures (see fig. 4.2.)

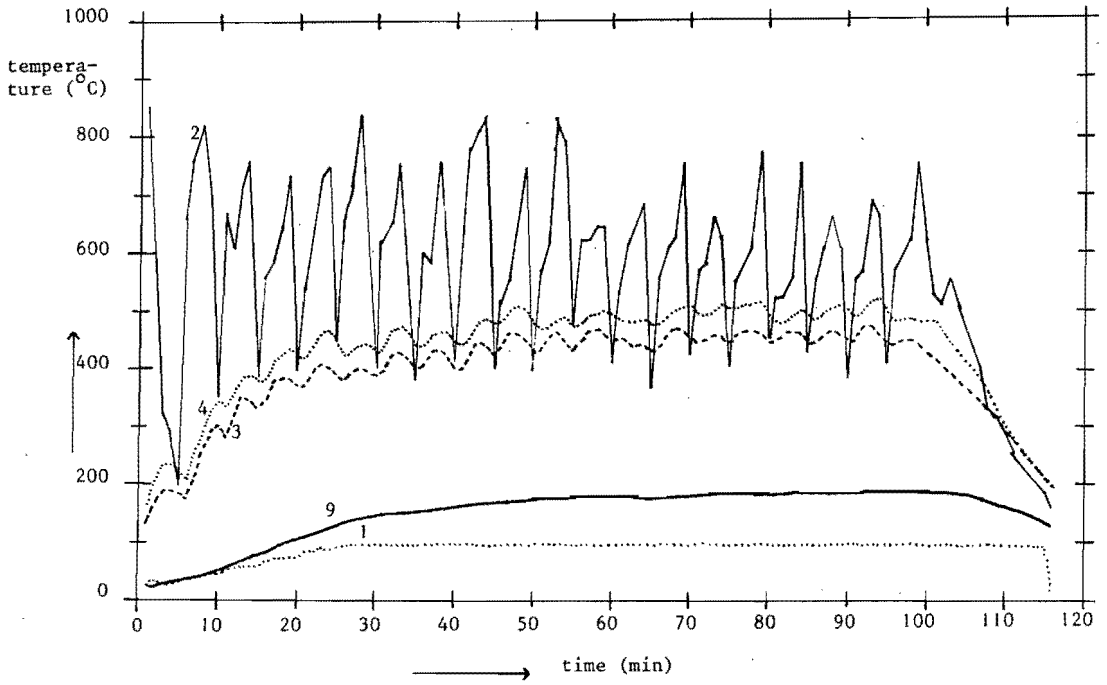


Fig. A.4.3. Temperature graph of experiment number 24

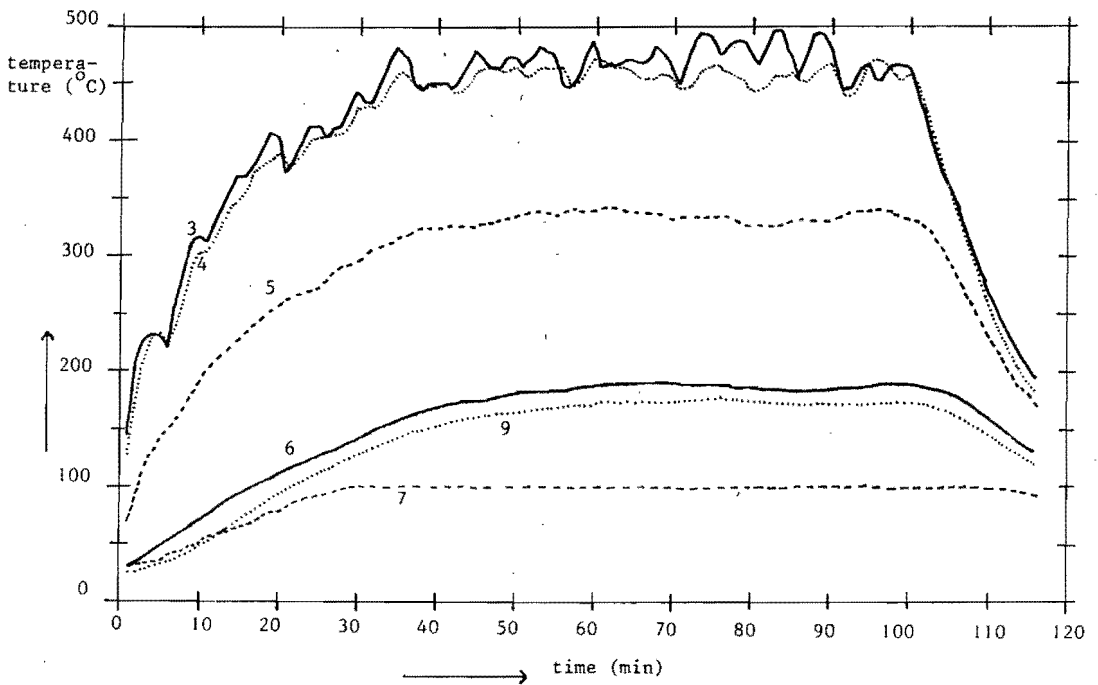


Fig. A.4.4. Temperature graph of experiment number 25

The numbers in the temperature graphs correspond with the measuring points of the temperatures (see fig. 4.2)

5. FUEL BED BEHAVIOUR

by

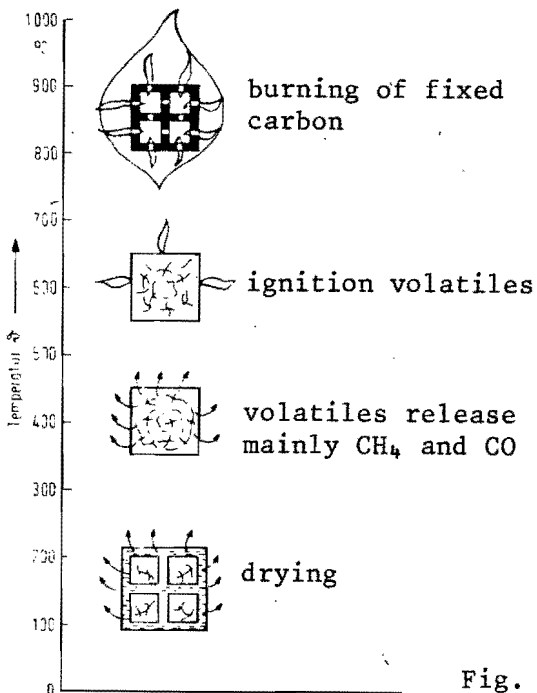
P. Bussmann and P. Visser

Eindhoven University of Technology,

Eindhoven, The Netherlands.

5.1. INTRODUCTION

The combustion process of wood is divided into two parts; the combustion of volatiles above the fuel bed and the combustion of fixed carbon (= charcoal) in the fuel bed. The behaviour of the fuel bed is important in that it controls the total power output from a fire as has been observed in earlier experiments. In chapter two it is shown that the distance between fuel bed and pan bottom has to obey the $P^{\frac{2}{5}}$ rule to make optimal use of the convection heat. This gave information about the combustion space that should be available for burning the volatiles. Nothing however is said about the way the volatiles are released in the fuel bed when fresh wood is added to the fire and nothing is said about the way charcoal burns in the fuel bed. For the construction of the combustion chamber in woodstoves this information is needed. One can ask three important questions in this respect.



The first question is: what is happening in the fuel bed?

Wagner [Wagner, 1978] studied the processes involved in burning of wood. He distinguished four successive periods, in which the temperature of each following period is higher (see fig. 5.1). Wagner stated that the volatiles and charcoal do not burn simultaneously because: "bei der intensive Gasentwicklung können die Sauerstoffmoleküle durch die expandierenden und brennenden Gase nicht in das Kohleteil gelangen."

Fig. 5.1.

Erst wenn die Gasentwicklung weitgehend abgeschlossen ist, kommt es zum Abbrand des verbleibenden Koksgerustes unter CO₂-entwicklung".*

This result means that no charcoal is burnt as long as there are flames above the fuelbed. This however is in contradiction with observations on fuel beds which show that, when the fire is fed several times with fresh wood, the fuel bed stops building up and volatiles as well as charcoal burn. Even in a single piece of wood one needs to take into account the anisotropic structure of wood, which sees to it that the release of gases is not homogeneous over the surface of the wood and thus it becomes well possible that charcoal and volatiles burn both at the same time, but at different places.

The second question one can ask is: what is the difference in the rate of combustion between small and large, wet and dry, soft and hard wood?

Some of these problems have been tackled earlier [Visser, 1980; Sielcken, 1930; Nievergeld, 1981; Delsing (this report); Visser (this report)] but need further investigation because of contradictory results. Experiments of Visser on open fires and Nievergeld on the Vandaele-De Lepeleire stove for instance showed only weak dependence of the efficiency numbers on the size of the wood blocks used, while the efficiency numbers of Sielcken on the Family Cooker and experiments of Delsing on a tubular combustion chamber showed a strong dependence.

The third and last important question one can come up with is: what is the influence of using a grate?

Efficiency measurements on open fires [Visser, 1980] showed an efficiency increase of 3 percentage points when a grate was used. It was supposed that a better airtion of the fuel bed through the grate might be the cause of this increase, but a good explanation of this phenomenon however was not given.

*) The oxygen can not reach the charcoal part when the volatiles production is high. This is caused by the expansion of burning gases. Only after the volatiles production has nearly stopped, the charcoal will be converted into CO₂.

5.2. RECORDING OF THE FUEL BED WEIGHT LOSS

The behaviour of the fuel bed is studied by recording the fuel bed weight loss as a function of time. For this the fire was placed on a balance and the change of weight of the fire was measured with a load cell. A characteristic picture of the experimental results is shown in fig. 5.2.

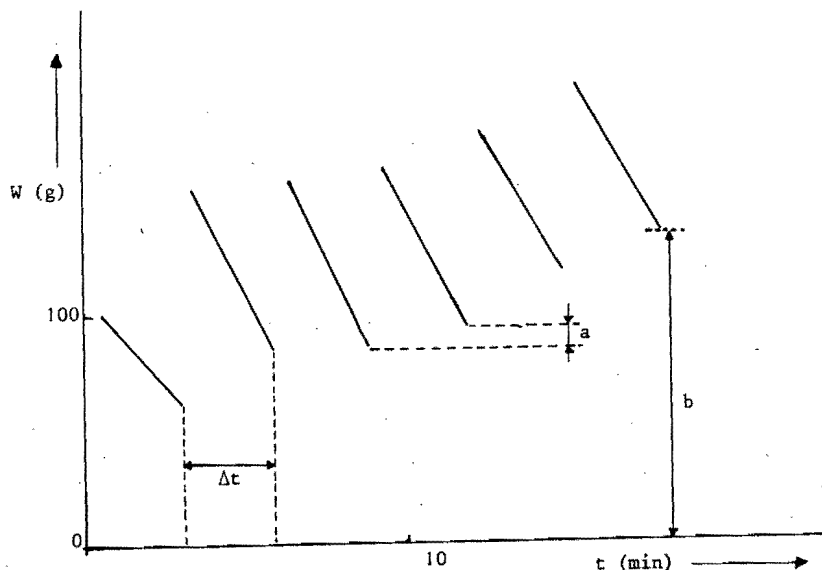


Fig. 5.2. Weight loss of the fuel bed as a function of time for an open fire without a grate $P = 10$ kW.

At $t = 0$ a charge of 100 g. of wood is fed to the fire and burns away with time until at $t = \Delta t$ a new charge of 100 g. is added, and so on. From a graph like this we can derive a number of important characteristics of the fire, which we shall discuss briefly.

5.2.1 Building up of fuel bed

At a time $3\Delta t$ a new charge is added to the fire. This charge burns away, but is not completely burnt at time $4\Delta t$, when the next charge is added. The part of the charge that is not yet burnt at that time has a weight of 'a' grams. It is assumed that this unburned part is mainly charcoal. This need not be necessarily true. Depending on the conditions it might still contain some volatiles, but we will assume this volatile part to be nearly zero. So, accumulating, the weight of the fuel bed after 6 charges, at $t = 6\Delta t$, is 'b' grams.

5.2.2 Amount of charcoal and volatiles burnt

If we assume the fuel wood to burn as 20 % charcoal and 80 % volatiles by weight [Brame and King, 1967] then after 6 charges of 100 g we have added 120 g charcoal and 480 g volatiles. With the assumption that the left overs of a charge are charcoal, we then know that 480 g volatiles and $120 - b$ g charcoal is burnt.

5.2.3 Time dependent power of the fire

If we assume the rate of burning of the charcoal during the experiment time (t_e) to be constant and equal to $\frac{120 - b}{t_e}$, then the slope of the weight loss curve $(\frac{\Delta W}{\Delta t})$ gives the momental evolution of the volatiles $(\frac{\Delta W_v}{\Delta t})$

$$\frac{\Delta W}{\Delta t} = \frac{\Delta W_v}{\Delta t} + \frac{120 - b}{t_e}$$

Because the heat of combustion of wood (18.7 MJ/kg), the heat of combustion of charcoal (33.0 MJ/kg) and thus the heat of combustion of volatiles $((18.7 - 0.2 * 33.0)/0.8) = 15.2$ MJ/kg) are known, the power output of the fire at any time is given by:

$$P(t) = \frac{120 - b}{t_e} * 33.0 + \frac{W_v}{t} * 15.2 \quad \text{kW}$$

In addition to the monitoring of the fuel bed weight, we could also constantly monitor the weight loss of water from the pan. With this we could calculate the power absorbed by the pan and the time dependent efficiency of the system. With these experiments this idea was not yet put into practice.

5.3. EXPERIMENTAL RESULTS AND DISCUSSION

The weight loss experiments were done for:

1. the 10 kW open fire (ϕ 26 cm) without a grate using wood blocks of 15 * 15 * 50 mm;
2. the 10 kW open fire (ϕ 26 cm) with a grate using wood blocks of 15 * 15 * 50 mm;
3. the 10 kW open fire (ϕ 26 cm) with a grate using wood blocks of 30 * 30 * 100 mm;
4. the 5 kW open fire (ϕ 19 cm) without a grate using woodblocks of 15 * 15 * 50 mm.

In experiments 1 and 2 the power output of 10 kW was obtained by charging the fire every 180 seconds with 100 g of oven dry wood. In experiment 3 by charging the fire every 225 seconds with 126 g. In experiment 4, the charges were 100 g every 375 seconds.

It appeared that the weight loss rate of the fuel bed was constant during the time interval Δt between two charges. This however is only correct if the fuel wood catches fire immediately after recharging, happening only when there are still flames, which means that not all the volatiles of the previous charge are burnt. As a consequence the time dependent power output of the fire is constant during the time interval Δt . If this is not true then the weight loss rate of the fire will be smaller just before and just after recharging. The straight lines in figure 5.2 then become S-shaped curves, as can be seen in fig. 5.3 for a 5 kW open fire (ϕ 19 cm) without a grate.

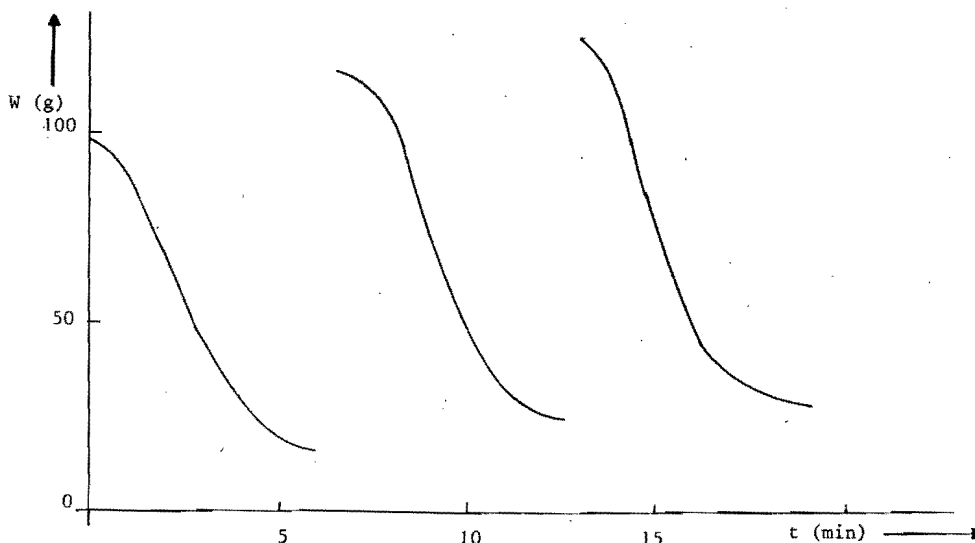


Fig. 5.3. S-shaped weight loss curves for an open fire (ϕ 19 cm) without a grate.

The weight of the fuel bed just before recharging is shown in figure 5.4. The figure shows the striking difference between the experiments with (experiment no. 2 and 3) and without (experiment no. 1) a grate. The 10 kW fire reaches a steady state period only when a grate is used. Without a grate the fuel bed keeps on building up, and the fuel bed diameter finally becomes too small to hold the charcoal. After 10 charges of 100 g there is 165 g charcoal stored in the fuel bed without a grate. Making use of the volatiles-charcoal ratio of 4 this means that only 17 % of the supplied charcoal is burnt when a new charge is added to the fire. The lack of oxygen in the fuel bed is obvious; this problem is solved when a grate is used.

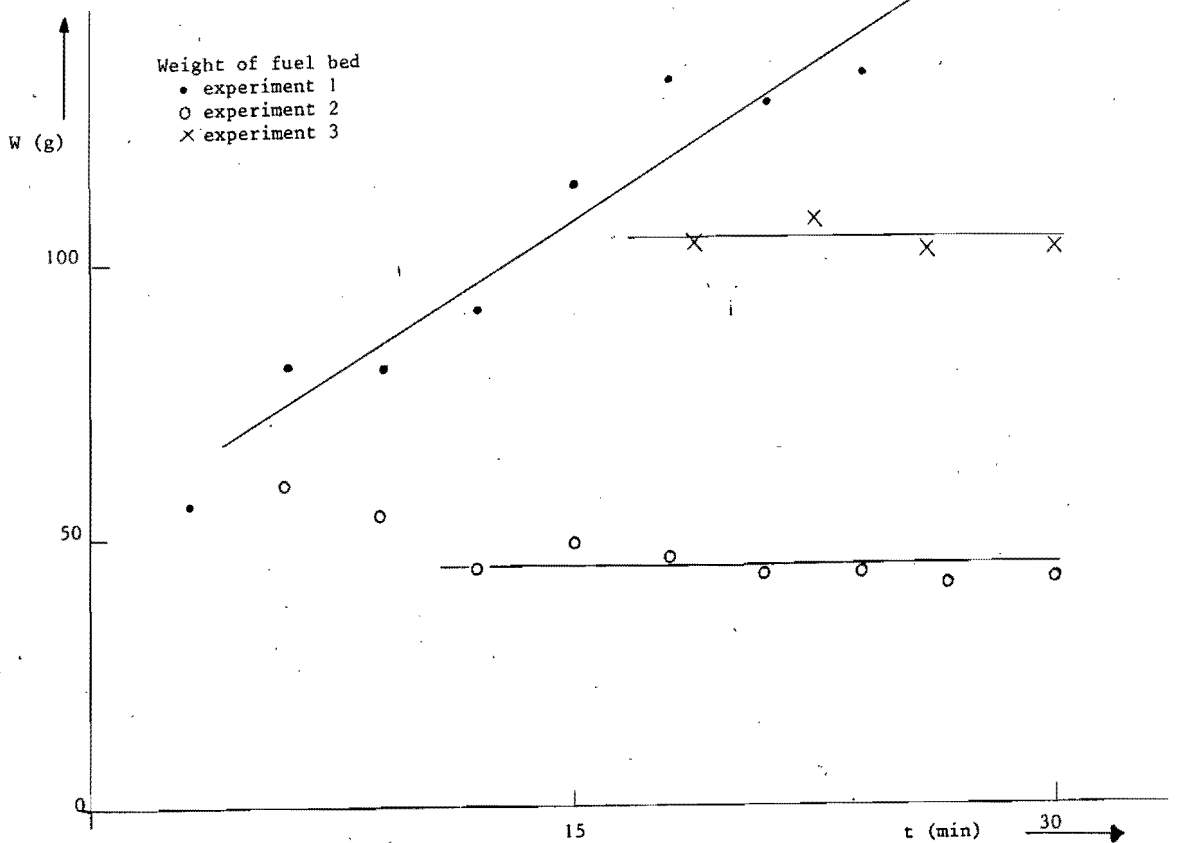


Fig. 5.4. Weight of the fuel bed before recharging.

The figure 5.4 shows that a steady state period is reached when a grate is used. The actual time at which steady state is attained is dependent on the history of fire at starting, the wood block sizes, and may be other factors. At any rate for both the experiments reported here this period is 10 minutes for the small blocks and 15 minutes for the larger blocks. The behaviour of the fuel bed in both the experiments becomes the same after this period. If the steady state period is much longer relative to the building up period then the efficiency will show only weak dependence on the size of the wood used. This explains the experimental results of Visser and Nievergeld [Visser, 1980; Nievergeld, 1981].

A striking difference between experiment 2 and 3 is the amount of charcoal stored in the fuel bed. With the bigger blocks of wood more than 2 times as much charcoal lies on the grate. A reason for this might be the following.

The surface area to volume ratio for the small blocks is twice that of the big blocks. So, for the same volume of wood, the surface area for the reactions to take place is for small blocks twice as much as for the big blocks. If we assume the same surface ratios to exist for the remaining charcoal pieces of the wood blocks, then this explains that there is twice as much charcoal on the grate for the big blocks as for the small blocks to give the same power output. Reducing the power output will reduce the amount of charcoal stored. It is obvious then that the power output reduction can be much larger when the bigger wood blocks are used, for the same charge weight. So using big wood blocks gives the possibility to drive the fire at low power outputs.

The weight loss experiments lasted 30 minutes. At that time the fire required a new charge of wood to keep it burning at a power of 10 kW. This however was not done; the experiment was brought to an end.

Table 5.1 shows that in the successive experiments, after 30 minutes, 29 %, 8 % and 18 % of the total heat input is stored. Here it is assumed that the remaining fuel is charcoal. As stated before this assumption is not completely true, because the fire keeps on burning after $t = 30$ minutes. Especially when big wood blocks are used there is a considerable amount of volatiles stored in the fuel bed, which can be seen in table 5.1 from the time periods after $t = 30$ minutes when there are still visible flames.

Table 5.1.

	m_s (g)	Q_s (%)	t_f (s)	m_1 (g)	Q_1 (%)
Experiment no. 1 (without grate)	165	29	120	117	20
Experiment no. 2 (with grate, small wood)	45	8	30	34	6
Experiment no. 3 (with grate, big wood)	105	18	240	40	7

m_s : charcoal stored in 30 min (g)

Q_s : heat stored in 30 min (%)

t_f : burning time with flames after 30 min (s)

m_1 : charcoal left unburnt (g)

Q_1 : heat not released (%)

After the flames disappear, only charcoal is left over. The power output from the charcoal bed in all experiments is about 3 kW. This differs by more than a factor 3 from the initial power output of the fire. In many cases this will be too low a power to accomplish the cooking task, so this charcoal is not completely used. For the open fire without a grate this means that 20 % of the total heat input might be wasted, while the open fire with a grate does not use 6-7 %! This is the reason for the 3 % efficiency difference in laboratory tests found by Visser [Visser, 1980]. It is believed that the difference will be much greater in practice!

REFERENCES

Brame, J.S.S. and King, J.G., (1967)

"Fuel", Arnold, London

Wagner, W., (1978)

"Berechnung van Holzfeuerungen für
Wärmeträgeranlagen" in "Wärme", 85, 4-5.

Nievergeld, P. et al, (1981)

"The De Leppeleire/ Vandaele Woodstove", in
"A study on the performance of two metal stoves",
Krishna Prasad, K., (ed), Eindhoven University of
Technology, Eindhoven and TNO, Division of Technology
for Society, Apeldoorn.

Sielcken, M.O. and Nieuwvelt, C.J., (1980)

"The family cooker", in "Some performance tests
on open fires and the family cooker", Krishna Prasad,
K., (ed), Eindhoven University of Technology, Eindhoven.

Visser, P. and Verhaart, P., (1980)

"Open fires", in "Some performance tests on open
fires and the family cooker", Krishna Prasad, K., (ed),
Eindhoven University of Technology, Eindhoven

6. THE PERFORMANCE OF THE NOUNA WOODSTOVE

by

J. Claus, W. Sulilatu, M. Verwoerd and J. Meyvis

TNO-Division of Technology for Society

Laan v. Westenenk 501, 7334 DT Apeldoorn

The Netherlands

SUMMARY

This report describes the measurements to determine the performance of the so called Nouna wood stove.

After description of the stove and the experimental details special attention is given to the efficiency and combustion performance of the stove. The influence of heat load, combustion air damper position, chimney draft and a baffle are discussed. A comparison with the performance of the De Lepeleire/Van Daele stove is made. It turns out to be possible to draw up a heat balance of the stove with a percentage unaccounted for varying between 10 and 20%.

Computer calculations of the wall temperatures show good agreement with measured values.

The efficiency of the Nouna stove lies between 15 and 23%. Higher heat load, lower chimney draft and smaller damper opening have a positive effect on the efficiency. However, the combustion performance then becomes poorer, leading to higher CO- and C_xH_y -concentrations. Further research is recommended to investigate the effect of a baffle and to optimise the stove construction and adapt it to the users behaviour.

6.1 Introduction

In the framework of the research project to improve the efficiency of wood stoves for the Sahel countries an experiment was carried out with a so-called "heavy" stove.

This stove "the Nouna wood stove" is one of the types of stoves already used in rural areas of the third world.

In contrast with the metal, De Lepeleire/Van Daele wood stove, which was investigated earlier in the programme the Nouna stove is made of bricks, sand and concrete.

The design and construction materials for the Nouna wood stove were reported by one of the many developing workers in the Sahel countries: Mrs. Rosemary Kempers.

The stove was made in the workshop of TNO's Division of Technology for Society at Apeldoorn.

In this report a full description will be given of the experiments that were carried out on the Nouna wood stove. After a description of the design and the experimental set-up the performance of the stove will be discussed.

Special attention will be given to the efficiency and the combustion performance. A comparison is made between the performance of the De Lepeleire/Van Daele-stove and the Nouna-stove.

6.2 Design of the stove

The design of the Nouna wood stove is shown in fig. 6.1 and 6.2.

It has a rectangular shape and consists of a combustion chamber, a flue gas channel, a second heating chamber and a chimney.

The combustion chamber has a cylindrical shape and is not provided with a grate. The volume of the combustion chamber is $0,0075 \text{ m}^3$.

The bottom and top plate of the stove are made of concrete, the walls are made of ordinary brick. The space between the in- and outside walls is filled up with sand.

The overall dimensions are:

length : 1.10 m

width : 0.60 m

height : 0.30 m.

The Nouna wood stove is provided with two pan holes with a diameter of respectively 0.25 m and 0.20 m. The first pan is situated directly above the combustion chamber and the second pan above the heating chamber. On their way to the chimney, which in most experiments has a length of 1.0 m and a diameter of 0.1 m, the flue gases will heat the second pan. During the experiments the distance between the bottom side of the pans and the bottom plate was 0,15 m for both pans.

To prevent air leaking a "fiber frax" cord is placed between the pan sides and pan holes. The fuel supply hole can be closed with a steel sheet. In this sheet a manually operated combustion damper is placed with a length of 0.14 m and a height of 0.06 m. It can arbitrarily be varied between fully open and fully closed.

6.3 Experimental details

The performance of the Nouna wood stove was determined for a number of variables which will be specified later by the boiling water tests [1]. For these experiments, two cylindrical aluminium cooking pans with a height of 0.145 m and 0.115 m were used. The diameter of the pans were

0.25 m and 0.2 m respectively, with a wall thickness of 0.002 m. For all the experiments the pans were filled with tap water and covered with a lid. The experiments were carried out in a laboratory, unaffected by wind or draft effects. The wood stove was placed on a low table. The space between the bottom of the wood stove and the table was filled up with glass wool. The experimental set-up of the measurements was similar to that of the De Lepeleire/Van Daele wood stove and is given in [1]. The experimental set-up is shown in figure 4.

The fuel used in the majority of the experiments was unchaved oven-dry white fir, the wood chips having sizes of 0.02 x 0.03 x 0.2 m. The density of this wood was 350 kg/m³. For all experiments the fuel was loaded through the fuel-supply entrance by lifting the steel sheet. The wood fuel was ignited with a Bunsen-burner. Because the chimney draft developed very fast, no starting problems were encountered. In order to determine whether the combustion rate of the wood was regular the decrease in the weight of the wood charge in the stove was followed by means of a load cell. Table 6.1 gives an example of the data collected with this experiment.

From this table it is clear that apart from the first wood charge that is burning in the relatively cold stove, the variations in the combustion rate of the different charges are small. The maximum deviation over the 2nd-9th charge for white fir is $\pm 12\%$, and for Merbau $\pm 21\%$. When the practical difficulties are taken into account in charging the stove in a reproducible manner, this result can be considered to be quite satisfactory. The beginning of the experiment was taken to be the moment at which the wood first caught fire. The end of the experiment was considered to be the moment at which the CO₂ content dropped below a value of about 1%. This moment corresponded with the moment at which the temperature in the first pan started to drop.

The duration of the experiments varied between 2 and 48 hours depending on the type of experiment. Compared with the trials with the De Lepeleire/Van Daele stove three new measurements were added to the experiments.

- For a few test runs the soot concentration in the flue gases was measured with the so-called "dust unit", which is normally used by TNO for measuring furnaces. The principle of this technique is that flue gases are sucked isokinetically out of the chimney (and next) through a filter, the dust load of which is subsequently determined by weighing.

- The unburnt hydrocarbons were measured with a Hydrocarbon analyser model 400 working on the ionisation principle.
- The evaporation rate of the water and the combustion rate of the wood were measured by means of a load cell.

The following factors influencing the performance of the stove were investigated:

- the heat output of the fire
- the combustion air damper position
- the effect of the chimney draft
- the effect of a baffle.

Only for a first impression some exploratory trials were made to investigate the following subjects:

- the effect of tangential air supply
- the effect of wood properties.

6.4 Efficiency of the stove

The efficiency for the Nouna wood stove is calculated using the formula as described in [1]. For all the experiments the initial amount of water for pan one was 4 kg and for pan two 2 kg.

6.4.1 The effect of the heat output of the fire

To investigate the influence of the heat output of the fire on the wood stove a number of experiments were performed in which the heat load of the stove was varied by changing the time between the different charges. The experiments were made with three different damper positions [12.5%, 25% and 37.5% open]. Because in the experiments with the De Lepeleire/Van Daele wood stove no effect of the number of wood pieces was determined only experiments with 4 pieces per charge were carried out.

The size of the wood pieces was 0.02 x 0.03 x 0.2 m, the length of the pans above the fireplate 0.15 m. The results of the experiments are summarized in Table 6.2. The efficiency as a function

of the heat output is plotted in Fig. 6.5 a,b and c. In these graphs also the efficiencies of the first and the second pan are plotted.

From Fig. 6.5 it is clear that the efficiency of the stove is not influenced very much by a change in the heat output of the fire. Under the conditions investigated the efficiency of the stove varies between 15% and 23%. The efficiency increases roughly by 3% when the heat output is doubled. This means from the point of view of efficiency it is advisable to operate the stove at a high heat load. The change in efficiency has to be attributed almost entirely to the first pan. In contradiction to the De Lepeleire/Van Daele stove the efficiency increases when the heat output of the fire increases. This trend is clearly noticeable for the three series of experiments performed. The explanation for this is that the heat transfer by radiation to the first pan is much higher in the well insulated combustion chamber of the Nouna stove than it is in the poorly insulated De Lepeleire/Van Daele stove where convective heat transfer to the pan is more important.

The efficiency of the first pan is about 4 times higher than that of the second pan. The operating range of the stove is very limited. With 4 pieces of wood per charge the Nouna wood stove can be operated with a minimum heat output of the fire of approximately 4 kW and a maximum heat output of about 9 kW.

The maximum output was limited by the size of the combustion chamber which limited the size of the charges that could be supplied. The minimum capacity was restricted by the fact that for lower capacities the fire was extinguished.

6.4.2 The effect of the combustion air damper position

To show the influence of the combustion air damper position on the efficiency of the Nouna wood stove, the experimental data of Table 6.2 are replotted in Fig. 6.6 a, b and c. The graphs show the efficiencies of the first and the second pan and the total efficiency. It is quite clear that the position of the combustion air damper has an important effect on the total efficiency of the stove.

A variation in the combustion air damper position from 12.5% to 37.5% of fully open, results in a decrease of the efficiency of about 6% absolute. This decrease is mainly noticeable in the efficiency of the first pan which accounts for a decrease of 4% absolute.

In fig. 6.6 C the efficiency measured with a fully opened damper is also given. It is obvious that the operation of the damper as far as efficiency is concerned still effective in the range >37.5% and that the efficiency drops further.

In Fig. 6.13 the measured CO₂- and CO-concentrations in the flue gases are given.

It is clearly shown that the CO-concentration increases strongly when the damper is closed. This is one of the reasons why no experiments with smaller damper openings were performed.

The increase in efficiency for smaller damper openings is due to the fact that the flame temperature increases because of the smaller excess air.

Compared with the 37.5% opened damper the excess air factor diminished with 29-42% depending on the heat load of the stove. In Fig. 6.14 a plot is presented of the excess air factor for different damper position as a function of the heat load. This figure shows that the amount of air is properly controlled by the damper.

6.4.3 The effect of the chimney draft

Because the height of a chimney is one of the construction variables that can easily be altered, a number of experiments were made with different chimney drafts (4.9 Pa and 6.9 Pa, corresponding with the draft of a chimney of 1 m and 1.5 m respectively). The test results are given in Table 6.4

For all the experiments the stove with the lower draft has a much higher efficiency. This effect is almost entirely due to the higher efficiency of the first pan. See also Fig. 6.7. This is due to the higher combustion temperature caused by the lower amount of combustion air.

The increase in efficiency varies between 2.4% absolute for a high heat load and a 37.5% opened damper to 4.3% absolute for the high heat load and the 12.5% opened damper. Although the number of ex-

periments is too small to draw definite conclusions with respect to the effect of heat load and damper position on the height of the increase, the results clearly indicate that an important change in efficiency can be obtained by altering the chimney draft and that from the efficiency point of view it is advisable to use as low a chimney as possible (see also chapter 6.5.3).

6.4.4 The effect of a baffle on the efficiency

To see what effect could be expected from a baffle between the combustion chamber and the heat transfer chamber the opening between these spaces was filled with a baffle leaving about 33% of the original cross-section in function. Also between the second chamber and the chimney the cross-section was filled with a baffle construction (see Fig. 6.8). The result of the experiments with the baffle are presented in Table 6.5 and Fig. 6.9. By comparing the efficiencies with and without baffle it is noticeable that for the stove with the baffle the efficiency of both pans is always higher than the efficiencies of the pans in the original stove. Although the limited number of experiments excludes a definite conclusion, there is a strong indication that the effect of the baffle increases with greater damper openings. In the trials with the fully opened damper the increase in efficiency due to the baffle is even 6%. Because of this positive effect of the baffle on stove efficiency further experiments should be performed to determine the effect of the baffle for other operating conditions and also to investigate different baffle dimensions.

6.5 The combustion performance

The combustion performance data of the Nouna stove are given in Table 6.6. Because the combustion performance is specially important from the point of view of health, the flue gas analysis was extended with the measurements of soot and C_xH_y . Because the instrumentation was not available during the whole testing period these data have not always been measured.

The measurements of the soot concentration show that the average concentration in the flue gases during a cooking period is of the order of

10 mg/nm³. This corresponds to 0.02% of the amount of wood that is burned.

The C_xH_y-concentration fluctuates much more strongly. Values between 30 and 1300 ppm were measured. To see whether CO-concentration could be diminished an experiment was performed with a tangential air intake. Comparison between the data of this experiment with the data of the stove with the original air intake at the same heat load and damper opening (runs 42, 43, 45 and run 38) shows no improvement.

6.5.1 The effect of the heat output of the fire

In Figs. 6.10 a, b and c the CO₂-and CO-concentration in the chimney is plotted versus the heat output of the stove. When the heat output increases the CO₂-concentration increases, because of the relatively smaller amount of air that is sucked through the stove. This has a favourable effect on the flue-gas losses. In Fig. 6.11 the change in the excess-air factor as a function of the heat output is given. This figure shows that even at the high heat output level and a small damper opening the amount of combustion air is still more than twice the stoichiometric value.

In spite of the fact that enough combustion air is available no complete combustion is achieved. Figs. 6.10 a, b and c show that the CO-concentration increases with the heat load, especially when the damper opening is small (12.5%). Apparently the mixing of the combustion gases with the combustion air is not ideal.

For the design of the stove it is interesting to know the relationship between efficiency and combustion performance. This relationship is shown in Fig. 6.12, where the CO-concentration is plotted versus the efficiency of the stove. This figure shows that the CO-concentration increases with the efficiency of the stove. This means that for this stove construction the aim to reach high efficiencies will also lead to high CO-concentrations, CO-concentrations that are so high that they are unacceptable for health reasons. A further investigation of the stove behaviour on this point and a search to possibilities to diminish the CO-concentration by altering the construction or the firing procedure will be necessary to improve this situation.

6.5.2 The effect of the combustion damper position (excess air)

The influence of the damper position on the combustion performance is presented in Figs. 6.13 a, b and c.

In chapter 6.1 it has already been discussed how the excess-air factor changes with the heat output (see Fig. 6.11). By replotting this figure the effect of the damper opening on the excess-air factor can be shown more clearly (see Fig. 6.14). It is obvious that the damper construction is adequate in controlling the amount of combustion air. Although for a damper opening of 12.5% the excess-air factor is still more than twice the stoichiometric value. The combustion performance becomes so poor that very high CO-(and C_xH_y -)concentrations occur. Experiment no. 35 is a good example of the danger that threatens when the damper opening becomes too small. The CO-concentration increases sharply to values that are unacceptable. In Fig. 6.15 all the CO-concentration measurements are plotted together as a function of the excess-air factor. The relative position of the data show that for the same excess-air factor the CO-concentration is lower for the higher heat loads.

From the test runs 49, 59 and 60 (Table 6.6) it is clear that also with a fully opened damper and at high heat loads the CO-concentration is still in the order of 0.14%. The poisoning index, defined as the ratio of the CO-and CO_2 -concentration, is 0.026 at this most favourable condition. This value is higher than the value that is considered as safe for gas-fired heating appliances. (CO/CO_2 max. 0.01 for normal operation and 0.02 for down blowing wind in the chimney).

It is therefore necessary to improve the combustion performance of the stove. In order to avoid extremely dangerous situations the construction of the damper should be such that a minimum damper opening is always guaranteed.

6.5.3 The effect of the chimney draft

In chapter 6.3 the favourable effect of a low chimney in the efficiency of the stove was discussed. In Fig. 6.16 the effect of the

draft on CO- and CO₂-concentrations is shown. However, the lower amount of combustion air leads to a poorer combustion with respect to CO-formation. The values in Table 6.4 show a systematic increase in the concentration of carbon monoxide for lower drafts. On the other hand these values show that it is possible to diminish the CO-concentration by increasing the chimney height. However, at the high draft CO is still present in the flue gases at concentrations that are too high to consider the flue gases as harmless.

6.5.4 The effect of a baffle on the combustion performance

In Fig. 6.17 the CO₂- and CO-concentrations for two series of experiments, one with and one without a baffle, are presented (see also Table 6.5). The most important conclusion from this graph is that the CO-concentration does not seem to change very much when a baffle is used. This effect, combined with the positive influence of the baffle on the efficiency, underlines the conclusion that more research should be done in the effect of a baffle on the stove performance.

6.6 The heat balance

To understand the stove performance it is necessary to draw up heat balances of the stove.

The measurements of pan efficiency, sensible heat output of the fire and loss of heat by unburnt constituents in the flue gases has already been discussed in the report on the De Lepeleire/Van Daele stove [1]. From the data collected in the soot emission it can be concluded that the average concentration during a cooking period is of the order of magnitude of 10 mg/nm³. This corresponds to 0.2 mg/kg fuel or an amount of heat of 0,002 kW, which can be neglected.

As described in chapter 6.5, the C_xH_y-concentration varied considerably. The contributions of C_xH_y to the heat load has been calculated by considering C_xH_y as CH₄. In Table 7 the influence of CO and C_xH_y on the heat losses is indicated by using different columns for the heat loss by unburnt constituents.

An important difference between the De Lepeleire/Van Daele stove and the Nouna stove discussed in this report is the mass of the stove body in which heat is accumulated during the cooking period.

To get an insight in the amount of accumulated heat two different methods have been used.

In the first approach the accumulated heat was determined by calculating the heat loss of the stove to the surroundings during a cooling down period using the same equations as in the experiment with the De Lepeleire/Van Daele stove.

Because the cooling-down period lasts for almost 48 hours and the temperature differences between stove and surroundings are very small, the environmental conditions have a strong effect in the accuracy of the calculations. It appeared that no proper calculations could be made for a number of experiments also because of irregular interruptions of the data acquisition system during the night. For those experiments the accumulated heat is presented in Table 6.7 in the column "Accumulated heat + unaccounted for". To improve this situation more thermo-couples were installed in the surroundings to get a better insight in the ambient temperature around the stove, the thermo-couples in the stove body were re-arranged on basis of infrared pictures so that a better mean temperature could be calculated and the test period was lengthened.

Heat balances drawn up for these tests are presented in Table 6.7 for the runs 47 etc.

The amount "unaccounted for" changes between 4% and 20% and is of the same order as found by the De Lepeleire/Van Daele stove. Taking into account the much longer period over which the calculations of the heat losses to the surroundings are made and the already mentioned smaller temperature differences the result is satisfactory.

For those test runs where no proper calculations could be made, the accumulated heat and the part "unaccounted for" are added together. Another approach was the use of an existing computer programme for kiln calculations (see Appendix 1). With this computer model calculations were made for three different cases, namely one with heat output of 4.7 kW, one with a heat output of 8 kW and one simulating the cooking behaviour (run 53). Each case consists of at least a period of heating followed by a period of cooling down.

With the computer programme the average surface temperatures of both the long and the short side walls of the stove were calculated.

In Fig. 6.19 the calculated values are given for run 57 (heat output 4.7 kW). In the same figure the measured values for the average surface temperature of each of the four sides of the stove are indicated. The results of the measurements and the calculations for the runs 49 (heat output 8,1 kW) and 53 (cooking behaviour) are plotted in the same way as run 57 in Figs. 6.20 and 6.21.

In the Figs. 6.22, 23 and 24 the accumulated heat as a function of time is given. The accumulated heat is calculated for the model and therefore represents only half of the value for the whole stove.

It can be seen from Figs. 6.19,20 and 21 that, especially during the cooling-down period, a good agreement exists between measurements and calculations.

Most of the aspects of the heat balance have already been discussed in detail in the foregoing chapters.

Therefore it will do to restrict the discussion in this chapter to the item "accumulated heat". As can be seen in Table 6.7, the accumulated heat is the greatest part of the heat balance. It does not change much with variables investigated and remains in the order of 30-40% of the heat input.

This heat can be made use of either for heating purposes or for heating water. In both cases the stove will be far more effective. When for instance after cooking the pans are filled with water, they can easily be heated to 60°C without adding any fuel to the stove. (Air damper and chimney damper in fully closed position, see Fig. 6,18.) Because the accumulated heat is so important for the fuel consumption that a further study into the behaviour of the stove body should be made to optimise the stove construction and adapt it to the user's behaviour. The computer model described before will be very useful in this respect.

6.7 The effect of wood properties

For exploration purposes two experiments were carried out using Merbau as a fuel. In Table 6.7 the proximate analysis of this wood is given. compared with the White Fir [1] the calorific value of the Merbau is the same. The greatest difference is found in the moisture content of the wood. The specific weight of the Merbau is 780 kg/m³. This is more than twice the specific weight of the White Fir used (350 kg/m³).

The result of the two trials are given in Table 6.3. It is clear that there is great effect of the fuel properties on the efficiency. The efficiency of the first pan increases even at low heat loads to levels that are about 6% higher than with White Fir. On the contrary, the efficiencies of the second pan drops below 3%. The most probable reason for this is the completely different way in which the volatiles burn. By visual observation it can be seen that the Merbau burns with short flames while the White Fir burns with long flames even in the second chamber of the stove. This means that for equal heat loads the combustion of the Merbau takes place in a much smaller space that higher temperatures are generated in particular under the first pan.

6.8 A comparison between the De Leppeleire/Van Daele wood stove and the Nouna wood stove

6.8.1 Efficiency

When the total efficiency of the De Leppeleire/Van Daele stove of 25-30% [1] is compared with that of the Nouna stove that lies between 17 and 20% it can be concluded that under the cooking conditions used in the field the performance of the De Leppeleire/Van Daele stove is much better. Furthermore it appears that this better efficiency is almost entirely due to the better efficiency of the second pan. To the De Leppeleire/Van Daele stove this efficiency amounts to 9-12%, for the Nouna stove the second pan efficiencies vareis between 3.2 and 3.9%.

When the two stoves are compared under equal firing and heat transfer conditions the picture changes, however, the main effect of this change is due to the effect of the depth of the pan in the stove on the efficiency, the De Leppeleire/Van Daele stove this depth is mostly taken as 0.5 m and for the Nouna stove it is 0 m. In Table 6.9 two experiments with the pan bottom flat with the top of the combustion chamber are compared.

Although the De Leppeleire/Van Daele stove performance is still better, the difference is not so striking as under field conditioning. When furthermore efficiency values of the Nouna stove are corrected for the different pan diameters by multiplying the

efficiency with the square of the diameter ratio of the pans, it comes out that the Nouna stove efficiency is higher than that of the De Lepeleire/Van Daele. The most probable reason for the higher heat transfer is the insulated brick construction of the stove that cools down the combustion gases to a less degree than the uninsulated De Lepeleire/Van Daele stove.

In this respect another important effect should be mentioned. As already indicated in the chapter on the heat balance, a considerable amount of heat is accumulated in the stove wall. This heat, however, can be used when after finishing the cooking, pans are placed in the stove for the purpose of heating water. In Fig. 6.18 is illustrated for a heat load of about 8 kW that this water can be heated to about 55°C. When the accumulated heat is made useful this way, the total efficiency of the Nouna stove increases with another 2%. This argument illustrates the necessity of a good definition of the efficiency and of the experimental conditions.

6.8.2 Combustion performance

Generally speaking the combustion performance in the Nouna wood stove under field conditions is much better than that of the De Lepeleire/Van Daele stove. In the latter CO-concentrations are several times higher for the same heat load. Values higher than 1% are no exception. An important reason for this is undoubtedly the higher excess-air factor for the Nouna stove and the fact that the combustion air enters the combustion chamber through a well-operating damper, this in contradiction to the De Lepeleire/Van Daele stove, where because of air leaks the combustion air can not be properly controlled. Another reason is the depths at which the pans are brought into the stove. These are much higher for the De Lepeleire/Van Daele stove. For the same pan depths (see Table 6.9) the combustion performance of both stoves is of the same order of magnitude.

6.9 Conclusions

- The main characteristic of the Nouna wood stove is that it can be operated at heat loads between 4.5 and 9 kW at an efficiency with two pans on top of the stove between 15 and 23%.

- The efficiency under operating conditions increases when the heat load increases, the damper opening becomes smaller or the chimney draft is lowered. In all these cases a higher efficiency is accompanied by a poorer combustion leading to higher CO- and C_xH_y -concentrations.
- The combustion air damper controls the amount of combustion air properly. Because of the strong increase in CO-concentration at smaller damper openings the minimum damper opening must be limited.
- Even with a fully opened damper the poisoning index of the flue gases is higher than that considered to be safe for gas-fired appliances.
- A baffle between the two chambers of the stove and in the channel to the chimney has a favourable effect on the efficiency without appreciably effecting the CO-concentration. This measure therefore deserves further consideration.
- Exploratory measurements indicate a strong effect of the type of wood used on the efficiency of the stove. Further experiments should be performed to clarify this effect.
- About 30-40% of the heat input is accumulated in the stove body. It will be useful to optimise the stove construction to the users behaviour by using a computer model.
- When stoves of a different construction are compared on efficiency and combustion performance, due consideration should be given to the operating conditions under which such a comparison is made.
- Under field conditions the efficiency the De Lepeleire/Van Daele-stove has a 8-10% higher efficiency than the Nouna-stove. However, the combustion performance of the De Lepeleire/Van Daele-stove is much lower and CO-concentrations are several times higher. The main reasons for this are the larger pan depth and the poorer combustion air control of the De Lepeleire/Van Daele-stove.

- When compared at almost equal heat loads and equal pan depths the efficiencies of the two stoves are of the same order of magnitude (21%) at equal combustion performance.

References

- [1] K. Krishna Prasad c.s. (1981)
A study on the performance of two metal stoves.
Report from the Woodburning Stove Group, Eindhoven
University of Technology, Eindhoven, The Netherlands
- [2] Ree, H. v.d., W.J. Basting and P.G.M. Nievergeld (1974)
Reduction of temperature distributions in cargoes with the aid
of a computer program using the method of finite elements.
Paper presented at the meeting of Commission D-2 of the International
Institute of Refrigeration 22-26 April 1974
Wageningen.

Description of the computer program used for the temperature calculations.

1. The program

TNO has developed a computer program, called Bertem, for the calculation of temperature distributions in constructions and for flows as function of time [2].

Both stationary and non-stationary temperature distributions can be calculated with this program.

The program can be applied to the solution of one-, two- and three-dimensional problems. It is based on the so-called finite-element method.

With this method a construction of a given configuration is divided into a large number of small parts, called elements. Each element has heat transport connections with its neighbouring elements.

The thermal properties of the elements, their connections and data, such as for instance the boundary conditions and their changes in time, can be supplied in the form of tables of figures and/or additional parts of the program in which required data are calculated or values are assigned.

The program integrates, starting from initial temperatures for the elements, with a step-by-step method in time, the heat transfer equation describing the heat exchange among the elements.

The time intervals used can be varied during computation. In the program use has been made of fundamentally stable integration methods. The computer program is a highly flexible program, which with relatively small efforts can be applied to a wide diversity of heat transfer problems.

2. Computer model of the stove

To translate the actual situation into a computer model some simplifications in the construction have been made. The outside dimensions are the same for the model and the stove. However, the holes for, among other things, the pans and the chimney, are concentrated in one big hole in the centre of the model.

For the calculations the stove is assumed to consist of one single material. The properties of this material, such as the thermal conductivity, the specific heat and the density, are based on the properties of the materials of which the stove is constructed, namely ordinary brick, concrete, sand and cement.

The model represents only half of the stove, because for reasons of symmetry the centre plane can be considered as an adiabatic surface.

The model and its division into elements are shown in figure 6.25.

The heat input in the model, caused by the combustion of the wood, takes place via the elements adjacent to the hole in the centre.

The heat leaves the model via the elements at the outside of the model where it is transferred to the ambient air.

In this way it is also possible to calculate the accumulated heat in the model at any point of time.

Table 6.1 Combustion rate of different charges of White Fir (WF) and Merbau (M) for an average heat load of ± 8 kW

Charge	g/min.		residu in grams	
	WF	M	WF	M
1	13	16.25	98	142
2	29.25	25.5	62	124
3	28.25	18	60	178
4	23.5	22	72	198
5	25	21	70	224
6	27.25	21.5	62	236
7	25.75	22.5	58	240
8	27	20.75	60	254
9	23.25	17.25	58	304

Table 6.2 Efficiency of the Nouna wood stove as a function of the heat output of the fire and the damper position

size of the wood pieces: 0.02x0.03x0.2 m
 depth of pans in stove : 0.11 m
 initial amount of water: first pan 4.0 kg
 second pan 2.0 kg

Symbols:

d.p.	- combustion air damper position	[%]	t_b	- time to boiling	:	t_{b1}	- of pan 1	[min]
Δm_f	- mass of charge	[kg]				t_{b2}	- of pan 2	[min]
Δt	- time between the two charges	[min]	m_s	- amount of water evaporated:	:	m_{s1}	- of pan 1	[kg]
\dot{Q}	- heat output of the fire	[kW]				m_{s2}	- of pan 2	[kg]
n_i	- number of charges	[1]	η	- efficiency	:	η_1	- of pan 1	[%]
m_f	- total amount of wood used	[kg]				η_2	- of pan 2	[%]
t_t	- total burning time	[min]				η_t	- total	[%]
T_i	- initial temperature of the water	[°C]						

run no.	d.p. [%]	m_f [kg]	Δt [min]	\dot{Q} [kW]	n_i [1]	m_f [kg]	t_t [min]	T_1 [°C]	t_b [min]		m_s [kg]		η [%]		
									t_{b1}	t_{b2}	m_{s1}	m_{s2}	η_1	η_2	η_3

Charge: 4 pieces

32	12.5	0.228	15	4.74	10	2.289	162	24	37	80	2.514	0.403	16.4	3.7	20.2
33	25.0	0.242	15	5.04	10	2.410	156	23	47	83	2.082	0.378	13.4	3.4	16.8
34	37.5	0.208	15	4.33	10	2.089	156	23	36	109	1.556	0.149	12.5	2.6	15.1
31	12.5	0.245	12	6.40	10	2.450	143	25	30	52	2.780	0.602	16.7	4.4	21.1
29	25.0	0.245	12	6.40	10	2.455	135	22	42	53	2.182	0.532	13.6	4.0	17.6
30	37.5	0.236	12	6.12	10	2.356	132	24	35	64	1.792	0.351	12	3.2	15.2
35	12.5	0.213	8	8.60	10	2.213	105	24	25	39	1.794	0.514	18.4	4.4	22.8
37	25.0	0.233	8	9.1	10	2.329	108	20	26	44	2.362	0.436	15.4	3.9	19.3
38	37.5	0.219	8	8.5	10	2.191	93	21	28	47	1.985	0.334	14.3	3.5	17.8

Table 6.3 Comparison of different kind of wood as fuel for the Nouna wood stove

run no.	damper position (%)	heat output (kW)	Efficiency			kind of wood		baffle	
			first pan (%)	second pan (%)	total (%)	White fir	Merbau	with	without
55	25	7.8	21.60	2.87	24.47		*	*	
51a	25	8.6	15.80	4.10	19.90	*		*	
53a	25	9.3	16.80	4.80	21.60	*		*	
56	25	5.1	21.3	2.20	23.50		*	*	

Table 6.4 Comparison of variation in draft

run no.	damper position (%)	heat output (kW)	Efficiency			draft		CO (%)	CO ₂ (%)	baffle	
			first pan (%)	second pan (%)	total (%)	4.9 (Pa)	6.9 (Pa)			with	without
50	12.5	8.32	18.3	5.60	23.90	*		-	8.35	*	
58	12.5	9.05	15.4	4.70	20.10		*	0.29	7.31	*	
52	12.5	4.40	20	3.20	23.20	*		0.43	5.40	*	
54	12.5	4.96	19.7	3.95	23.65	*				*	
57	12.5	4.67	17.2	3.10	20.30		*	0.23	4.24	*	
22	12.5	9.2	14.2	4.3	18.5		*	0.21	4.21		*
23	25	9.6	12.3	3.9	16.2		*	0.18	4.48		*
25	37.5	8.5	11.8	3.6	15.4		*	0.16	4.67		*
35	12.5	8.6	18.4	4.4	22.8	*		0.60	9.3		*
37	25	9.1	15.4	3.9	19.3	*		0.24	6.8		*
38	37.5	8.5	14.3	3.5	17.8	*		0.22	5.87		*

Table 6.5 Comparison of the Nouna wood stove with and without the presence of a baffle
 wood charge :4 pieces
 size of wood:0.02x0.03x0.2m

run no.	damper position (%)	heat output (kW)	Efficiency			baffle				boiling time	
			first pan (%)	second pan (%)	total (%)	with	without	CO (%)	CO ₂ (%)	first pan (min)	second pan (min)
50	12.5	8.0	18.3	5.60	23.9	*		-	8.35	25	36
35	12.5	8.6	18.4	4.40	22.8		*	0.6	9.30	25	39
51	25	8.65	15.8	4.10	19.9	*		0.46	7.18	24	34
53	25	9.30	16.8	4.80	21.5	*		0.25	5.14	21	40
37	25	9.10	15.4	3.90	19.3		*	0.24	6.80	26	44
52	12.5	4.40	20.0	3.20	23.2	*		0.43	5.40	35	100
54	12.5	4.96	19.7	3.95	23.65	*		-	-	34	71
32	12.5	4.76	16.4	3.70	20.10		*	0.43	6.29	37	80
48	100	8.12	15.24	5.0	20.24	*		-	-	25	37
49	100	8.10	14.10	5.0	19.10	*		0.13	5.73	28	40
59	100	7.84	13.0	4.40	17.40	*		0.17	5.70	25	45
60	100	8.20	9.90	2.70	12.60		*	0.12	4.60	30	88

Table 6.6 Combustion performance of the Nouna Wood stove as a function of the heat output of the fire, the wood pieces per charge and the combustion air damper position.

Symbols: d.p. - combustion air damper position [% open]
 n. - number of the wood pieces [1]
 \dot{Q} - heat output of the fire [kW]
 T_g - flue gas temp. [°C]

initial amount of water
 pan 1: 4 kg; pan 2: 2 kg

run no.	d.p. [%]	n. [1]	\dot{Q} [kW]	Flue gas composition						excess air factor
				CO ₂ [%]	CO [%]	O ₂ [%]	C _x H _y [ppm]	Soot [$\frac{mg}{nm^3}$]	T_g [°C]	
22	12.5	4	9.2	4.21	0.21	16.8	30	6.6	254.17	4.7
23	25	4	9.6	4.48	0.18	16.48	500	4.1	340.54	4.4
25	37.5	4	8.5	4.67	0.16	-	38.5	6.4	268.12	4.3
31	12.5	4	6.4	7.09	0.36	13.94	440	-	231.36	2.8
29	25	4	6.4	5.91	0.28	14.97	-	-	249.01	3.4
30	37.5	4	6.12	4.63	0.20	16.54	740	14	234.63	4.3
32	12.5	4	4.76	6.29	0.43	14.59	665	-	187.21	3.1
33	25	4	5	4.77	0.23	16.1	185	-	215.21	4.1
34	37.5	4	4.35	3.68	0.20	17.27	147	-	183.63	5.3
35	12.5	4	8.6	9.3	0.6	11.59	1321	-	263.88	2.1
37	25	4	9.1	6.8	0.24	13.98	160	-	275.85	2.9
38	37.5	4	8.5	5.87	0.22	15.01	160	-	278.32	3.4
60	100	4	8.2	4.59	0.12	16.81	-	-	269.79	4.4
42	*	4	8.3	5.71	0.22	15.27	370	-	229.28	3.5
43	*	4	8.25	5.79	0.25	14.98	-	-	233.22	3.4
47	*	4	8.15	6.94	0.28	14.14	-	-	249.30	2.9
44	+	4	5.5	3.85	0.15	17.02	-	-	199.08	5.2
41	+	4	8.5	3.94	0.11	17.01	80	-	247.72	5.1
50	12.5	4	8.32	8.35	-	12.67	-	-	230.99	2.5
51a	25	4	8.6	7.18	0.46	14.09	-	-	232.00	2.7
53a	25	4	9.1	5.14	0.25	15.87	-	-	219.19	3.8
59	100	4	8.2	5.69	0.17	15.92	-	-	236.27	3.5
49	100	4	8.1	5.73	0.13	15.40	-	-	274.78	3.5
52	12.5	4	4.4	5.40	0.43	15.34	-	-	165.75	3.6
56	25	4	5.1	3.91	0.25	16.79	-	-	181.52	5.0
57	12.5	4	9.05	7.31	0.27	13.8	-	-	266.40	2.7

*) tangential air intake = 33% of damper position fully open
 +) steel sheet and damper removed [open air intake]
 -) no measurement available

Table 6.7 Heat balance of the Nouna wood stove for the test period as a function of the heat output of the fire, the wood pieces per charge and the combustion air damper position

initial amount of water;
pan 1: 4 kg pan 2: 2 kg

run no.	damper position (%)	wood charge (pieces)	heat output (kW)	first pan (%)	second pan (%)	sensible heat in flue gas (%)	unburnt constituents (%)		Rad. en conv. to surroundings (%)	accumulated heat (%)	unaccounted for (%)	accumulated heat + unaccounted for (%)	remarks
							CO	C _H y					
22	12.5	4	9.20	14.2	4.3	40.8	2.75	0.10	2.7			35.15	
23	25	4	9.60	12.3	3.9	52.1	2.2	1.80	2.3			25.40	
25	37.5	4	8.50	11.8	3.6	39.0	1.9	0.10	1.9			41.70	
31	12.5	4	6.40	16.7	4.4	22.7	2.8	1.0	3.5			48.90	
29	25	4	6.40	13.6	4.0	28.7	2.0	-	3.4			48.30	
30	37.5	4	6.12	12.0	3.2	35.1	2.4	2.5	4.0			40.80	
32	12.5	4	4.76	16.4	3.7	20.0	3.7	1.6	3.6			51.0	
33	25	4	5.0	13.4	3.4	30.2	2.7	0.6	2.6			47.1	
34	37.5	4	4.35	12.5	2.6	33.0	2.9	0.6	3.4			45.0	
35	12.5	4	8.60	18.4	4.4	19.9	3.4	2.2	1.5			50.2	
37	25	4	9.10	15.4	3.9	28.1	1.8	0.4	1.6			48.8	
38	37.5	4	8.50	14.3	3.9	32.6	2.1	0.4	1.2			45.5	
60	100	4	8.20	9.9	2.7	38.5	1.5	-	1.4			46.0	
42	**	4	8.30	18.6	4.1	27.6	2.2	1	1.5			45.0	*
43	**	4	8.25	14.1	4.5	27.2	2.3	-	1.8			50.1	variation in pan * depth
47	*	4	8.15	18.6	5.3	22.7	2.3	-	0.5	32.4	18.		*
44	0	4	5.50	15.3	3.5	34.3	2.2	-	2.6			42.1	*
50	12.5	4	8.32	18.3	5.6	18.2	-	-	3.1	40	16.5		*
51a	25	4	8.60	15.8	4.1	19.9	3.4	-	1.9			54.9	*
53a	25	4	9.30	16.8	4.8	25.8	2.6	-	4.1			45.9	*
59	100	4	8.20	13.0	4.4	27.3	1.8	-	2.5	30.7	20.2		experiment with * accumulated heat
49	100	4	8.10	14.1	5.0	31.1	1.4	-	2.1	38.0	8.4		*
52	12.5	4	4.40	20.0	3.2	16.9	4.7	-	4.6	36.0	14.5		*
57	12.5	4	4.67	17.2	3.1	29.8	3.2	-	4.4	35.4	6.9		draft variation *
58	12.5	4	9.05	15.3	4.7	23.3	2.2	-	2.6	39.0	12.9		draft variation *
56	25	4	5.10	21.3	2.2	25.5	3.8	-	3.9	39.2	4		Merbau *
61	12.5	4	8.20	15.3	3.8	20.5	2.7	-	2.4	38.1	17.3		

** tangential air intake = 33% damper position

0 steel sheet and damper removed [air intake fully open]

- not measured

* with baffle

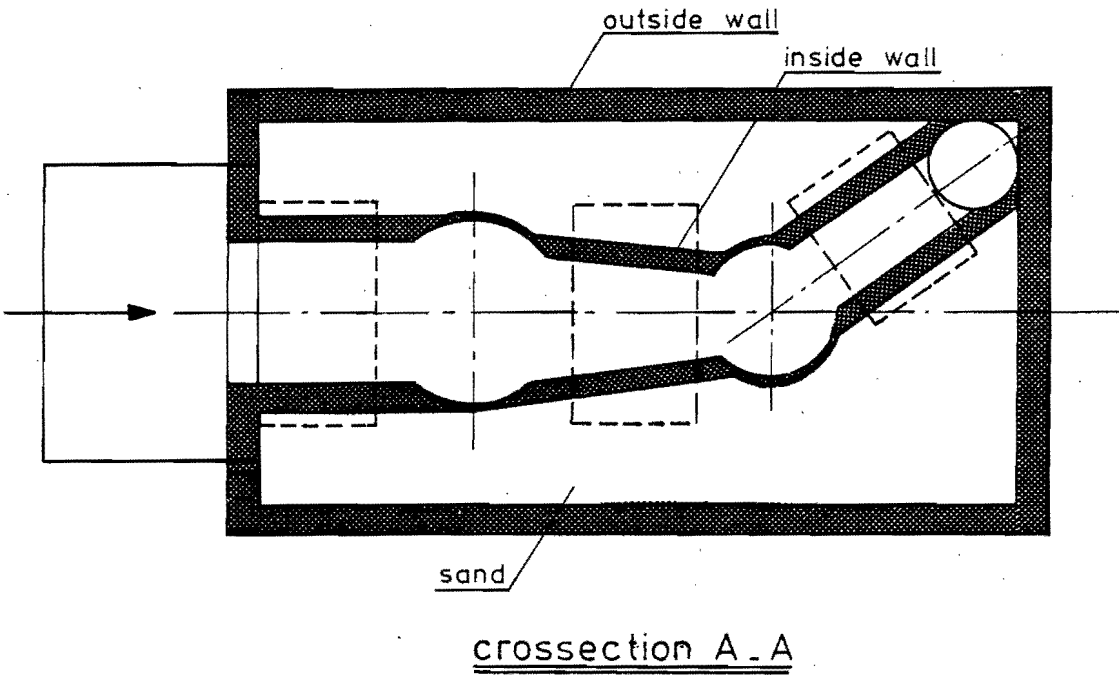
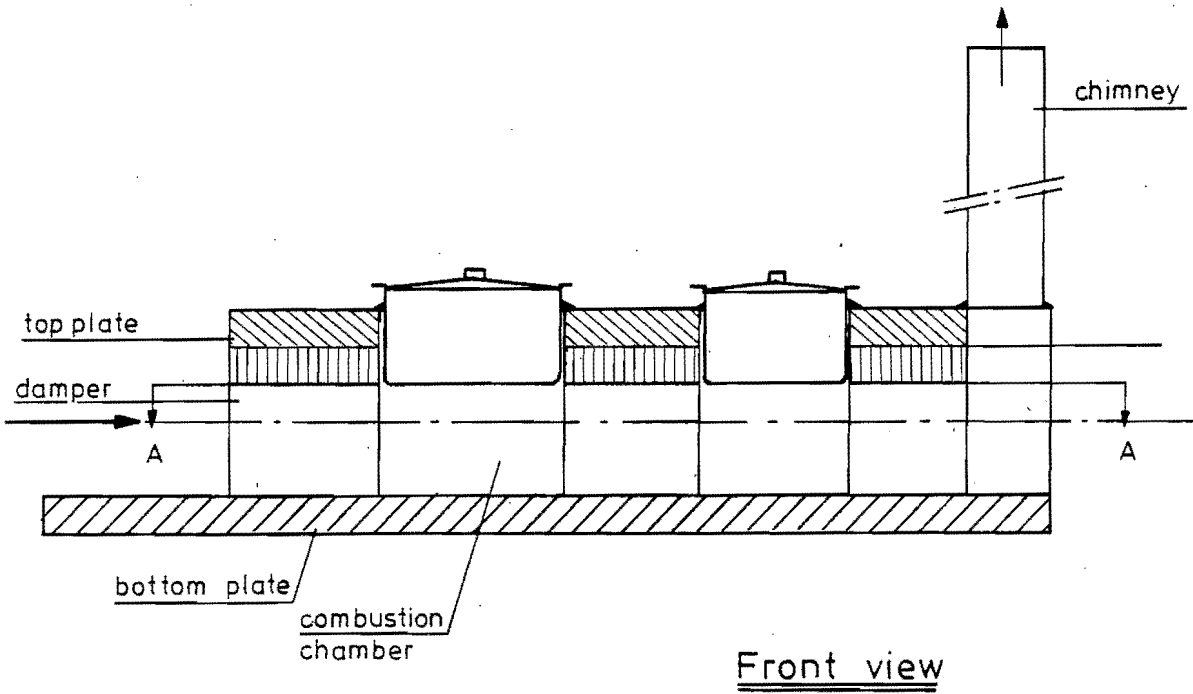
Table 6.8 Proximate analysis (wet wood) of the Merbau used during the trials

Moisture content (wt %)		45.	%
Volatile matter (wt %)		77.1	%
Ash (wt %)		0.6	%
fired carbon (wt %)			
Gros calorific value	(wet)	19.6×10^3	kJ/kg
	(dry)	20.5×10^3	kJ/kg
Net calorific value	(wet)	$18.1 \cdot 10^3$	kJ/kg
	(dry)	$18.95 \cdot 10^3$	kJ/kg

Table 6.9 Comparison of the De Lepeleire/Van Daele stove and the Nouna stove for equal pan depth's and almost equal heat inputs

	DL/vD	Nouna
Heat output	8.2 kW	8.5 kW
CO ₂	5 %	5.8 %
CO	0.3 %	0.23%
Depth of the pan in the stove	0 m	0 m
Diameter 1st pan	0.26m	0.25m
2nd pan	0.26m	0.2 m
Distance above the grate of the pan; 1st pan	0.24m	0.15m
2nd pan	0.125m	0.15m
Efficiency; 1st pan	13.7 %	14.3 % (15.5%)
2nd pan	6.6 %	3.5 % (5.9%)
total	20.3 %	17.8 % (21,4%)

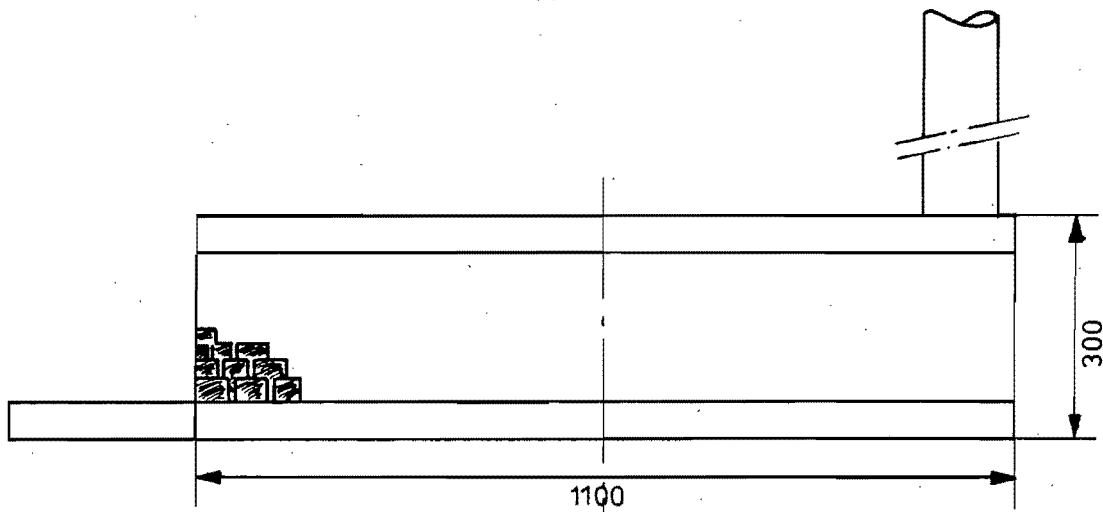
(Numbers between brackets refer to efficiencies corrected for the pan diameter)



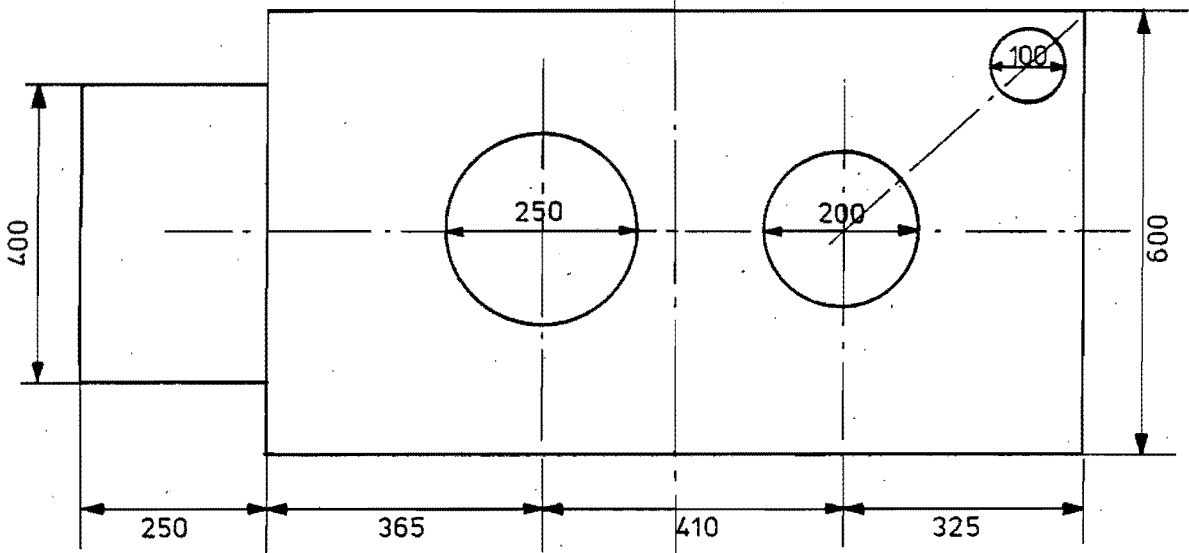
The Nouna wood stove

scale 1:10

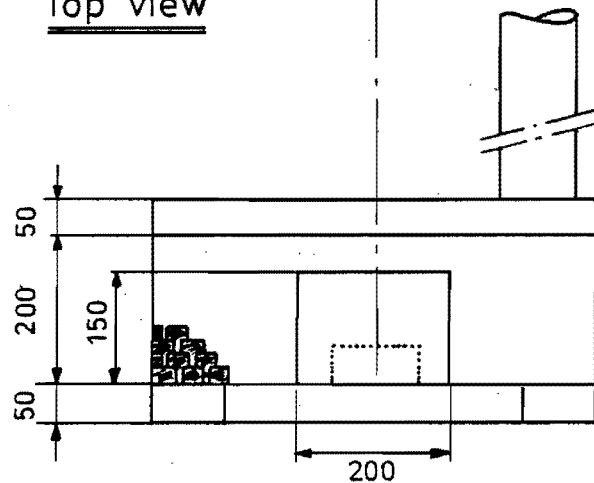
MT_TNO
84940
Fig. 6.1



Front view



Top view

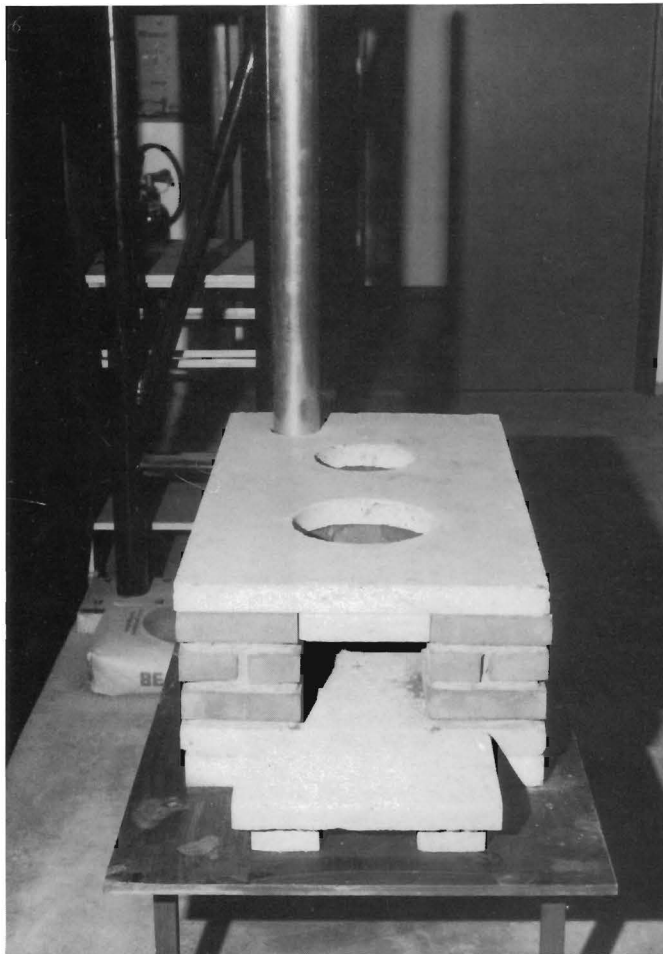


Side view

The Nouna wood stove

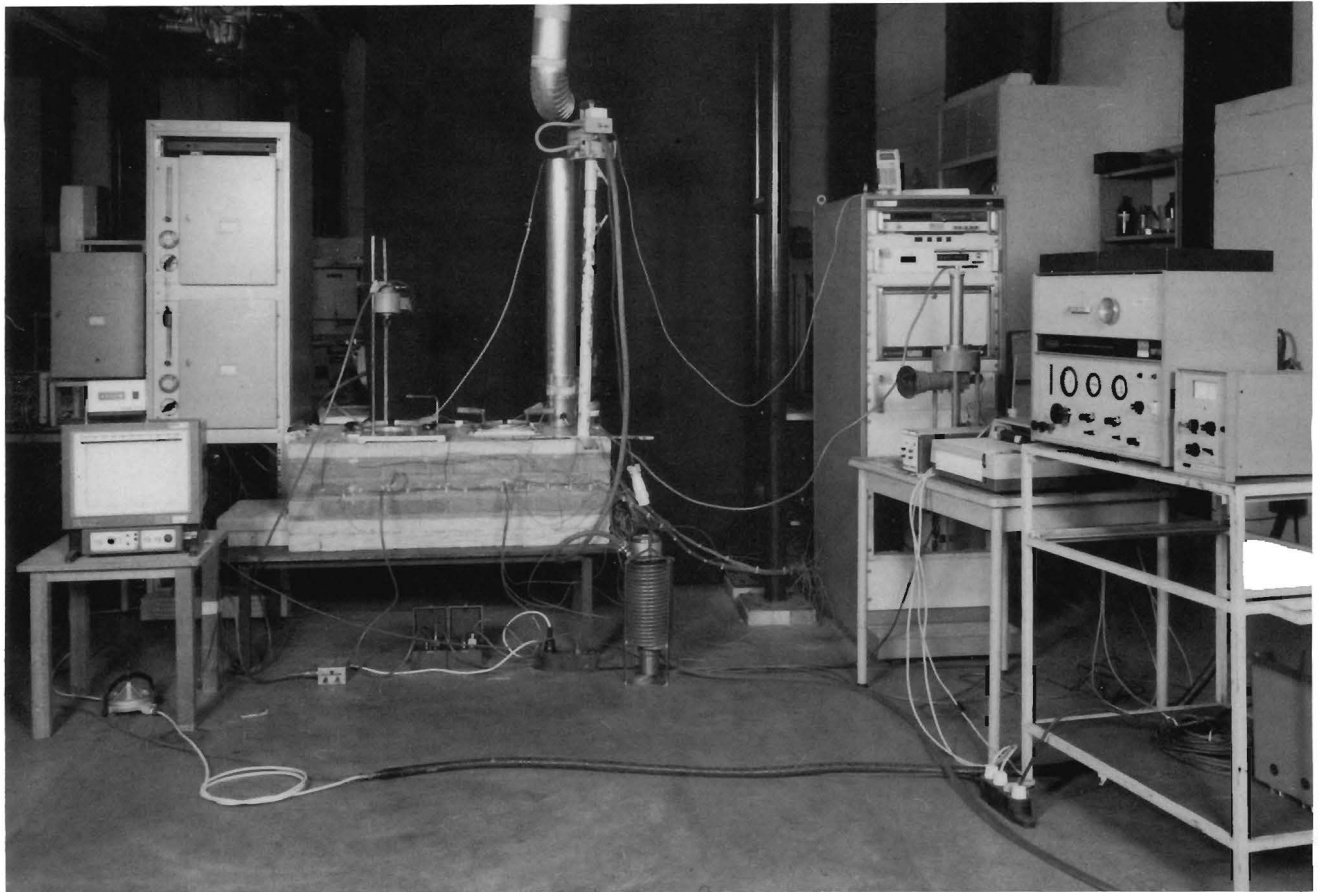
scale 1:10

MT.TNO
84940
Fig. 6.2



The Nouna wood stove

MT-TNO
84940
Fig. 3



Experimental set-up of the Nouna wood stove

MT-TNO
84940
Fig. 4

Efficiency of the Nouna woodstove as a function of the heat output of the fire

wood charge : 4 pieces
 size of wood : 0.02x0.03x0.2 m
 mass of charge : 0.232 kg
 damper position : 12.5 % open

▲ efficiency first pan
 ■ efficiency second pan
 ● total efficiency

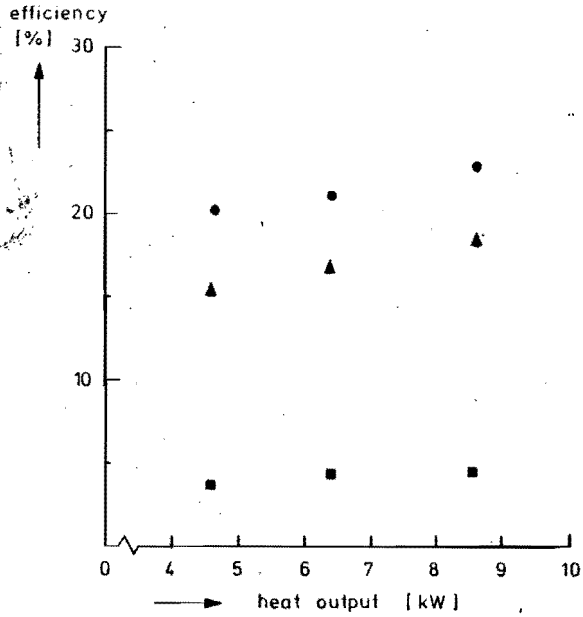


Fig. 6.5a

wood charge : 4 pieces
 size of wood : 0.02x0.03x0.2 m
 mass of charge : 0.240 kg
 damper position : 25 % open

▲ efficiency first pan
 ■ efficiency second pan
 ● total efficiency

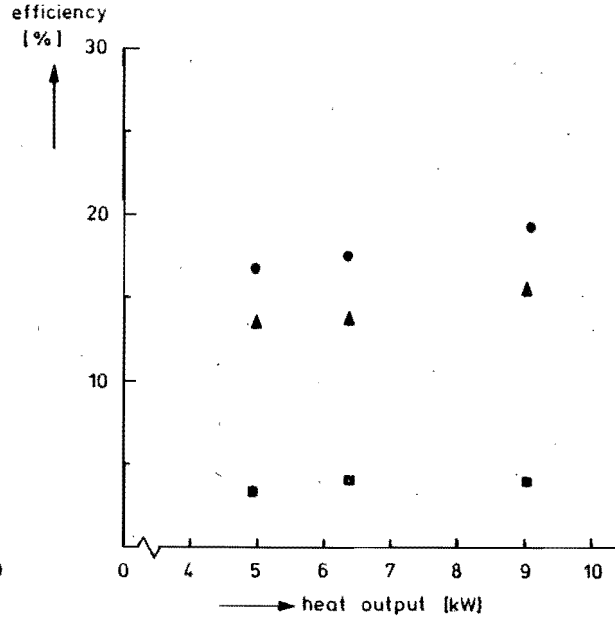


Fig. 6.5b

wood charge : 4 pieces
 size of wood : 0.02x0.03x0.2 m
 mass of charge : 0.221 kg
 damper position : 37.5 % open

▲ efficiency first pan
 ■ efficiency second pan
 ● total efficiency

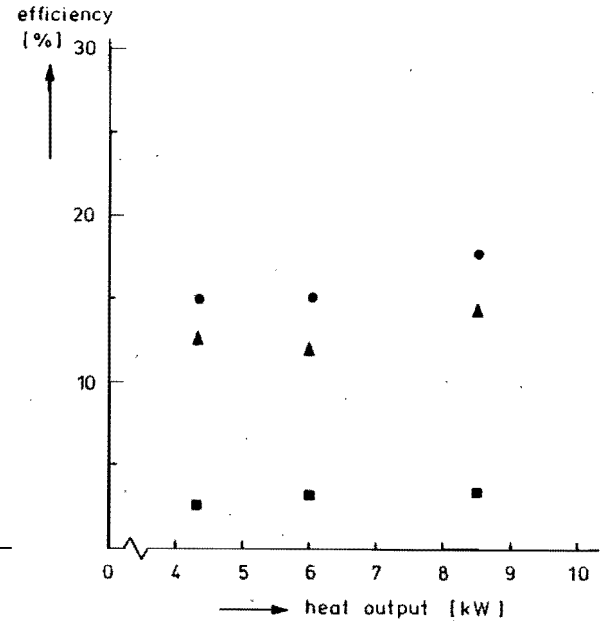


Fig. 6.5c

Efficiency of the Nouna woodstove as a function of the combustion air damper position

wood charge : 4 pieces
 size of wood : 0.02x0.03x0.2m
 mass of charge : 0.226 kg
 time between two charges: 15 min.
 average heat output of fire : 4.7 kW

▲ efficiency first pan
 ■ efficiency second pan
 ● total efficiency

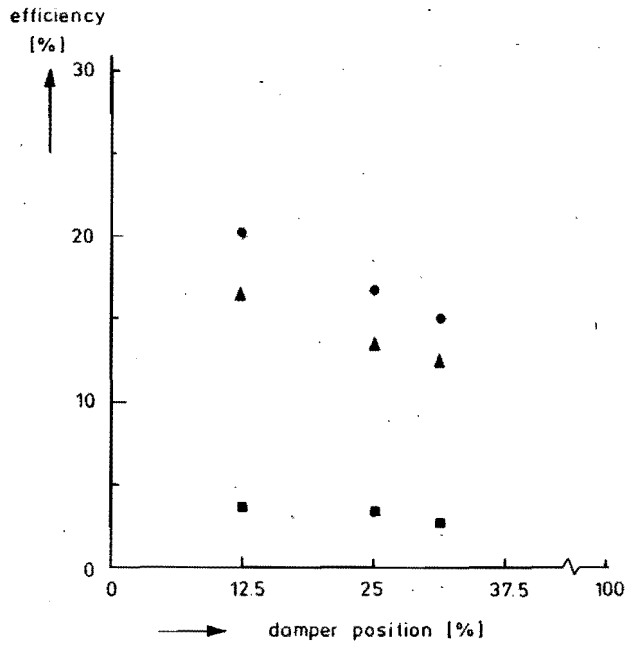


Fig. 6.6 a

wood charge : 4 pieces
 size of wood : 0.02x0.03x0.2m
 mass of charge : 0.242 kg
 time between two charges: 12 min.
 average heat output of fire : 6.3 kW

▲ efficiency first pan
 ■ efficiency second pan
 ● total efficiency

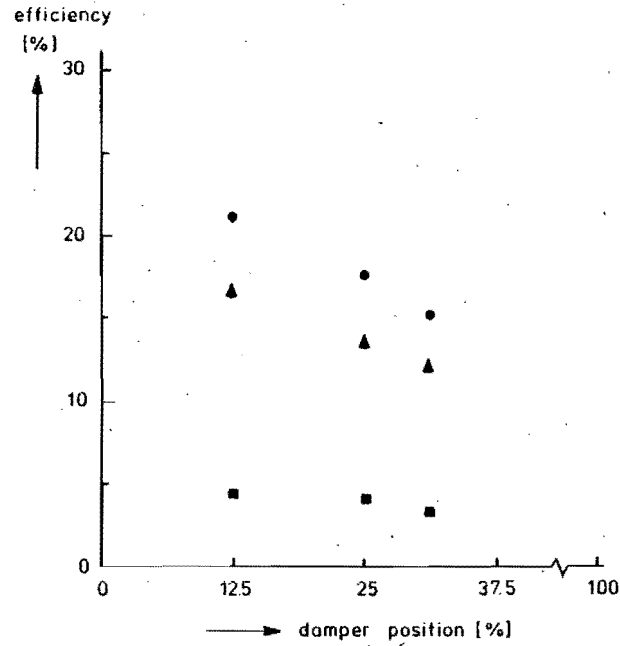


Fig. 6.6 b

wood charge : 4 pieces
 size of wood : 0.02x0.03x0.2m
 mass of charge : 0.222 kg
 time between two charges: 8 min.
 average heat output of fire : 8.7 kW

▲ efficiency first pan
 ■ efficiency second pan
 ● total efficiency

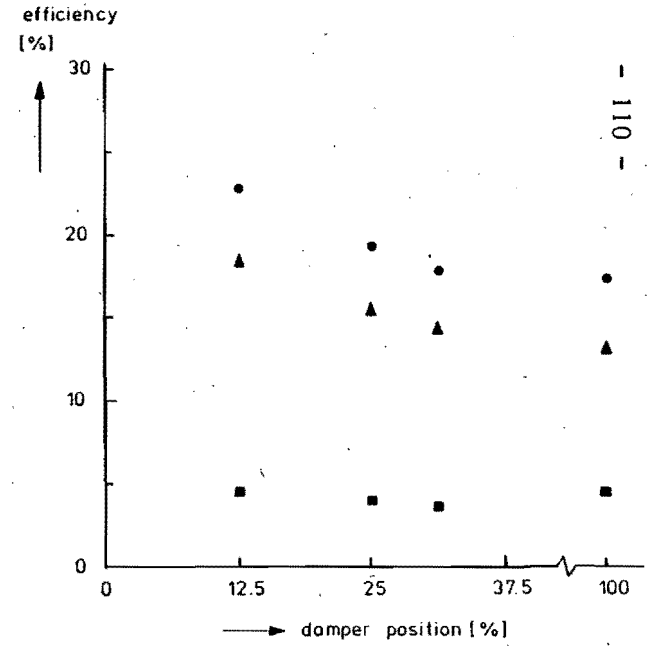
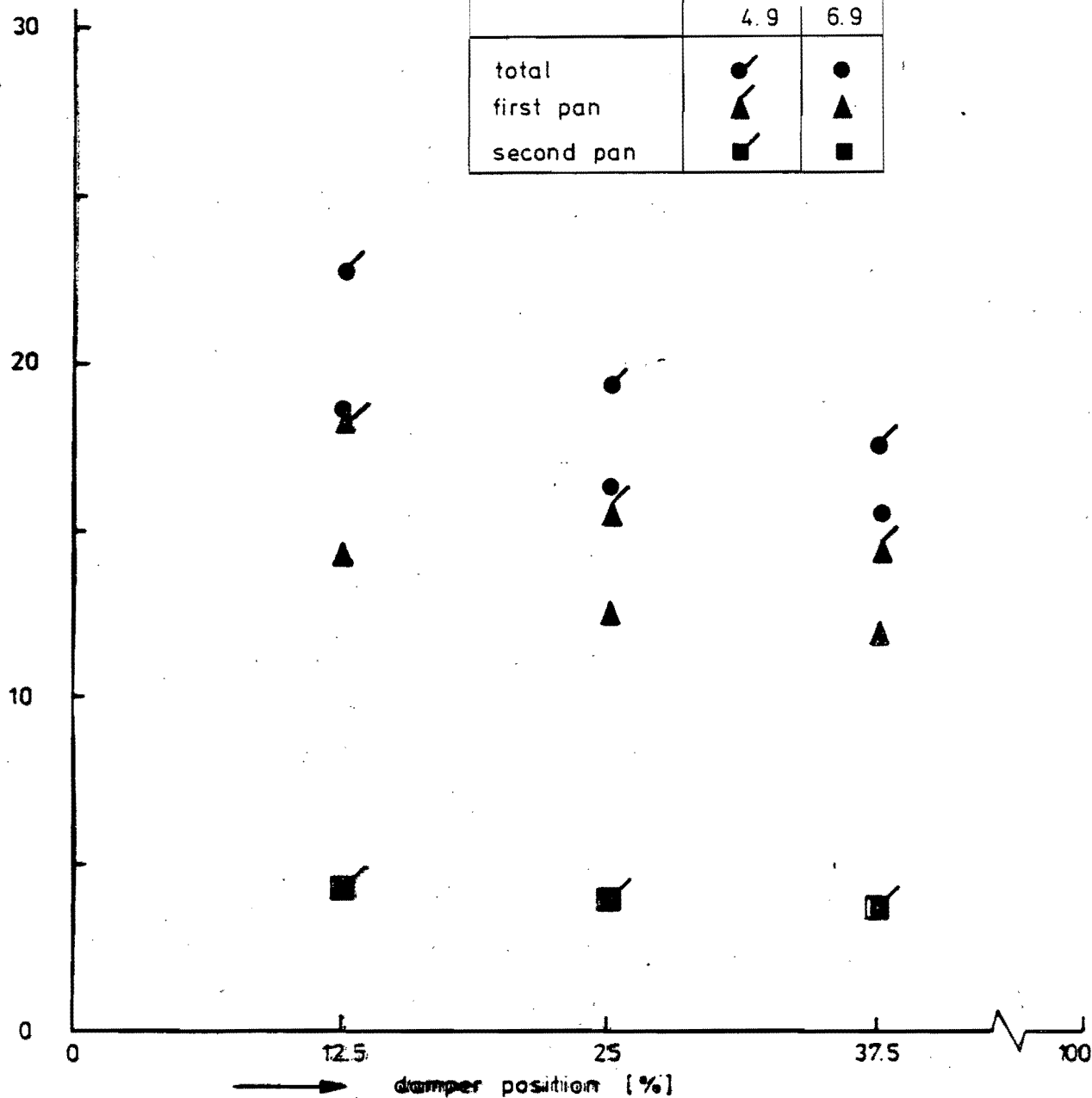


Fig. 6.6 c

wood charge : 4 pieces
 size of wood : 0.02x0.03x0.2 m
 time between two charges : 8 min.
 average heat output of fire : 9 kW

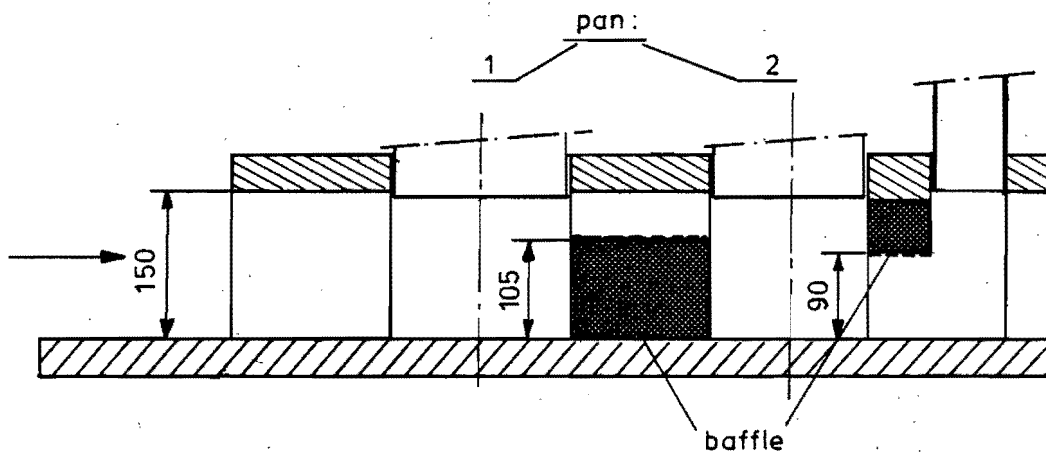
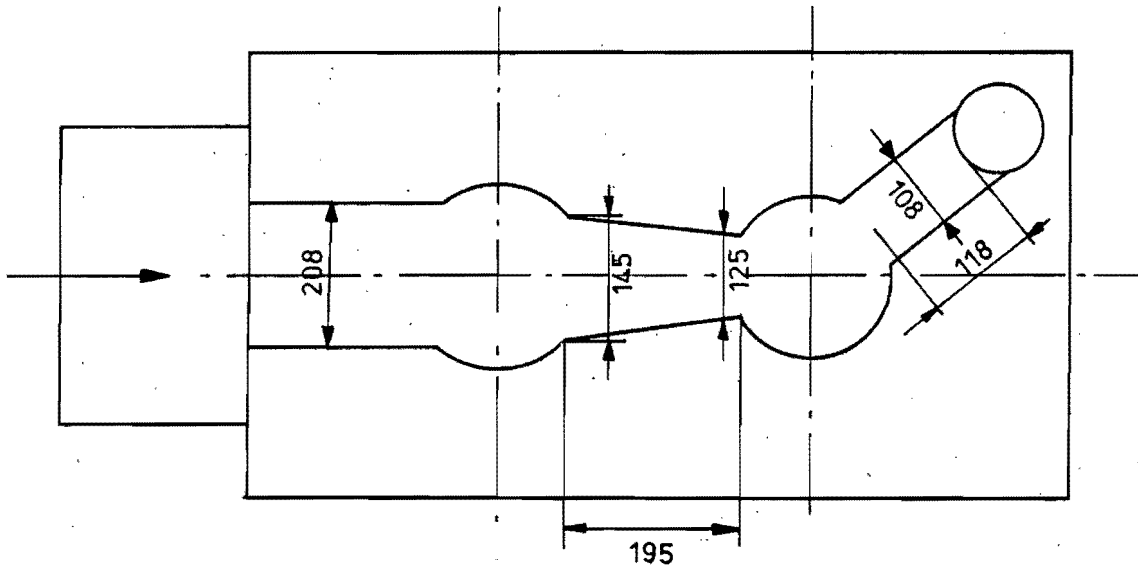
efficiency [%]

efficiency	draft [Pa]	
	4.9	6.9
total	●	●
first pan	▲	▲
second pan	■	■



Efficiency of the Nouna wood stove as a function of the damper position with a variation in draft

MT_TNO
 84940
 Fig. 6.7

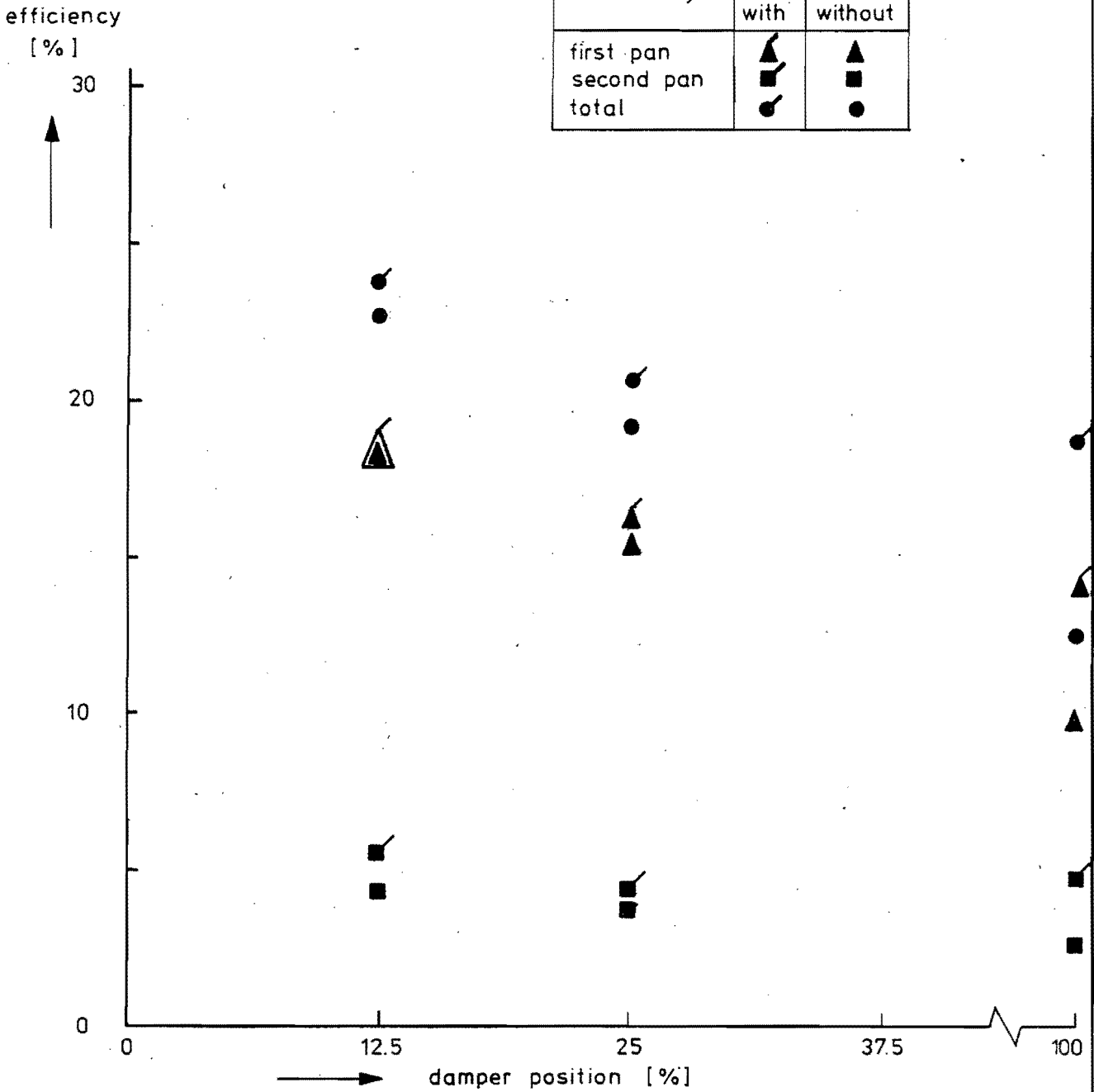


Schematic design of the Nouna wood stove with baffle

MT.TNØ
84940
Fig. 6.8

wood charge : 4 pieces
 size of wood : 0.02×0.03×0.2m
 time between two charges : 8 min.
 average heat output of fire: 8.4 kW

efficiency	baffle	
	with	without
first pan	▲	▲
second pan	■	■
total	●	●



Efficiency of the Nouna wood stove as a function of the damper position with and without a baffle

MT_TNO
 84940
 Fig.6.9

CO₂ and CO concentration as a function of the heat output of the Nouna wood stove

wood charge : 4 pieces
 size of wood : 0.02x0.03x0.2m
 damper position : 12.5 %

▲ CO₂ %
 ■ CO %

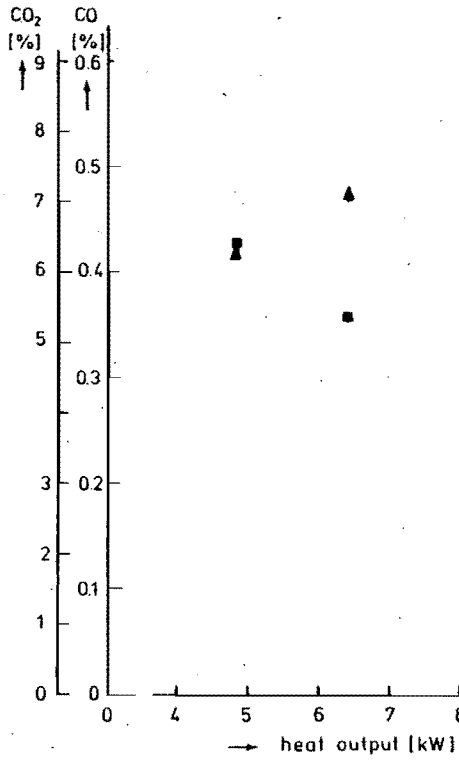


Fig. 6.10 a

wood charge : 4 pieces
 size of wood : 0.02x0.03x0.2m
 damper position : 25 %

▲ CO₂ %
 ■ CO %

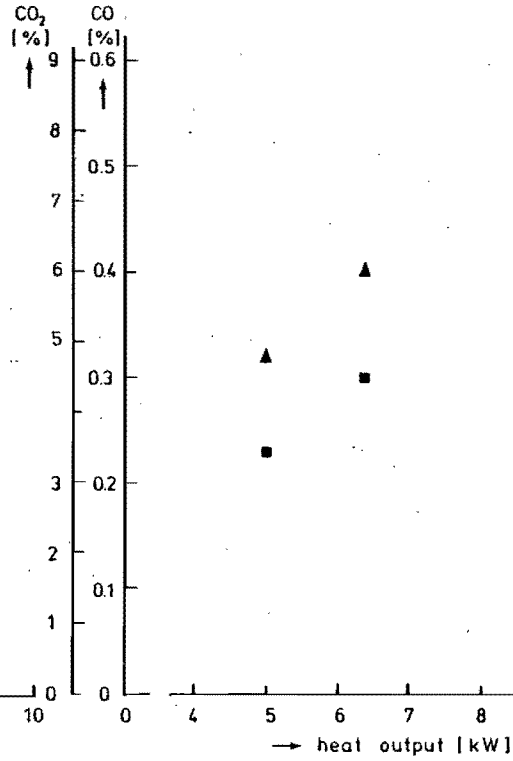


Fig. 6.10 b

wood charge : 4 pieces
 size of wood : 0.02 x 0.03 x 0.2 m
 damper position : 37.5 %

▲ CO₂ %
 ■ CO %

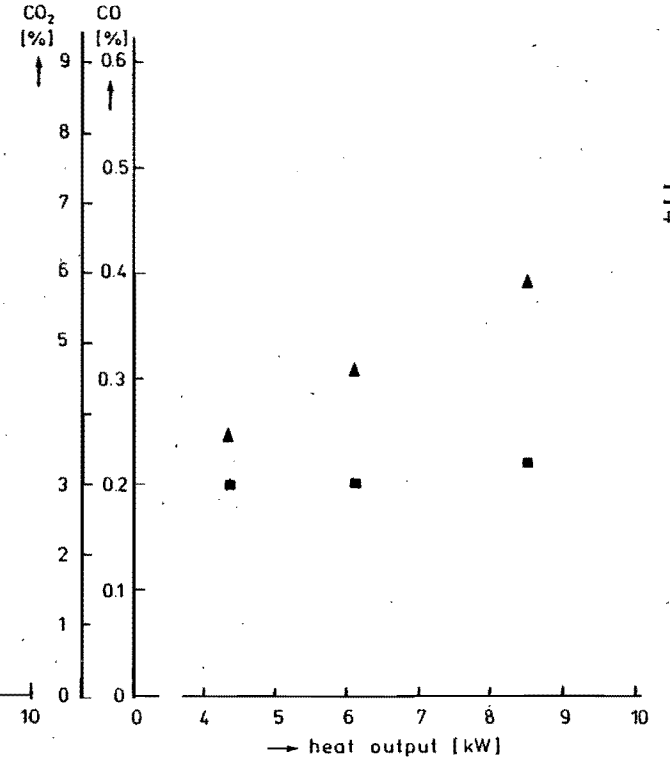
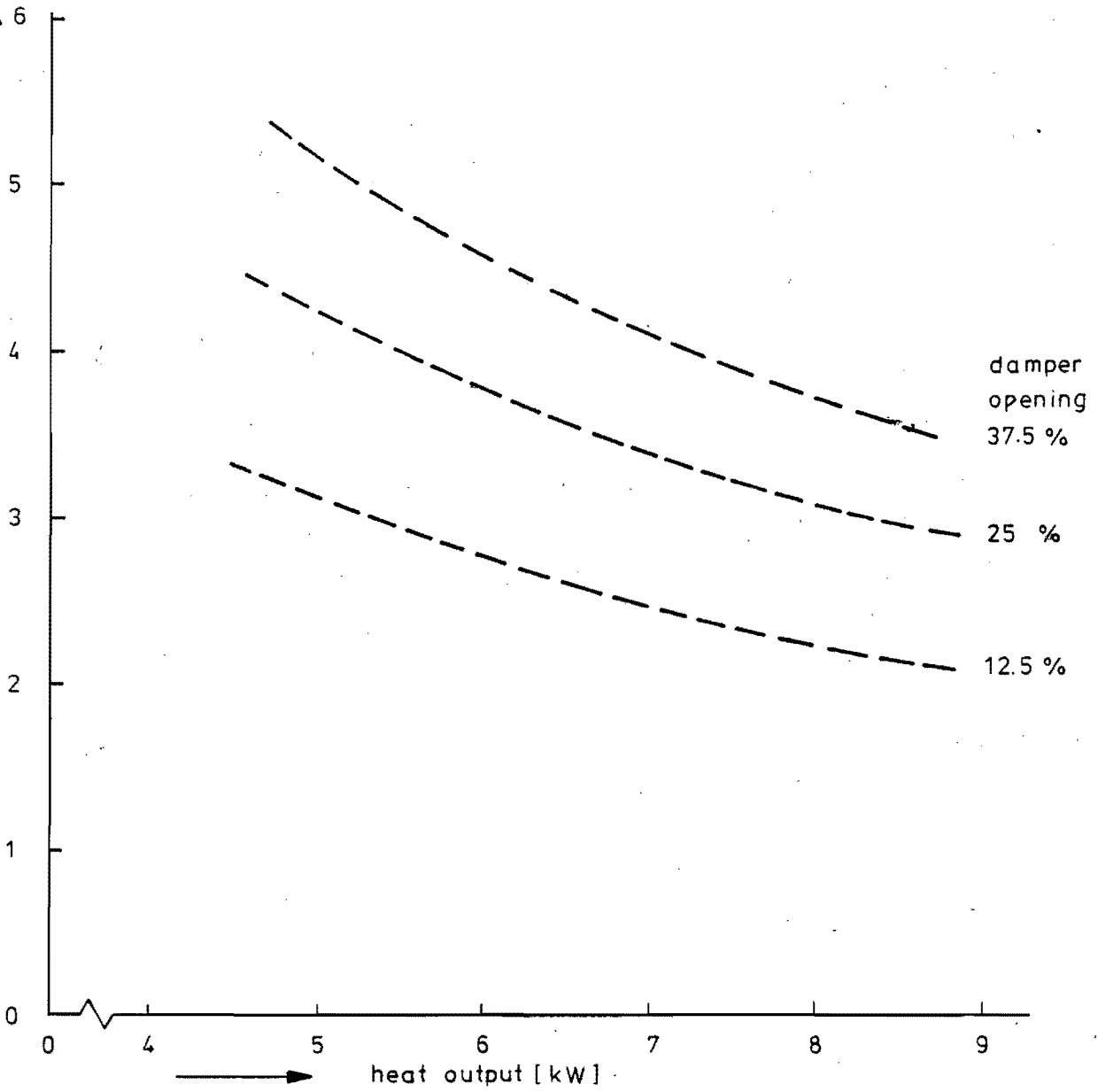


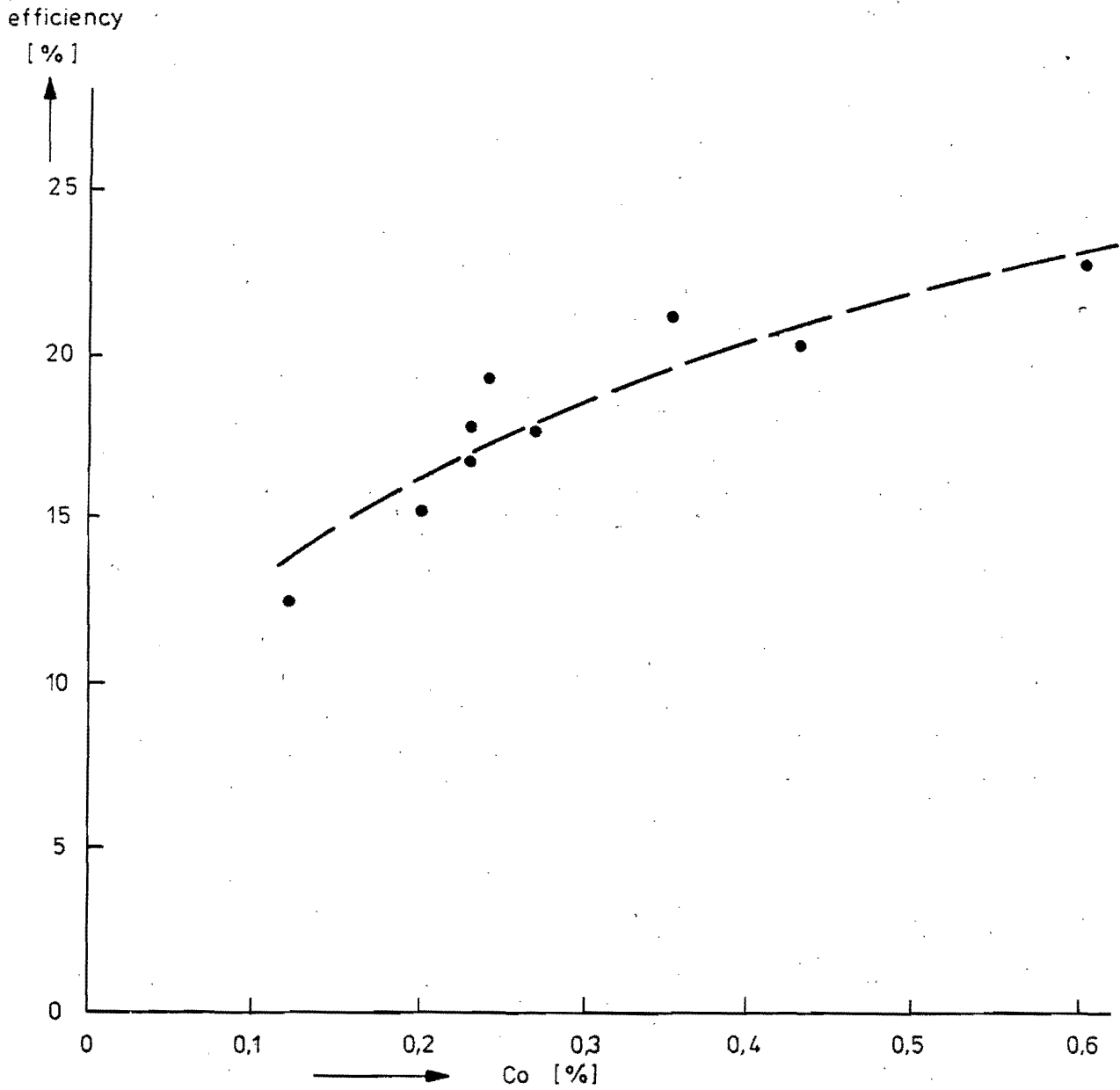
Fig. 6.10 c

excess
air factor



The excess air factor as a function of heat output for different damper positions

MT_TNO
84940
Fig. 6.11



The relation between Co concentration and the efficiency of the stove

MT-TNO
84940
Fig. 6.12

wood charge : 4 pieces
 size of wood : 0.02 × 0.03 × 0.2 m
 heat output : 4.7 kW

▲ CO₂ %
 ■ CO %

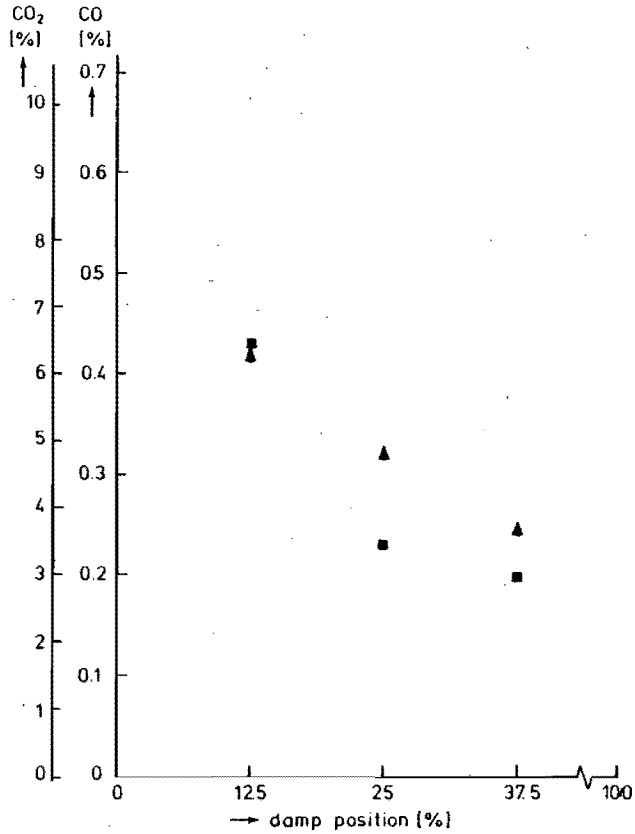


Fig. 6.13 a

wood charge : 4 pieces
 size of wood : 0.02 × 0.03 × 0.2 m
 heat output : 6.3 kW

▲ CO₂ %
 ■ CO %

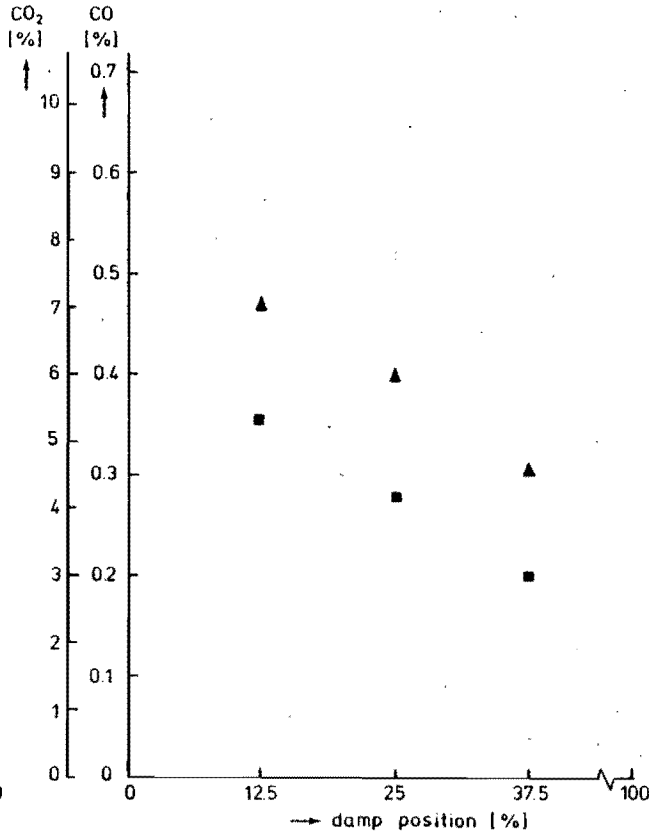


Fig. 6.13 b

wood charge : 4 pieces
 size of wood : 0.02 × 0.03 × 0.2 m
 heat output : 8.7 kW

▲ CO₂ %
 ■ CO %

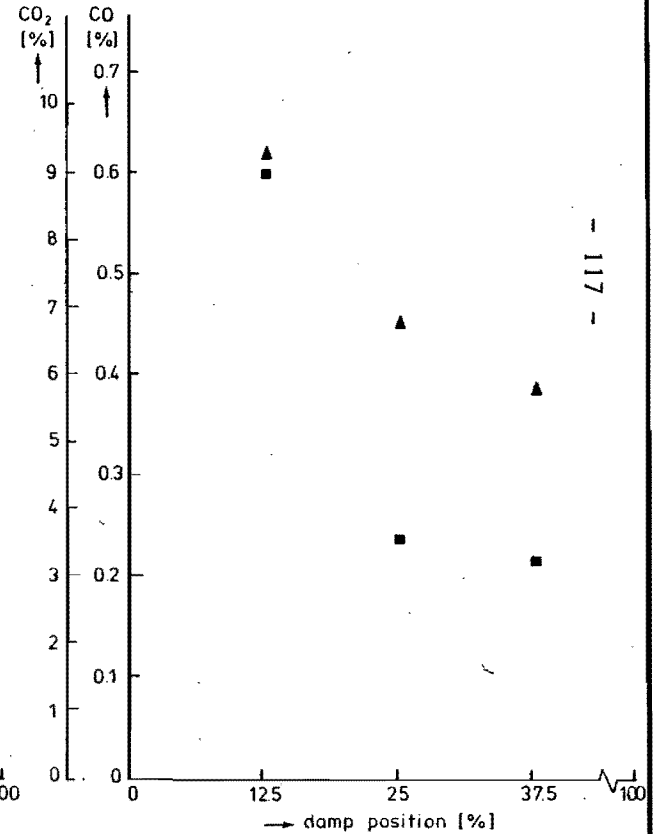
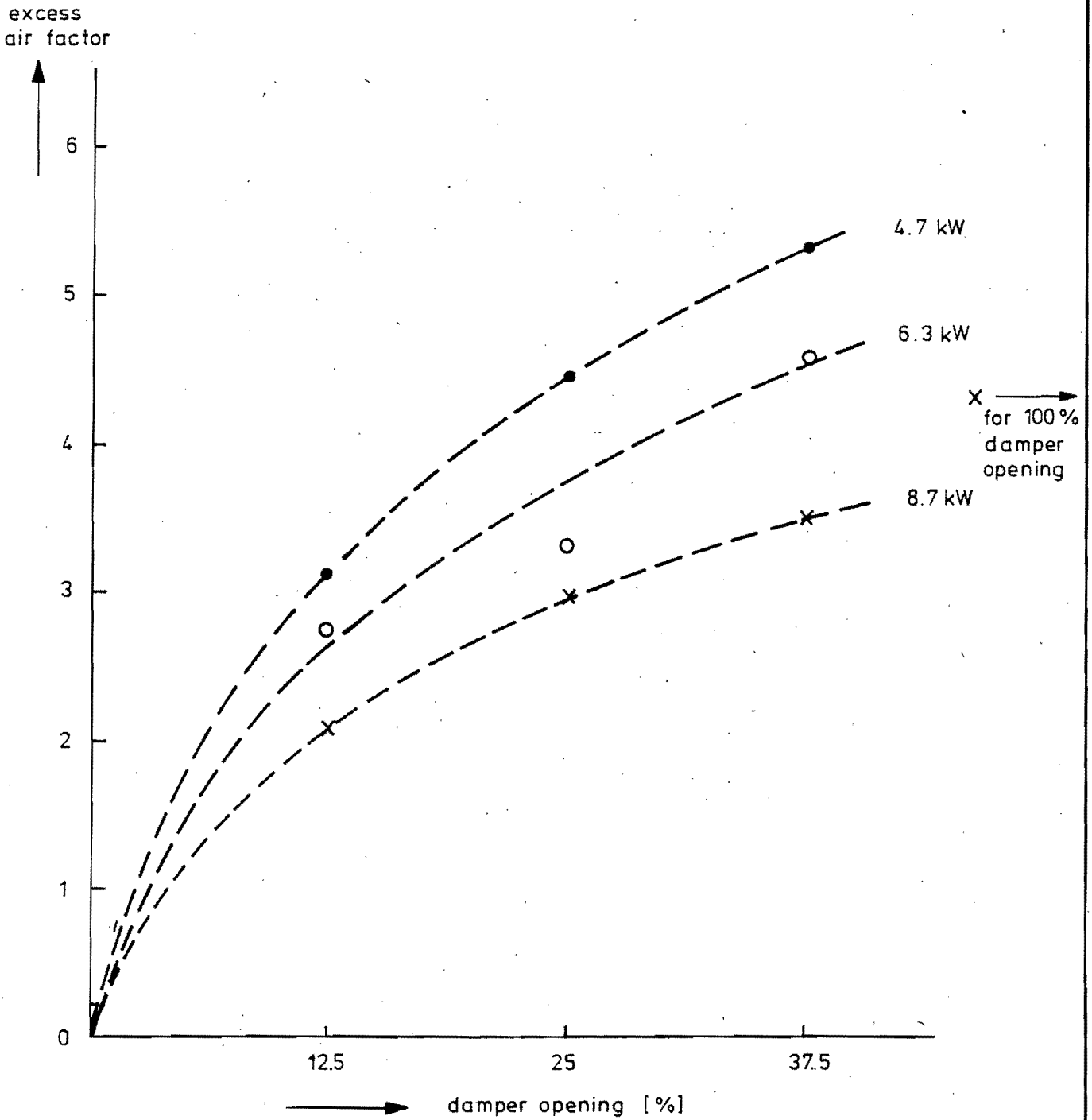


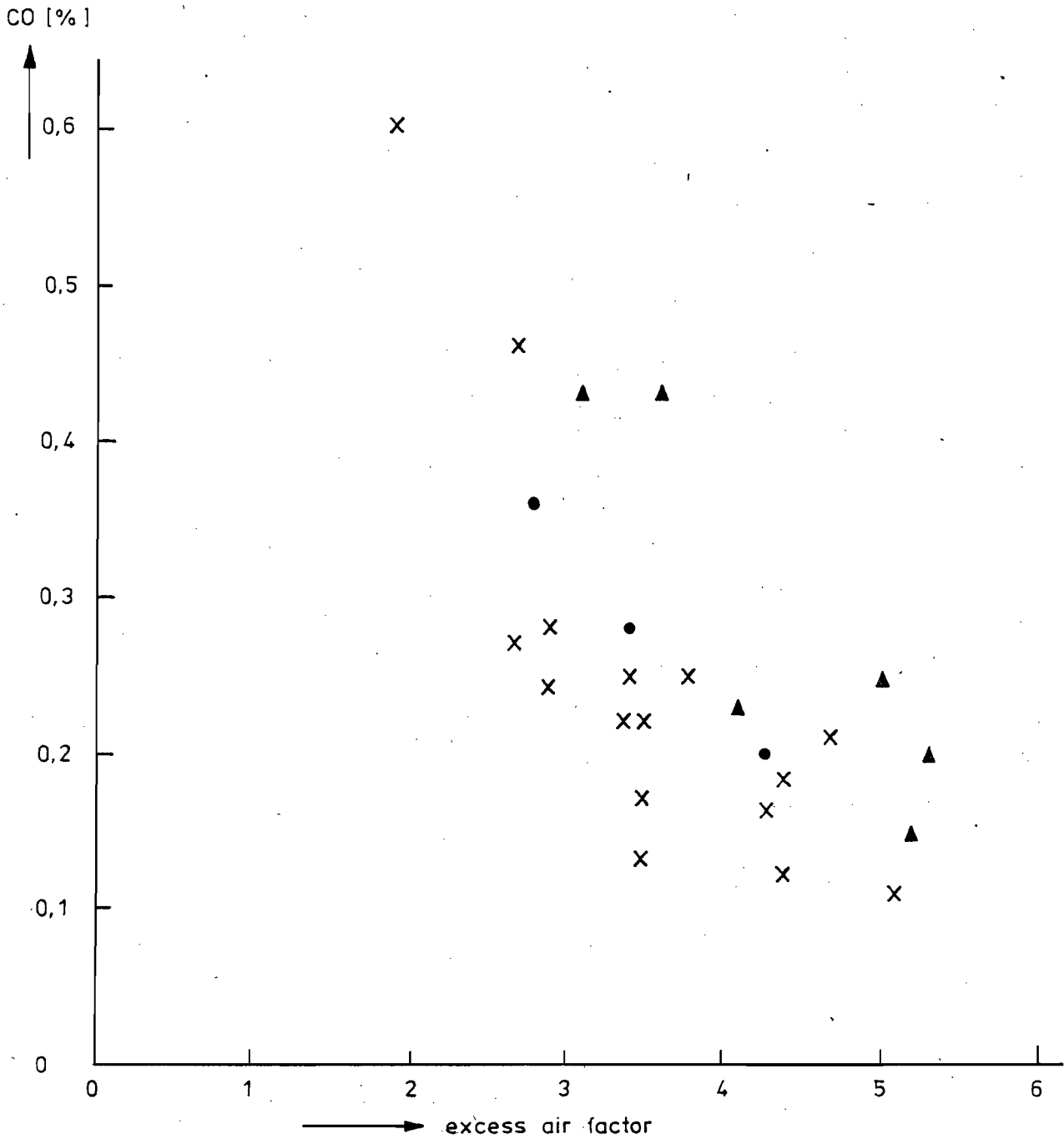
Fig. 6.13 c



The effect of the damper opening in the excess air factor

MT-TNO
84940
Fig.6.14

- X heat load \approx 8,7 kW
- heat load \approx 6.3 kW
- ▲ heat load \approx 4.7 kW

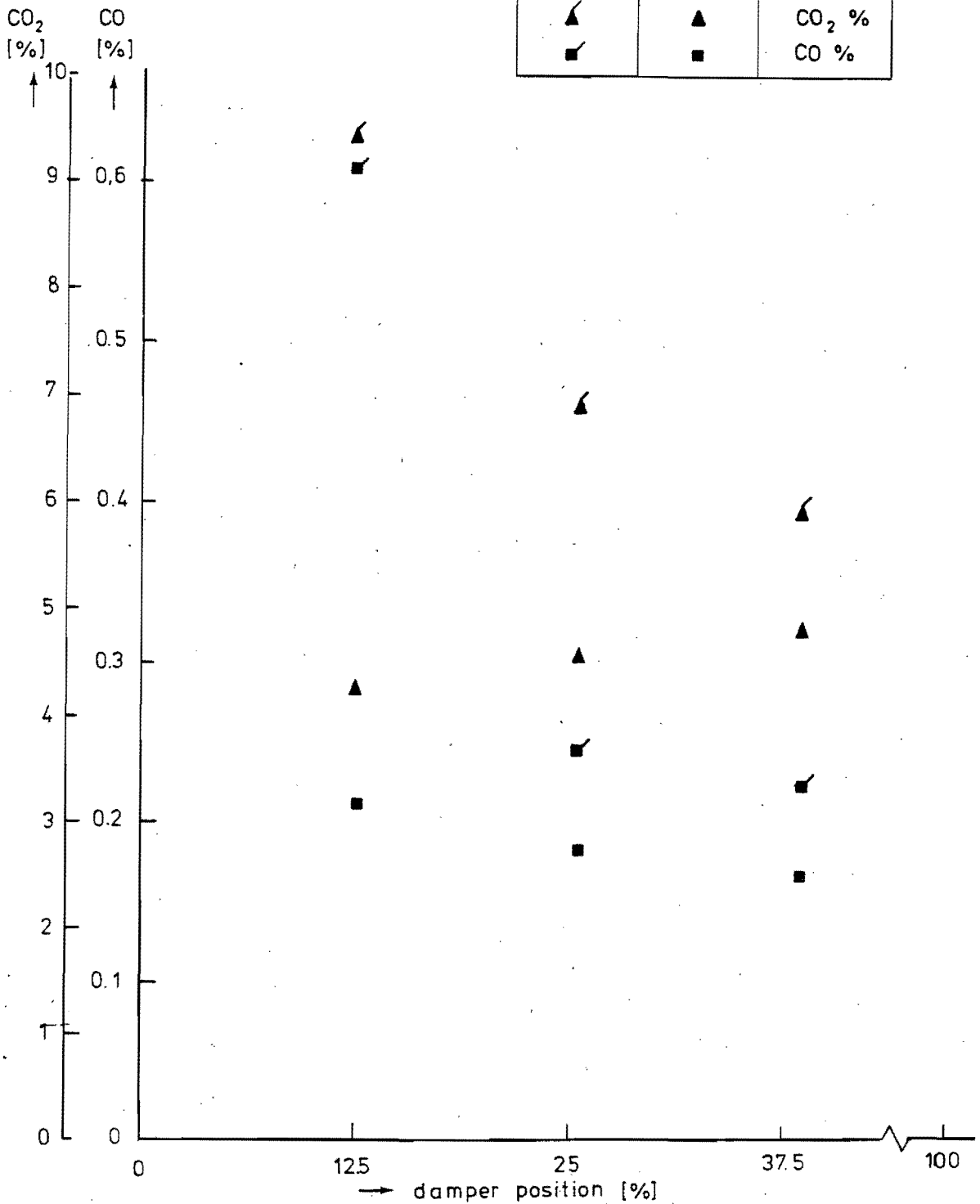


CO. concentration as a function of the excess air factor

MT_TNO
84940
Fig. 6.15

wood charge : 4 pieces
 size of wood : 0.02x0.02x0.2m
 time between two charges : 8 min.
 heat output : 9 kW

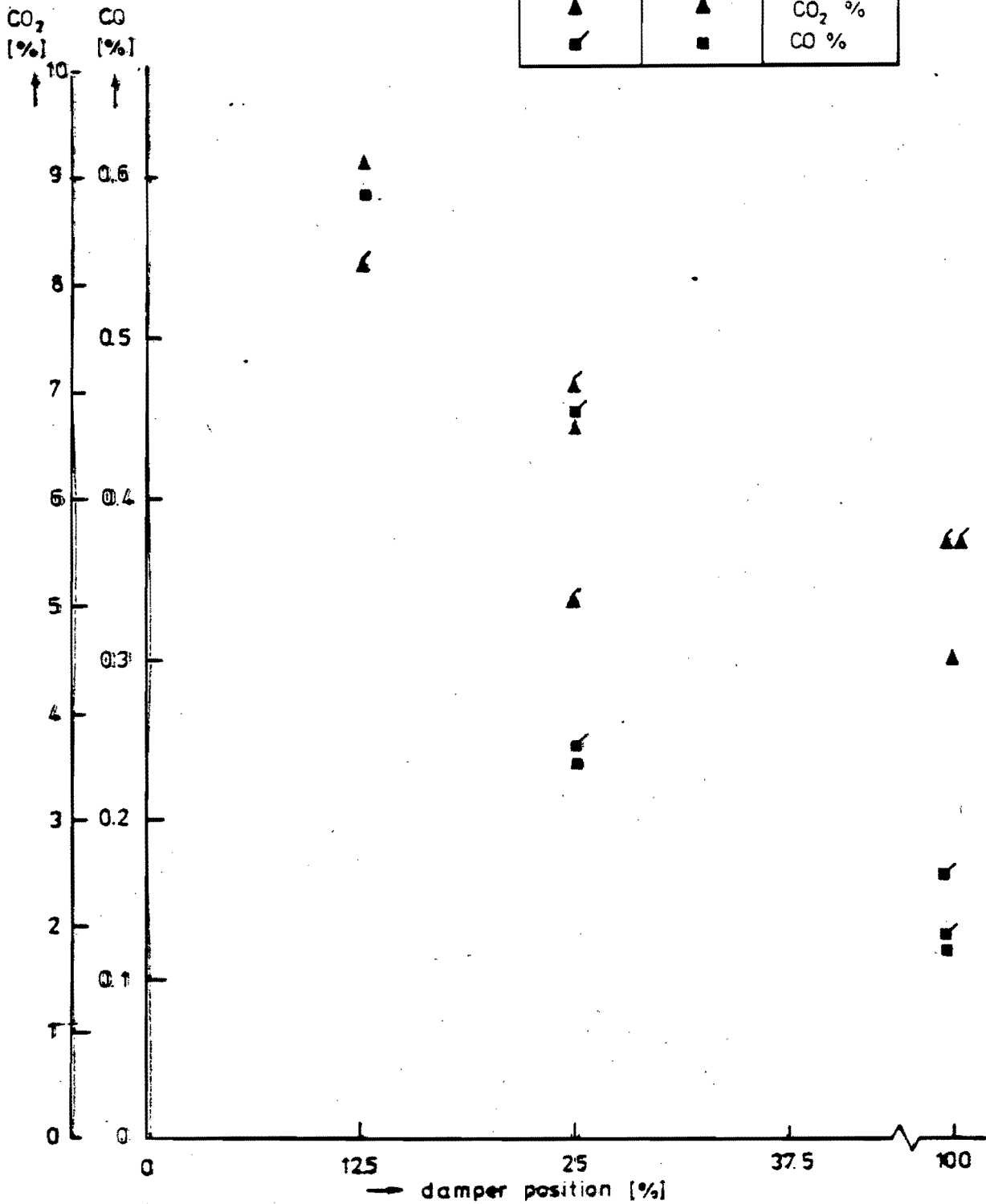
draft [Pa]		
4.9	6.9	
▲	▲	CO ₂ %
■	■	CO %



CO₂ and CO concentration as a function of the damper position with a variation in draft

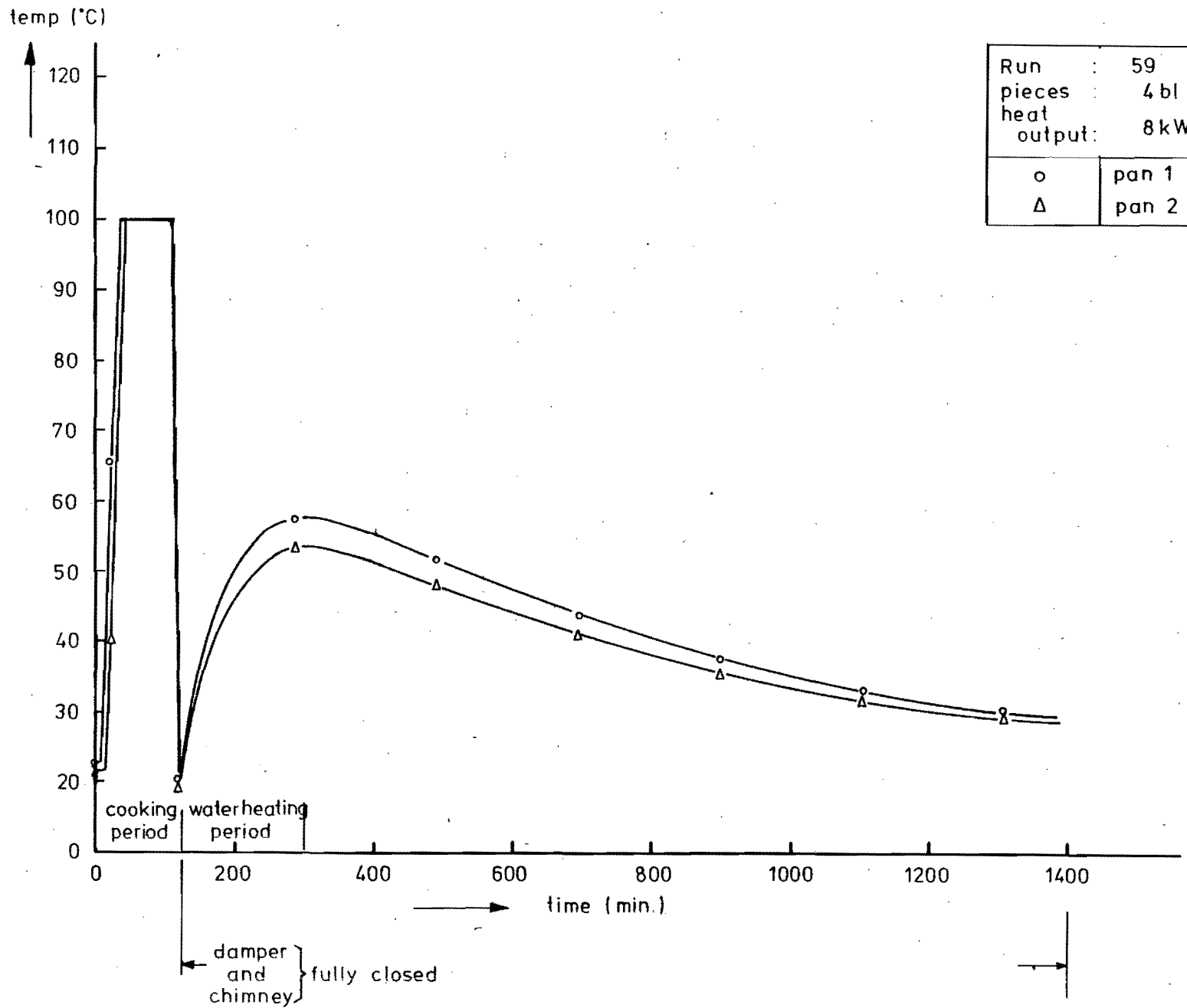
wood charge : 4 pieces
 size of wood : 0.02x0.03x0.2 m
 time between two charges : 8 min.
 heat output : 8.4 kW

baffle		CO ₂ % CO %
yes	no	
▲	▲	CO ₂ %
■	■	CO %



CO₂ and CO concentration as a function of the damper position with and without a baffle

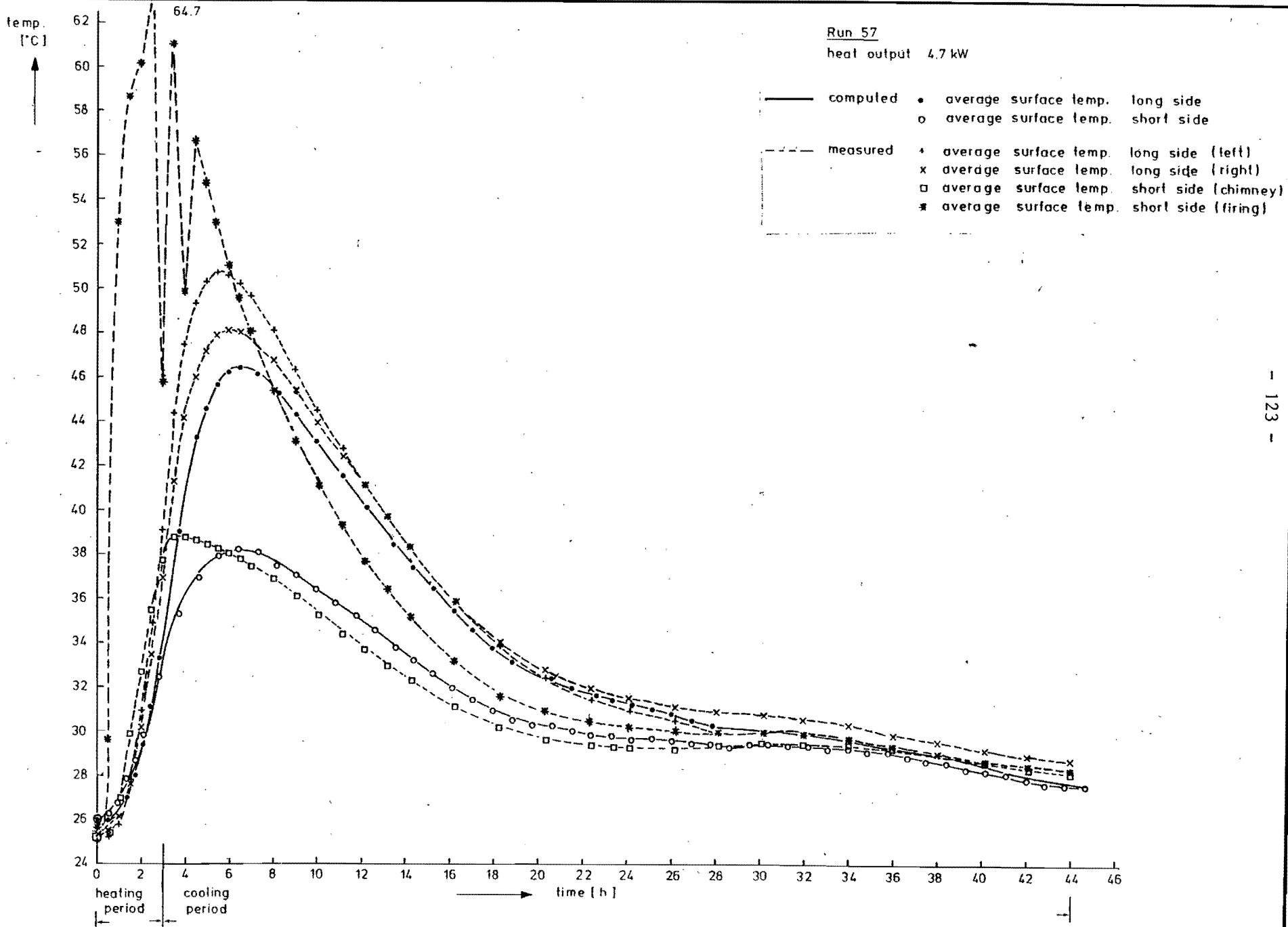
Water temperature as a function of time

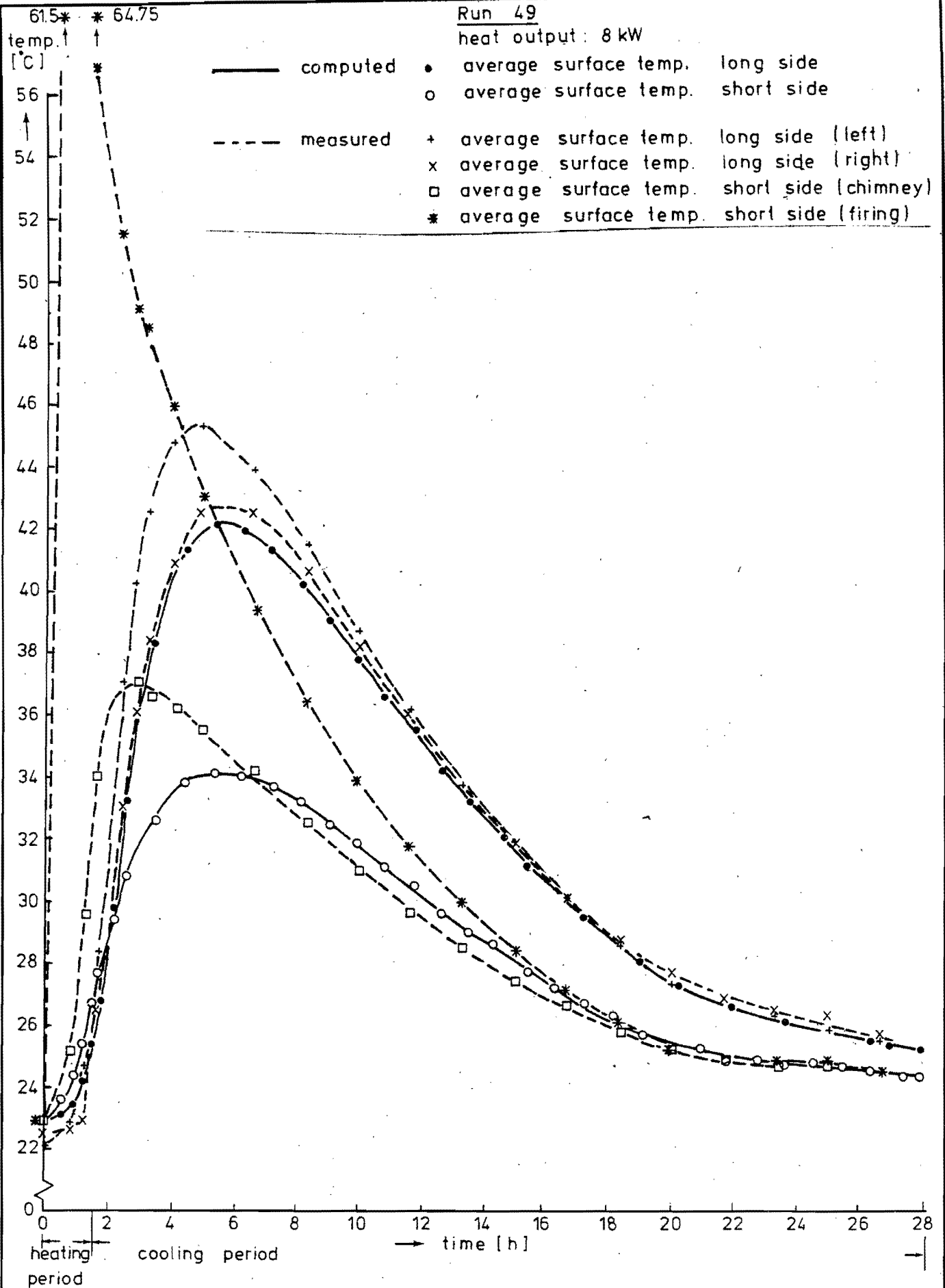


MT, TNO
84940
Fig. 6.18

Measured and calculated temperatures of the side walls

MT-TNO
84940
Fig. 6.19



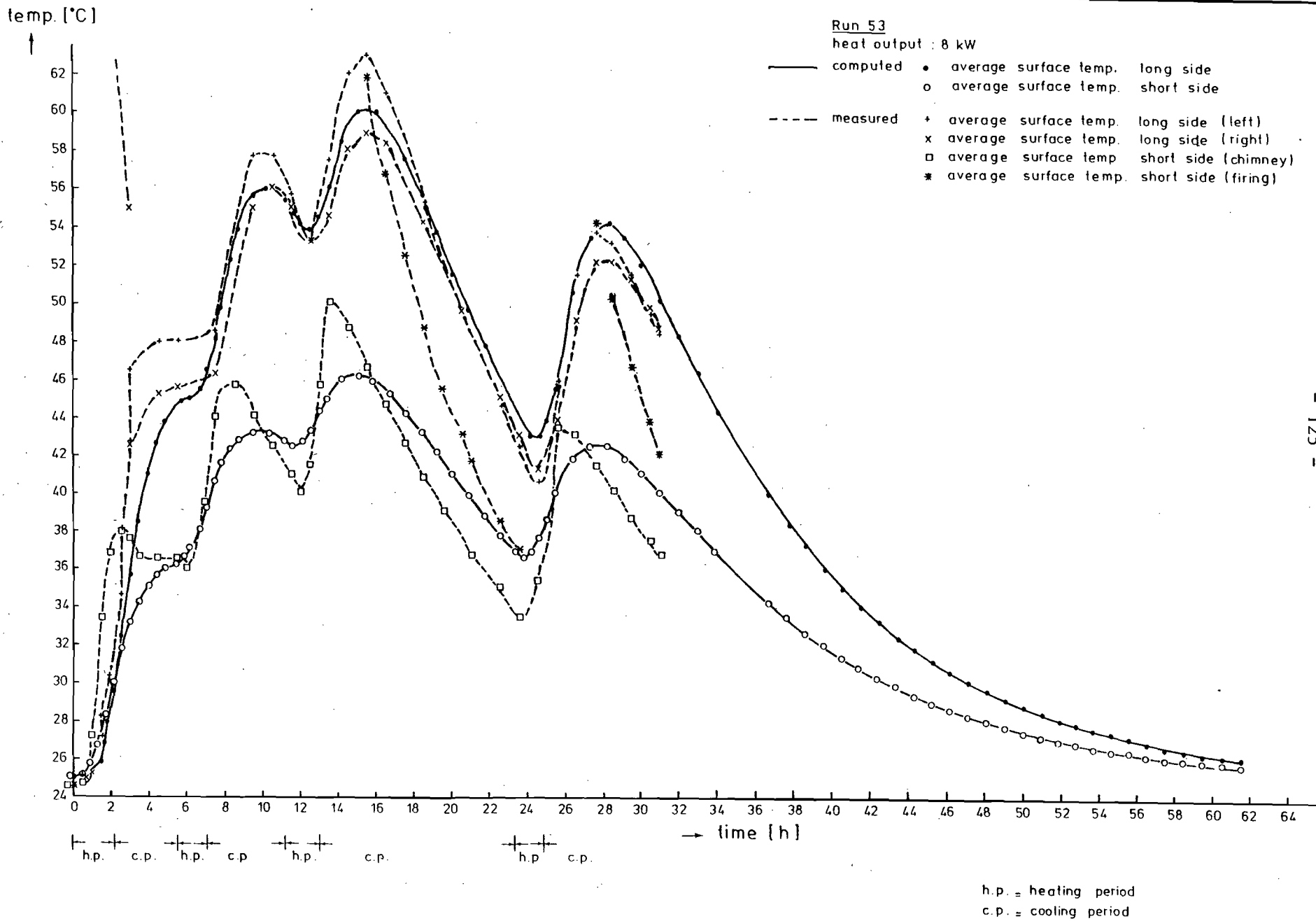


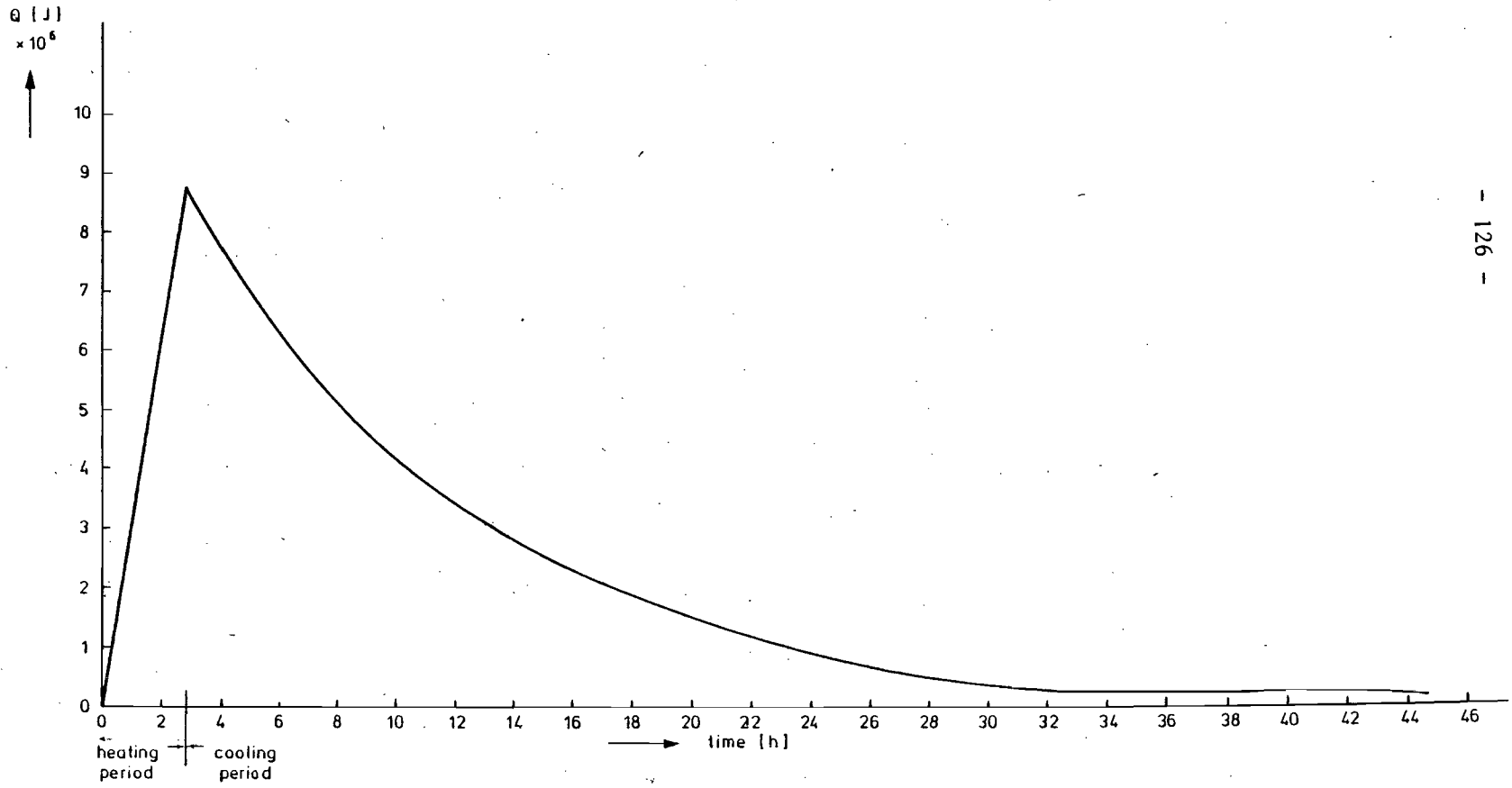
Measured and calculated temperatures of the side walls

MT_TNO
84940
Fig. 6.20

Measured and calculated temperatures of the side walls

MT - TNO
84940
Fig. 6.21

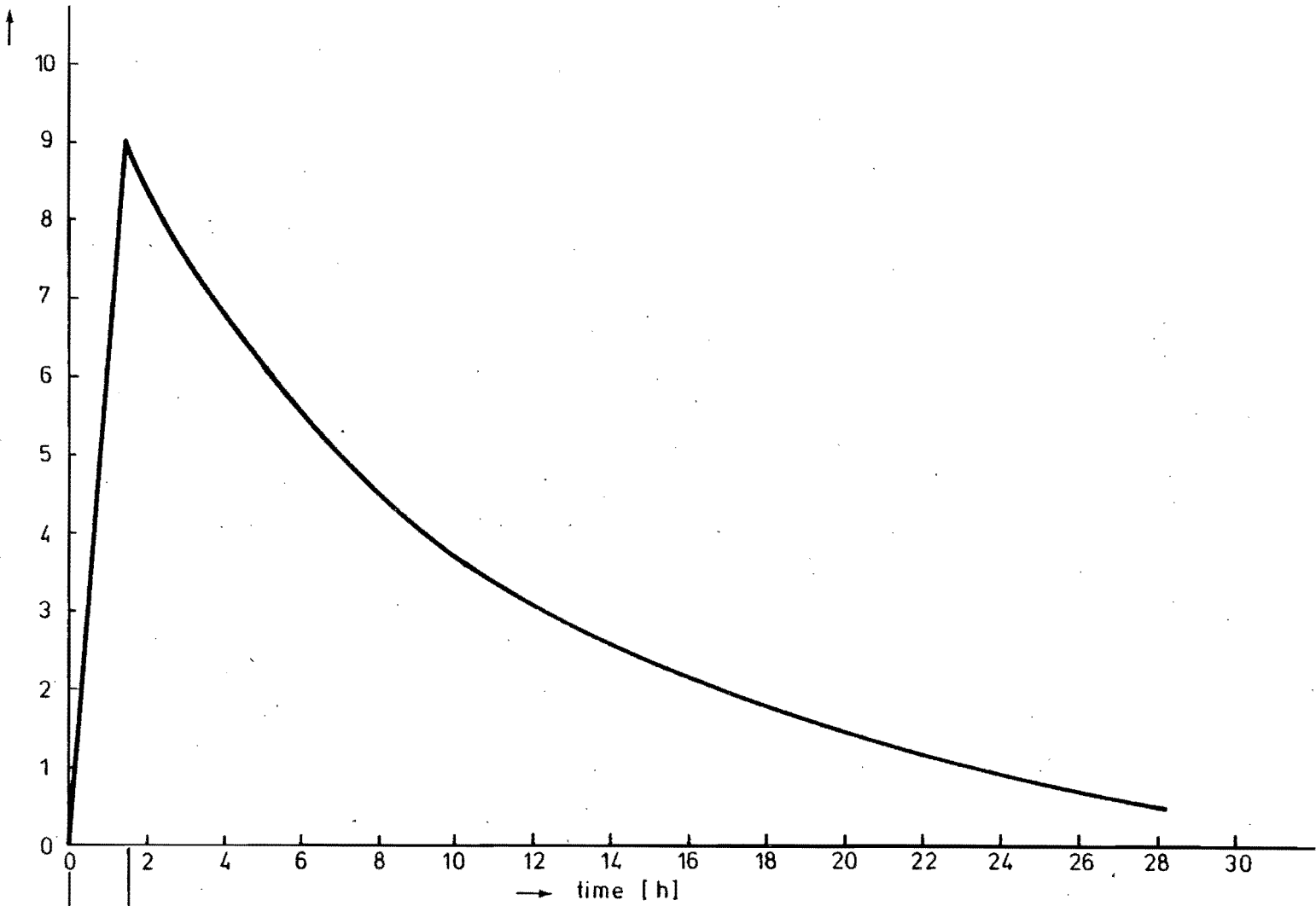




Calculated accumulated heat for half of the stove as a function of time

MT_TNO
84940
Fig. 6.22

$Q [J] \times 10^6$

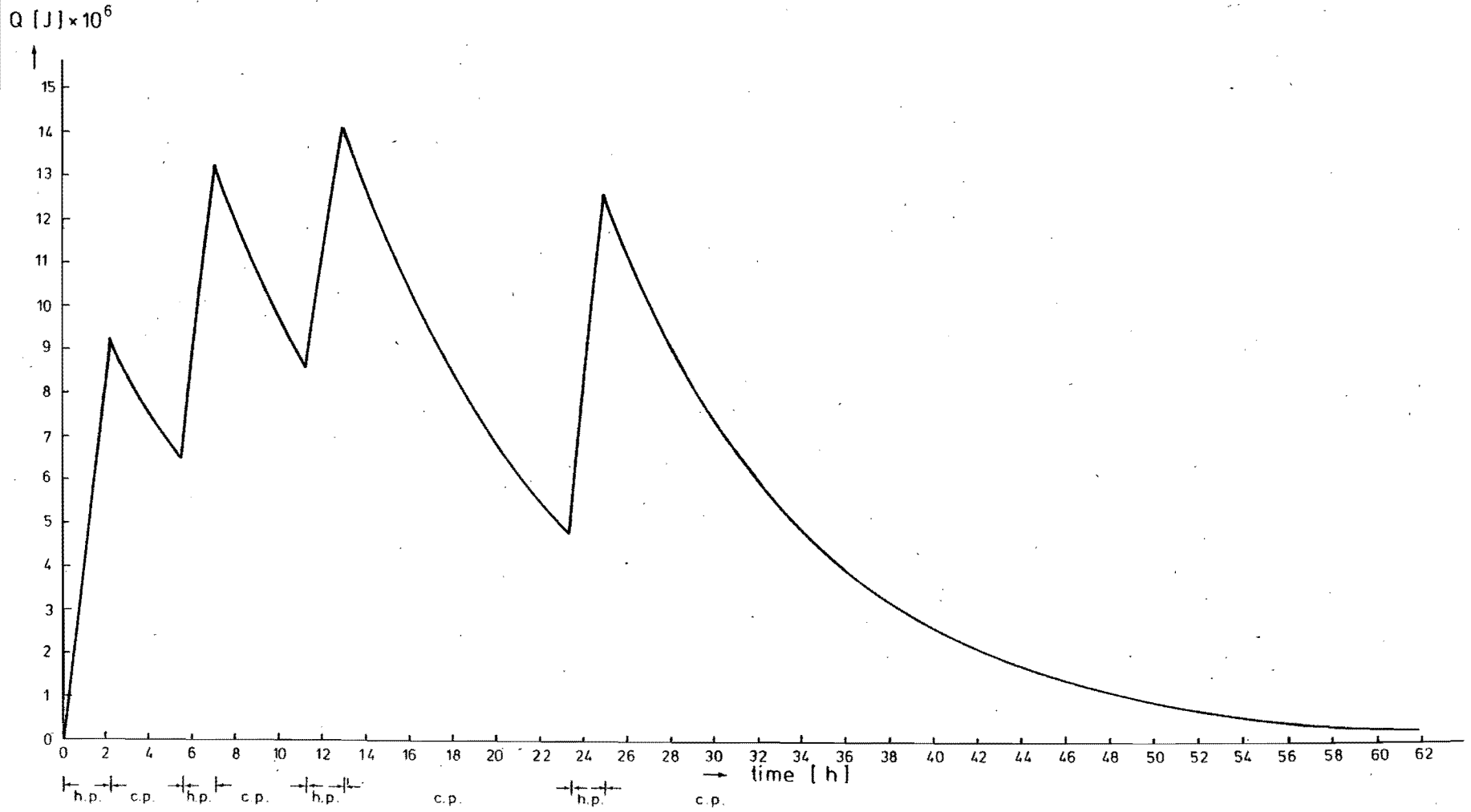


heating period cooling period

Calculated accumulated heat for half of the stove
as a function of time

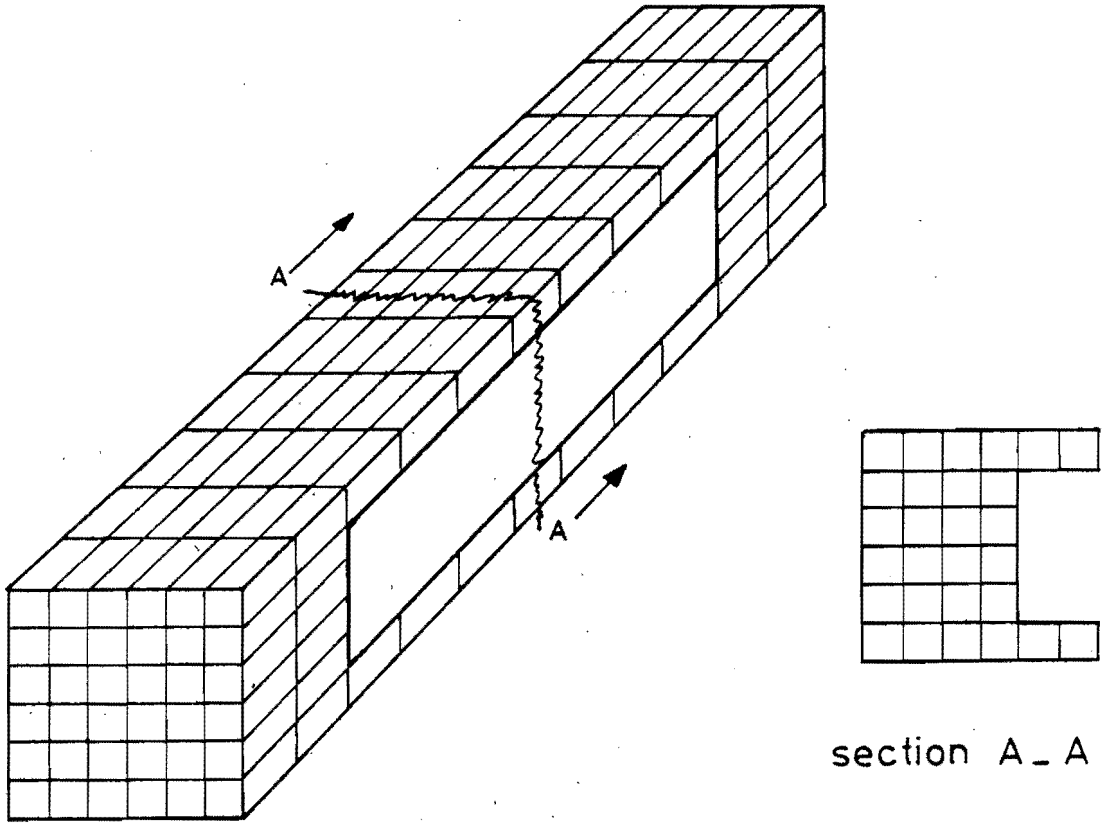
MT_TNO
84940
Fig.6.23

Calculated accumulated heat for half of the stove
as a function of time



h.p. = heating period
c.p. = cooling period

MT-TNO
84940
Fig. 6.24



section A - A

7. SOME EXPLORATORY STUDIES ON AN EXPERIMENTAL HEAVY STOVE

by

Marlies Knoll

Eindhoven University of Technology,

Eindhoven, The Netherlands.

7.1. INTRODUCTION

From time to time various suggestions have been made to improve the performance of wood burning stoves. Some of these suggestions have been actually incorporated in a few designs (see De Lepeleire, et al, 1981 for a description of some of these designs). Unfortunately there has been no attempt to systematically assess the effects of these design ideas on the performance of a stove.

The present paper makes a beginning for such a study. It describes a heavy stove whose configuration can be changed with relative ease so that several design ideas can be checked out under fairly controllable conditions. It goes on then to describe the results obtained for the basic configuration of the stove.

7.2. DESIGN DESCRIPTION

The main consideration in developing the design was the ability to change the configuration of the stove with relative ease. To achieve this, the stove was constructed out of refractory bricks. The bricks were cemented over at the joints with a refractory cement that has fast drying properties.

The joints can be loosened rather easily. A configuration change that is executed on a Friday is ready for firing the next Monday morning.

The work reported here is part of the final year assignment towards the Ingenieur degree in Environmental Sciences at the Agricultural University at Wageningen.

Fig. 7.1. The experimental heavy stove

Principle design features
 Main measures:
 0.93 x 0.52 x 0.45 m
 Power range..... 2.5-12 kW
 Efficiency..... 20-33 %
 Charge..... 300 g

the topplate : Aluminium ; 0.01 m thick
 the chimney : Aluminium ; 1 m high
 the grate : Steel ; 0.25 x 0.25 m²
 the door : Steel
 the maximum damper inlet area : ; 0.050 x 0.134 m²

distance grate - bottom of first pan : 0.12 m
 distance grate - stove bottom : 0.03 m
 distance second pan bottom - stovebottom : 0.03 m
 distance side walls of pans - stove walls : 0.01 m

Height of the baffle between part I and part II of the stove : 0.12 m

THE CHIMNEY
 The chimney is for providing the draught to overcome the resistance to flow inside the stove-body. The height and diameter of the chimney are to be matched with the maximum desired heat-output from the stove. It also serves to remove the smoke from the kitchen

THE CHIMNEY DAMPER
 Reduction of the draught to meet the low output-needs of some cooking operations is possible to a certain extent by the use of the chimney damper

THE LIDS
 The lids bring the food to the boil faster by reducing the heat-losses. Lid on the second pan is a must

THE SECOND PAN
 The main purpose of this pan is to extract heat from the combustion gases which would otherwise have been wasted up the chimney

THE TOP PLATE
 most difficult problem for all-clay stoves
 -problems:
 -construction of passages inside the stove body is difficult
 -crumbling of the pan-holes between the two pan-holes etc etc
 -can be overcome when the plate is made of a separate material (like metal, concrete or ferroccement)

BAFFLES
 to direct the hot gases closer to and around the pans
 1 a step at the bottom of the stove-body to confine the flames under the first pan
 2 side-baffles and back baffles:
 -help increasing heat-transfer surface area to the second pan
 -reduce the area of gas-flow passages to increase flow-velocities thus increasing heat-transfer to the second pan

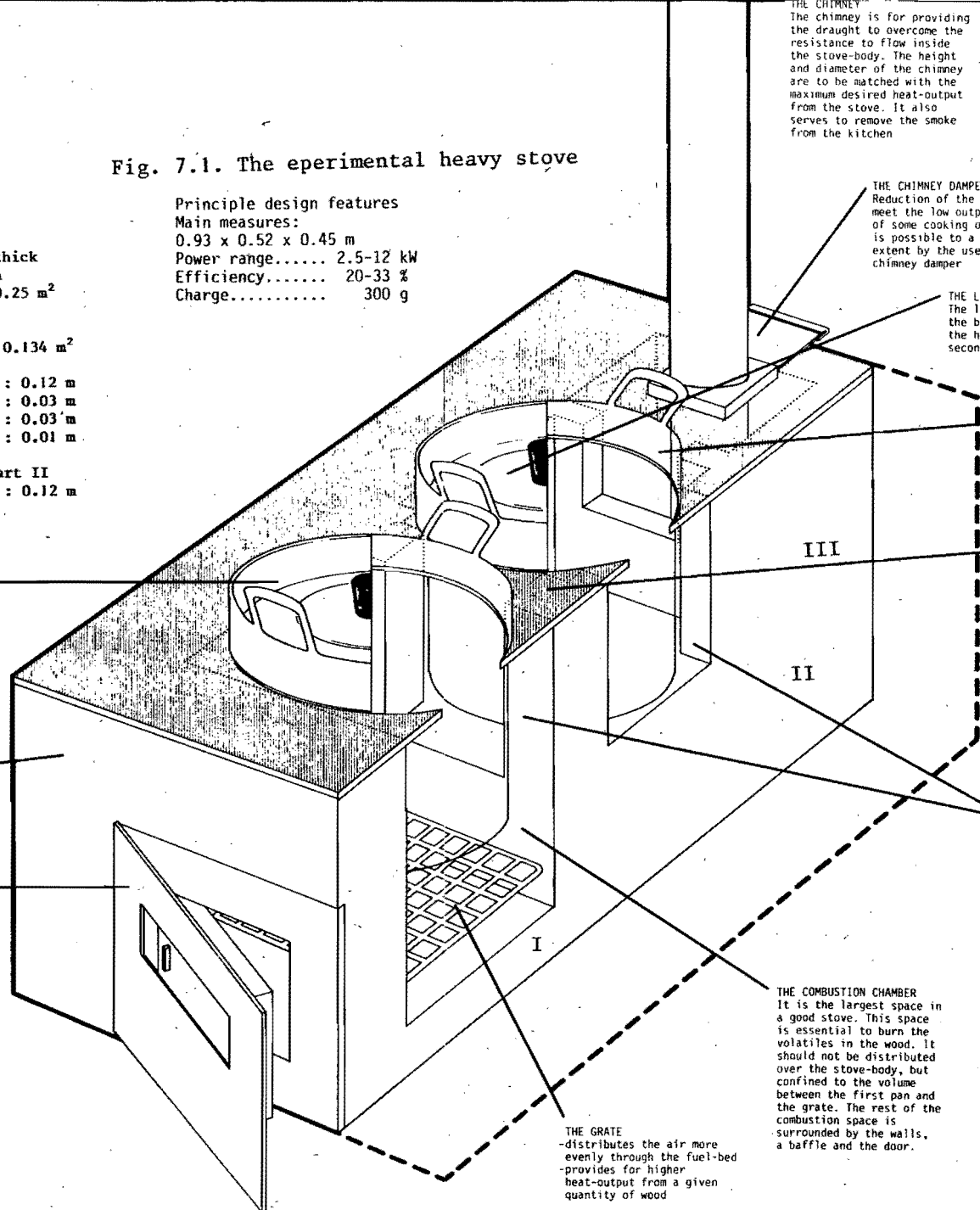
THE COMBUSTION CHAMBER
 It is the largest space in a good stove. This space is essential to burn the volatiles in the wood. It should not be distributed over the stove-body, but confined to the volume between the first pan and the grate. The rest of the combustion space is surrounded by the walls, a baffle and the door.

THE GRATE
 -distributes the air more evenly through the fuel-bed
 -provides for higher heat-output from a given quantity of wood

THE WALL
 -can be built of clay, cement-clay mixes, refractory bricks, etc

THE DOOR
 -to prevent too much air getting into the fire
 -by providing a double-walled arrangement, possible to pre-heat the combustion-air
 -provision for an inlet air-damper helps to match the air-flow to the heat-output of the fire, for example, for simmering operations
 -but, will require short lengths of wood

THE FIRST PAN
 -receives the major portion of the useful heat
 -pan to be sunk inside the stove-body to increase heat-transfer to the pan from the fire and to reduce the heat loss from the pan to the outside environment
 -special provisions required to position the pan at the desired height



The basic configuration and dimensions of the stove are illustrated in fig. 7.1. The figure also provides the list of materials used and some of the important dimensions. The several possibilities that are available for changing the basic configuration are described in the following sections.

7.2.1 The combustion chamber

Several options are available to change the volume of the combustion chamber.

- (i) The grate position can be altered by the addition/removal of layers of bricks from the support structure.
- (ii) The entire top plate can be lifted up or lowered down by adding/removing a layer of bricks on the top of the stove.
- (iii) The depth of the pan inside the stove body can be varied with the aid of a locating ring clamp. The basic configuration provides for the maximum depth of the pan inside the stove body.

The combustion chamber configuration will be altered when smaller pan sizes are employed with suitable rings in the panhole.

7.2.2 Second pan configuration

A crucial aspect for study as far as the second pan is concerned is the amount of convective heat transfer to it. This is controlled by the gap between the pan bottom and the stove bottom. Removal/addition of a brick layer at the stove bottom permits changes in the gap. In particular, if the top plate position is changed to alter the combustion chamber volume, the gap can be held constant by adding/removing a layer of bricks from the floor of the stove under the second pan.

Provisions to alter the pan depth in the stove body and pan size are made in a manner similar to that of the first pan.

7.2.3 Air-handling system

The basic configuration of the stove has a door of the type shown in fig. 7.1. It provides for preheating of the inlet air. The door has a damper to control the amount of air that is drawn into the stove. A more primitive form of door can be fitted so that the air preheating can be eliminated. Of course the door can be left out completely to permit the use of long pieces of wood.

The basic configuration of the stove comes with a chimney of 1 m height. The actual position of the gas entry to the chimney can be changed in height as well as orientation by the use of a separate chimney insert. Needless to say a damper is provided in the chimney to study the relative merits of inlet air/chimney control. The chimney height can be varied by using pipes of different lengths.

The baffle height between the combustion chamber and the part of the stove with the second pan can be changed by procedures described for changing the combustion chamber volume. All other baffles shown in the basic configuration can be either removed or changed at will.

The firing door can be set in-line with the chimney or it is possible to adopt a L-firing position. Such a change will provide for changes in air and gas flow paths.

Summing up, essentially three artifices provide for the design flexibility described above:

- (i) stove sealing is done only on the outer stove skin;
- (ii) standard size bricks cut into convenient sizes; and
- (iii) the chimney insert along with the clamping rings.

7.3. INSTRUMENTATION

Fig. 7.2. is an illustration of the set-up used for testing the stove. It also shows the instrumentation used.

The stove temperatures were measured at 19 locations using Chromel-Alumel thermocouples.

The temperatures were recorded by a data acquisition system every minute and punched on a papertape. By means of a computerprogramme the data were processed to get temperature plots.

Rough percentages of CO_2 and O_2 in the fluegas stream, were estimated by a commercial gas analysis apparatus supplied by Bacharach.

With a handpump a fixed amount of fluegas is drawn in the absorbing fluids for CO_2 and O_2 . The separate volume change in the level is a measure for the percentages of CO_2 and O_2 .

Thermo-couple position in the first 14 experiments:

1. inside wall near the first pan; top.
2. inside wall near the first pan; bottom.
3. inside wall near the second pan; top.
4. inside wall near the second pan; bottom.
5. 5 mm. in the outside wall near the first pan.
6. 5 mm. in the inside wall near the first pan.
7. 5 mm. in the inside wall near the second pan.
8. 5 mm. in the outside wall near the second pan.
9. in the water of the first pan.
10. in the water of the second pan.
11. in the chimney at the bottom.
12. in the chimney at the top.
13. at the entrance of the grate.
14. 5 mm. in the bottom of the stove under the second pan.
15. between the first and the second pan on the bottom of the stove.
16. on the baffle between the second pan and the chimney entrance.
17. on the aluminium topplate near the first pan.
18. on the aluminium topplate near the second pan.
19. 30 mm in the backwall of the stove.

The new position of the thermo-couple after the 14th. experiment:

12. under the second pan on the stove bottom.
13. at the entrance of the grate.
14. on the inside wall oposite 3 and 4; middle.
15. between the first and second pan on the bottom of the stove
16. on the baffle at the entrance of the chimney.
17. on the aluminium topplate near the first pan.
18. on the inside wall oposite 3 and 4; top.
19. on the inside wall oposite 3 and 4; bottom.

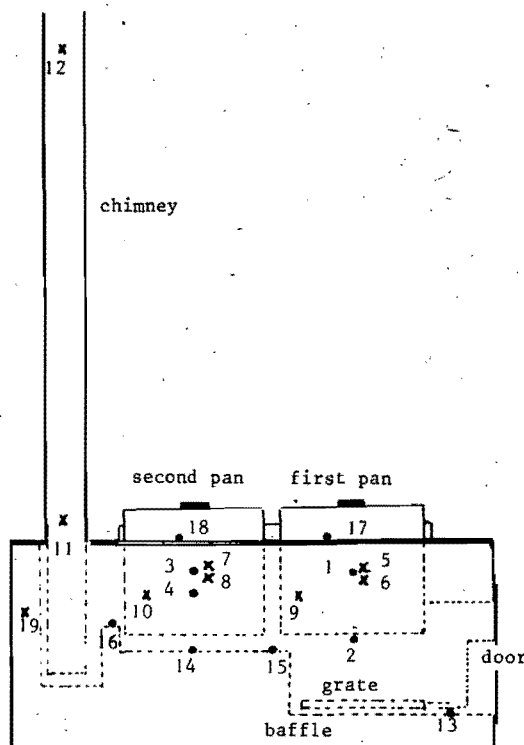


Fig. 7.2.a. Thermo couple position in the first 14 experiments. (see table for the description of the thermo couple positions.)

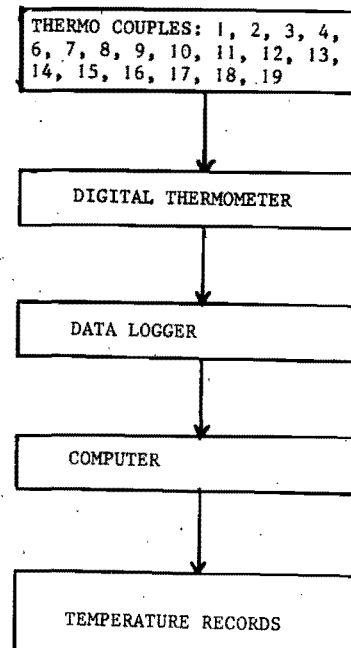


Fig. 7.2.b. Data processing procedure

7.4. EXPERIMENTAL PROGRAMME

In the experiments described below only the basic configuration of the stove is used.

In the first set of experiments the range of power outputs at full damper opening was determined.

By reduction of the damper opening the power output range is reduced as far as possible.

To find an optimum damper position at a certain power output (for two cases), tests were done with two different damper openings.

To extend the upper limit of the range of power outputs the chimney height was doubled.

In addition a few other experiments were done:

The effect of doubling the chimney height on performance and efficiency.

Firing the stove at the highest power output with normal chimney height to be able to compare the results of the doubled chimney height also for the highest power output.

The effects of using an other frontloading door, which provides the unpreheated inlet air right under the grate, on the performance and efficiency.

To be able to do as many experiments as possible, 2 experiments were done per day which means that the initial temperature of the walls of the stove is different at the start of the second test. For two power outputs the effect of this difference in initial temperature on performance and efficiency was tested.

7.5. GENERAL EXECUTION OF THE EXPERIMENTS

Table 7.1. Summary of the test characteristics.

pan type	: ordinary Aluminium household pan
pan size	: diameter : 0.28 m, height: 0.26 m
initial amount of water in both pans	: 5 kg
initial temperature of the water in both pans	: 20 °C
type of wood used	: oven dry white fir
size of the woodblocks	: 8 x 12 x 50 mm
combustion value of the wood	: 18700 kJ/kg
amount of wood used per charge	: 300 g
time between 2 charges	: 8 - 31 min
duration of the experiments	: 2 hours

All the experiments were water boiling tests. Basically the experiments were done in the way described in this chapter and summarized in table 7.1.

Before each experiment the ashes were swept out of the stove and the soot was brushed from the bottom of the pans. Better cleaning of the pans seemed impossible, because of a thick layer of brittle smooth tar. Later it was suggested to clean the pans and use a coating of soap. It appeared, in that case, most of the tar could be washed off at the end of the experiment.

The fire was lit by a propane burner, which takes less than a minute. The moment the wood caught fire was regarded as the start of the experiment.

With low initial temperature of the stove there were often starting problems. To avoid these an electric heating wire of 200 W was used to heat the chimney during the first 15 minutes of the experiment. Starting the stove with the door open could possibly help to avoid starting problems, but this was not tried.

It is also possible to adjust the baffle configuration and/or the passages in the stove more precisely.

In all the tests 300 g of tiny blocks of oven dry white fir were used.

After the last charge the end of the experiment was indicated by the temperature drop of the water in the first pan below boiling point. The duration of the experiments is limited to approximately two hours or less. During the first seven experiments CO₂ and O₂ were measured by Bacharach's approximately every five minutes. So the number of gas samples analysed between two charges differed with the power output.

The efficiencies have been calculated according the definition given by THE, Eindhoven and TNO, Apeldoorn (see paragraph 3.2.1).

7.6. RESULTS AND DISCUSSION

A summary of all the results can be found in appendix 7.1. In the next paragraphs the results of the tests done according to the experimental programme are discussed.

7.6.1 The power output range

Table 7.2. summarizes the results of the tests done to find the range of power outputs.

Table 7.2.: power output range.

Mass of water in first and second pans : 5 kg
 Mass of the charges : 300 g
 Chimney height : 1 m
 Door type : heavy

Run no.	T _i	d.p. (%)	P (kW)	t _{b1} (min)	t _{b2} (min)	t _t (min)	η ₁ (%)	η ₂ (%)	η _t (%)
22	C	100	11.7	19	80	80	22.0	3.8	25.8
* 5	C	100	10.4	45	92 ^o C	96	12.4	5.8	18.2
6	H	100	10.4	20	50	90	20.1	7.1	27.2
1	C	100	7.8	23	62	90	21.4	6.2	27.6
2	H	100	6.7	23	80	90	22.0	7.3	29.3
3	C	100	5.8	38	101	120	24.7	6.2	30.9
* 7	C	90	4.9	43	116	116	18.8	5.8	26.6
8	C	80	4.9	27	95	116	20.5	7.8	28.3
**23	C	70	3.9	31	101	120	25.0	6.6	31.6
13	C	60	3.9	33	92 ^o C	120	23.4	6.5	29.9
**10	C	50	3.9	50	93 ^o C	120	19.8	7.0	26.8
**11	H	40	3.0	40	88 ^o C	124	22.3	8.4	30.7
14	C	30	2.5	45	62 ^o C	111	19.8	4.0	23.8

(The meaning of the symbols can be found at the end of chapter 7.7)
 * experiments with starting problems
 ** chimney heated for at least 50 min. The efficiencies are corrected for the extra heat input

From this table can be seen that the power output range, without using the damper, is 11.7 - 5.8 kW.

By closing the damper the stove can be forced to produce a lower power output. As is shown in the second part of table 7.2. the lowest power output is 2.5 kW.

7.6.2 The efficiency at different power outputs

Leaving out the experiments with starting problems (*) it appears that the total efficiency slightly increases with decreasing power output, from 27 % to 31 % for the higher power output range. For the lower power outputs the efficiency increases from 25 % to 30 %. The efficiency for the second pan is about 6 - 8 % and independent of the power output.

A possible explanation for increasing efficiency at decreasing power outputs is a better combustion at an optimum amount of excess air. The average percentages of O₂ and CO₂ measured by the commercial gas-analyzers are used to estimate the percentages of excess air in the flue gas.

Table 7.3. The change in the amount of excess air with the power output.

Run no.	T	d.p (%)	P (kW)	excess air (%)	η_t (%)
1	C	100	7.8	77	27.6
2	H	100	6.7	82	29.3
3	C	100	5.8	100	30.9
* 7	C	90	4.9	122	24.6

* experiments with starting problems.

The results are not very accurate but show a tendency to an increasing excess air factor at lower power outputs. There are no gas analyses available for the other experiments.

Therefore it is not possible to estimate the optimum excess air factor. From table 7.3 it seems that the optimum amount of excess air is about 100 % or perhaps a little more.

7.6.3 The efficiency in the heating-up period

For power outputs of over 4.9 kW the efficiency in the heating-up period of the first pan is lower compared to the average efficiency of the first pan. From 4.9 kW down to 2.5 kW the opposite is true (see table 7.4)

Table 7.4. The efficiency in the heating-up period for high and low power outputs.

Run no.	d.p. (%)	P (kW)	η_{1H} (%)	η_1 (%)	t_{ba1} (min)
22	100	11.7	12.0	22.0	> 40
* 5	100	10.4	6.1	12.4	-
6	100	10.4	13.4	20.1	50
1	100	7.8	15.9	21.4	40
2	100	6.7	18.9	22.0	30
3	100	5.8	18.1	24.7	40
* 7	90	4.9	13.7	18.8	10
8	80	4.9	22.4	20.5	0
**23	70	3.9	23.1	25.0	-
13	60	3.9	22.2	23.4	-
10	50	3.9	14.7	19.8	-
**11	40	3.0	24.4	22.3	0
14	30	2.5	26.1	19.8	7

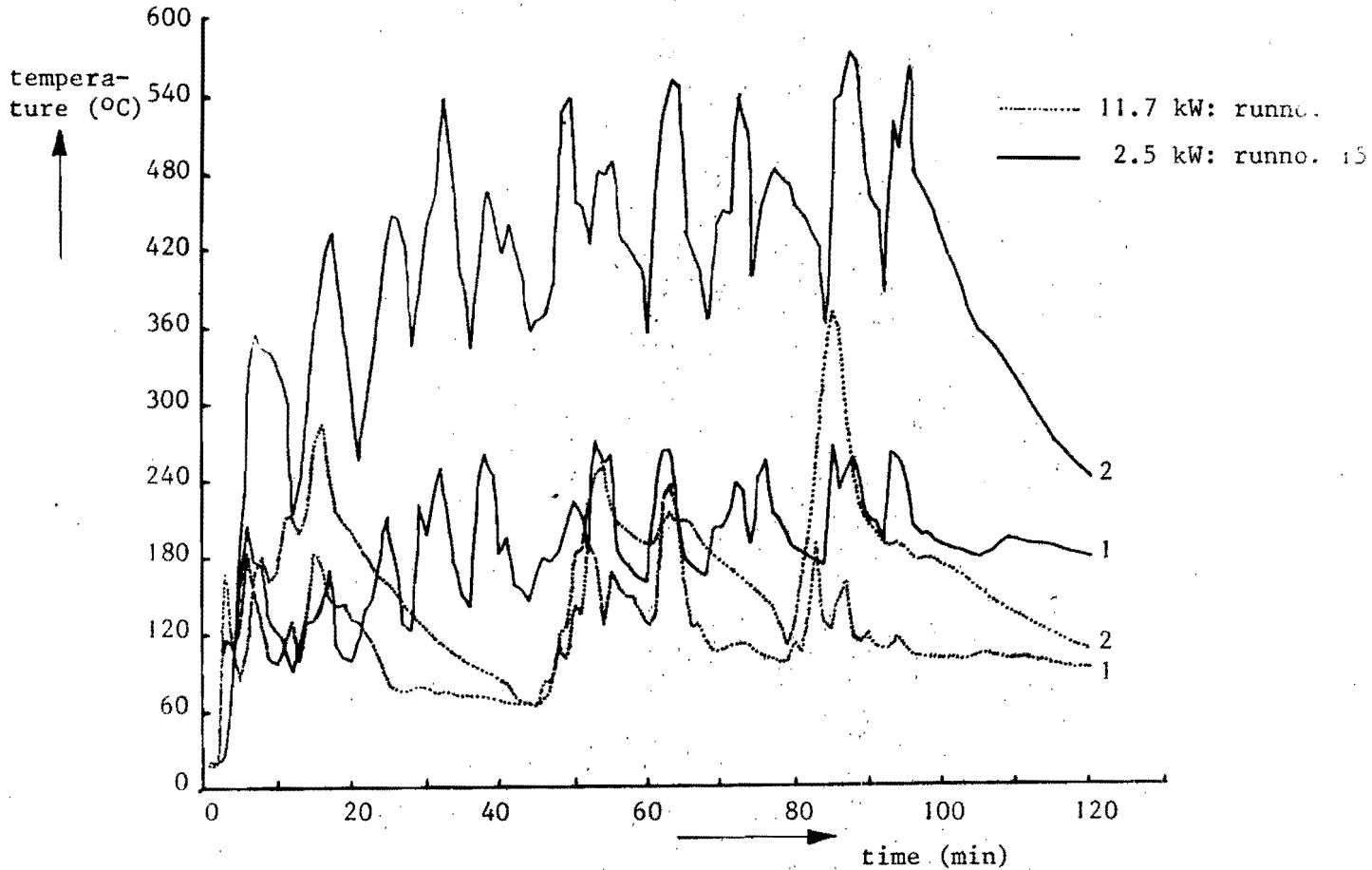
* experiments with starting problems

** chimney heated for at least 50 minutes.

The cause of this difference is the enormous heat capacity of the stove. An average of 0.65 kg of wood is needed to bring the stove to its main operating temperature (see chapter 7.6.8).

In case of a high power output the operating temperatures are considerably higher than at low power outputs, as it is clearly shown by the examples in figure 7.3. for the wall temperatures near the first pan.

Fig. 7.3. Temperature records of the wall temperatures near the first pan (1 and 2) for high and low power output.



At high power outputs the time interval between two charges is short. About 20 % of the energy used for bringing the stove to operating temperature can be regained but only after the theoretical ending of the experiment (calculated from the power output and used amount of wood).

The heat recovered from the walls and released by the charcoal remaining after the experiment keeps the water in the first pan boiling for 30 to 50 minutes longer (t_{ba1}). These 30 to 50 minutes are not taken into account in the efficiency calculations.

Thus it is clear that the efficiency during the heating-up period equals the average efficiency over the whole experiment. In the calculation of the total efficiency the end of the experiment is indicated by the moment the first pan stops boiling. For the higher power outputs this results in a lower efficiency in the heating-up period compared to the total efficiency. The somewhat higher efficiencies for the heating-up period at low power outputs are due to the better heat transfer in this period because of a larger temperature difference between the pan and the fire.

7.6.4 The efficiency of a hot and a cold stove

In order to do as many experiments as possible sometimes two experiments were done on one day.

At the first experiment the stove would be cold, for (about 20°C) and at the start of the second experiment the stove was at about 60°C. This must be taken into account when attempting to interpret the results.

Table 7.5. The efficiency of the hot and cold stove at the same power output.

Run no.	T _i	P (kW)	d.p. (%)	τ _t (min)	τ _{b1} (min)	τ _{b2} (min)	η ₁ (%)	η ₂ (%)	η _t (%)
* 5	C	10.4	100	90	14	92.5°C	12.4	5.8	18.2
6	H	10.4	100	90	20	50	20.1	7.1	27.2
13	C	3.9	60	120	34	92.5°C	23.3	6.5	29.9
9	H	3.9	60	120	33	103	23.4	7.6	30.9

* experiments with starting problems.

It is a pity that experiment no. 5 is not reliable because of the starting problems.

A difference of one percentage point is found for the experiments 13 and 9, respectively for a cold and a hot stove. This efficiency increase compared to the cold stove is mainly due to an extra heat gain of the second pan.

With a cold stove there are usually serious starting problems. To avoid these problems in the experiments, the chimney was electrically heated for 15 minutes with two 100 W electric heating tapes wrapped around it.

To be able to compare the experimental results the chimney was heated in every experiment, although it was not always necessary.

7.6.5 The effect of the damper-opening

Table 7.6. The efficiency at different damper openings.

Mass of water in the first and second pan : 5 kg
 Mass of the charges : 300 g
 Chimney height : 1 m
 Door type : heavy

Run no.	T_i	P (kW)	d.p. (%)	t_{b1}	t_{b2}	t_t	η_1	η_2	η_t
* 7	C	4.9	90	43	116	116	18.8	5.8	24.6
8	C	4.9	80	27	95	116	20.5	7.8	28.3
⊙13	C	3.9	60	34	92.5°C	120	23.4	6.5	29.9
10	C	3.9	50	37	93°C	120	20.0	6.8	26.8

* starting problems

⊙ chimney heating for 60 minutes.

For a decrease in the damper opening of 10 % for 4.9 kW the efficiency increases while for 3.9 kW the efficiency decreases considerably.

This might indicate that there is an optimum damper position for every power output which will probably provide for an optimum amount of excess air.

It is also imaginable that the effect on the efficiency in the one experiment at 4.9 kW is due to starting problems (experiment number 7). There were no gas analyses available to check on this.

7.6.6 The effect of the chimney height

Originally the chimney height was doubled to be able to reach higher power outputs. Later it appeared that by heating the chimney for 15 minutes the stove could be operated at higher power outputs even with a 1 m chimney. Furthermore the effect of a doubled chimney height was checked for 11.4, 5.8 and 2.5 kW.

From the results in table 7.7 the overall efficiency increases for all power outputs with doubling the chimney height.

This efficiency increase is the result of an efficiency increase of the second pan, because of an convective heat gain, due to higher velocities of the flue gases. With a taller chimney the amount of excess air increases, which provides a better combustion as long as the optimum is not exceeded.

Table 7.7. The effect of 1 and 2 m chimney.

Mass of water in first and second pan : 5 kg
 Mass of charges : 300 g
 Door type : heavy

Run no.	T _i	P (kW)	d.p. (%)	chimney height (m)	t _{b1} (min)	t _{b2} (min)	t _t (min)	η ₁ (%)	η ₂ (%)	η _t (%)
16	C	11.7	100	2	14	36	96	19.2	7.8	27.0
27	C	11.7	100	1	19	80	80	22.0	3.8	25.8
18	C	5.8	100	2	22	68	112	23.8	8.7	32.5
3	C	5.8	100	1	38	101	144	24.7	6.2	30.9
15	C	2.5	30	2	52	64.5°C	111	21.6	6.3	27.8
14	C	2.5	30	1	54	49.5°C	111	19.8	4.0	23.8

7.6.7 The effect of the door construction (see fig. 7.4)

With the heavy door (H) the inlet air temperatures are quite high. A more primitive door (L) was designed to bring the cold inlet air directly under the grate.

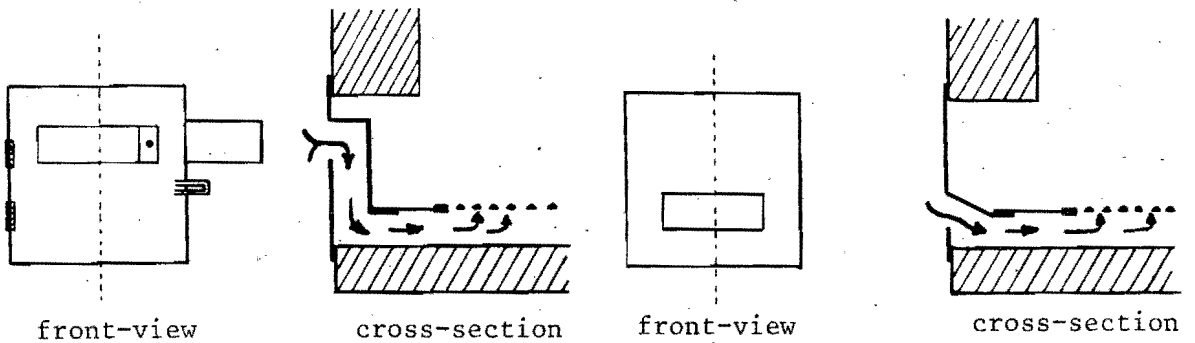


Fig. 7.4.a. Heavy door type (H)

Fig. 7.4.b. Light door type (L)

Because of pressure of time two experiments per day were conducted. Therefore the effect of a hot or cold stove on top of the effect of non preheating the inlet air was inevitable.

Table 7.8. The effects of preheating the combustion air.

Mass of water in the first and second pan : 5 kg
 Mass of the charges : 300 g
 Chimney height : 1 m

Run no.	T_i	P (kW)	d.p. (%)	Door type	t_{b1} (min)	t_{b2} (min)	t_t (min)	η_1 (%)	η_2 (%)	η_t (%)
17	H	11.7	100	L	16	46	80	20.3	6.2	26.5
22	C	11.7	100	H	19	80	80	22.0	3.8	25.8
19	H	5.8	100	L	43	112	112	25.4	7.3	32.7
3	C	5.8	100	H	38	101	144	24.7	6.2	30.9
21	H	2.5	30	L	47	61.5°C	111	21.5	7.2	28.7
14	C	2.5	30	H	52	64.5°C	111	19.8	4.0	23.8

The preheating of the inlet air was expected to have a positive effect on the efficiency. However, the experiments with the light door clearly show higher efficiencies. This can not be explained by the difference in initial temperature of the stove, as this an effect is only 1 % absolute efficiency (see chapter 7.6.4).

The effect of reducing the resistance completely overrules the effects of preheating the combustion air.

With a smaller resistance which is unwillingly also introduced with the primitive door, the airflow through the stove will increase. Accordingly, a larger excess air factor and higher flue gas velocities results. This explains the efficiency increase when the L-type door is used. (see fig. 7.4.b.)

7.6.8 Global heat balance of the stove

The heat balance of this stove is meant as an aid in defining where the major heat losses occur.

The temperature estimates are not very accurate; for the heat transfer coefficient and the emission coefficient the most likely values are given.

The heat loss from the pans

The heat loss from the pan can be calculated from the cooling of the water in one pan after the end of the experiment. The following equation is used:

$$\ln \left(\frac{T_1 - T_\alpha}{T_0 - T_\alpha} \right) = \frac{hA}{m_w C_p} * t,$$

in which:

T_1	: temperature after cooling	(K)
T_α	: ambient temperature	(K)
T_0	: temperature at the beginnging of the cooling process	(K)
h	: heat transfer coefficient	(W/m ² K)
	Assumed to be independent to temperature	
A	: area of the pan surface above the stove	(m ²)
m_w	: Mass of the water in the pan	(kg)
C_p	: heat capacity of the water	(kJ/kg K)

The cooling characteristic of run no. 7, 12, 14, 15 and 18 (thermo-couple number 9 or 10) are used in the calculation of h, the combined coefficient for convection and radiation heat transfer.

The total heat loss from the pans is estimated by use of the following formula with Q as the only unknown parameter:

$$Q = h * A * (T_w - T_{\alpha}) ,$$

in which

Q : heat loss (W)

T_w : temperature of the water (K)

T_α : ambient temperature (K)

The average heat loss is 75 W, for each pan, according to this estimation.

Heat storage in the stove

The stove can roughly be divided in parts of different materials and operational temperatures at a certain power output (table 7.9).

Table 7.9. The stove divided in parts of different operational temperatures and materials.

Part of the stove	Mass of Al. top-plate (kg)	Mass of Br. stove-body (kg)	Mass of steeldoor + grate (kg)	Number of the representative thermo couple	
				Al. topplate	Br. stovebody
I	3.9	90	6	17	the average of 5 and 6
II	2.4	110	-	18	the average of 7 and 8
III	3.1	80	-	18-(10°C)	19

Br = refractory bricks

Al = aluminium

I = front part of the stove near the first pan

II = middle part of the stove near the second pan

III = back part of the stove near the chimney

(see fig. 7.1)

The main operating temperatures are derived from the temperature records of the thermocouples. These are representative for the temperatures of part I, II and III of experiments at high medium and low power outputs.

For the frontpart (I) of the stove the temperature records are given in figure 7.5.

Temperature records similar to those in figure 7.5., for different parts of the stove were used to calculate the total heat absorbed to bring the cold as well as the hot stove to its operating temperature.

$$\text{formula: } \Delta H = m C_p (T_o - T_i) \quad |$$

in which

ΔH	: the amount of heat absorbed	(kJ)
m	: Mass of the material	(kg)
C_p	: specific heat at constant pressure for the varies materials	(kJ/kg K)
T_o	: operating temperature	(K)
T_i	: initial temperature	(K)

An initial temperature of 20°C is adopted for the calculations on a cold stove.

The specific heat for aluminium is 0.92 kJ/kg K, for brick (baked clay) 1.0 kJ/kg K for steel.

The heat loss from the walls, the top-plate and the chimney

The heat losses from the walls and top-plate are caused by radiation and convection.

The radiant heat losses are calculated by the following formula:

$$Q_{\text{rad}} = \epsilon \sigma . A . (T_1^4 - T_0^4) ,$$

in which

Q_{rad}	: radiative heat loss	(W)
σ	: Stefan - Boltzmann constant	$= 5.7 * 10^{-8}$ (W/m ² K ⁴)
A	: area size of the surface	(m ²)
T_1	: temperature of the surface	(K)
T_0	: ambient temperature	(K)
ϵ	: emission coefficient	

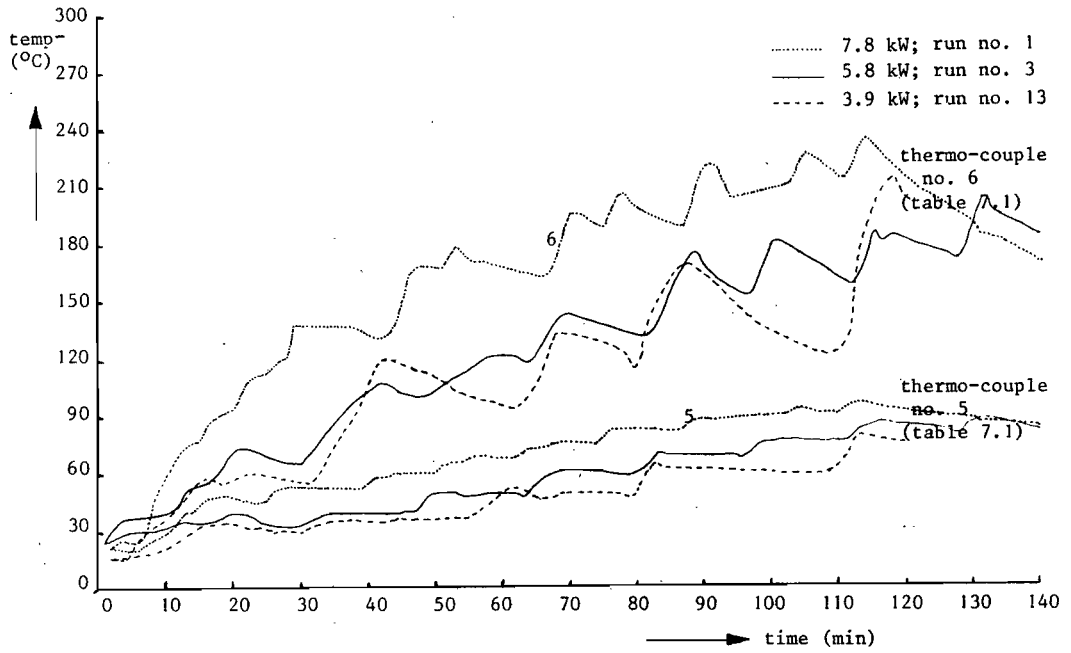


Fig. 7.5.a. Temperature records of representative thermo-couples of part I of the cold stove.

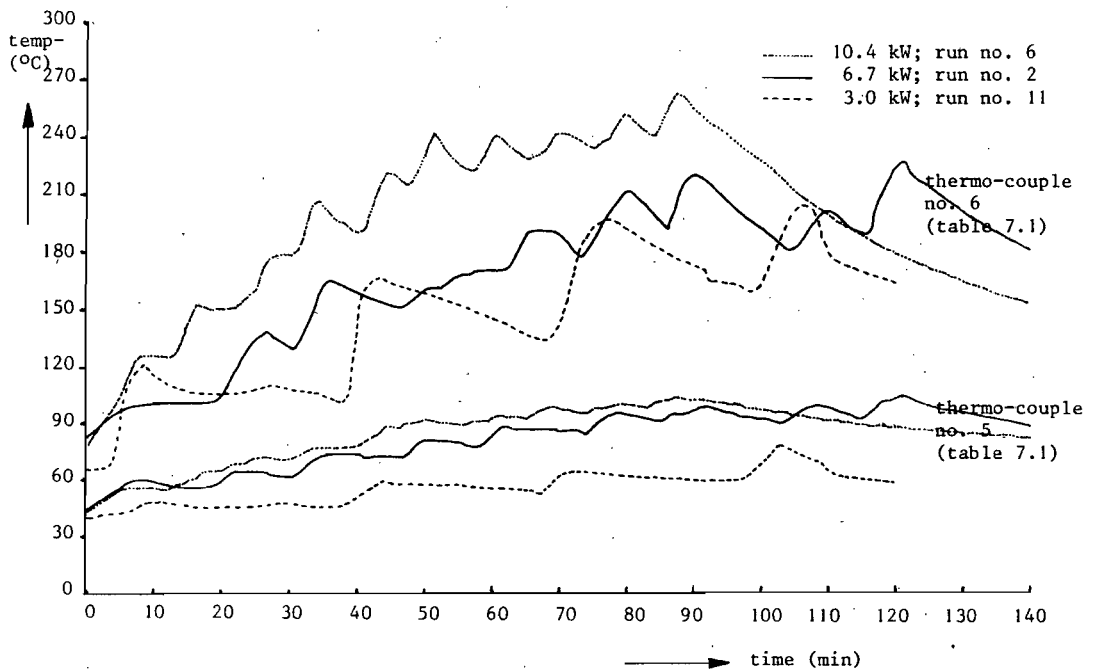


Fig. 7.5.b. Temperature records of representative thermo-couples of part I of the hot stove.

For ϵ the following values are used:

- ϵ_{st} : 0.75, refractory bricks
- ϵ_{Al} : 0.15, aluminium
- ϵ_{Wo} : 0.90, wood
- $\epsilon_{pan\ lid}$: 0.09, polished aluminium

Table 7.10. Cross sectional area of the three different parts of the stove.

	I			II			III		
	Br	Al	Wo*	Br	Al	Wo*	Br	Al	Wo*
(m)	0.469	0.1516	0.2132	0.210	0.944	0.156	0.336	0.1094	0.114

*Wo : Table area on which the stove is placed.

The convective heat losses are calculated from:

$$Q_{conv} = h \cdot A (T_1 - T_0),$$

in which

- Q_{conv} : convective heat loss (W)
- A : area size of the surface (m^2)
- T_1 : temperature of the surface (K)
- T_0 : ambient temperature (K)
- h : heat transfer coefficient (W/m^2K)

The heat transfer coefficient h for free convection is $4.5 W/m^2K$.

h is calculated from $Nu = 0.508 * \frac{Pr}{(0.952 + Pr)^{\frac{1}{4}}} * (Gr Pr)^{\frac{1}{4}}$, in which $Pr = 1$ and $Gr = 2.2 * 10^8$

The same operating temperatures as used for the calculation for the heat storage are used in this case as well.

The temperatures of the table under the stove are supposed to be roughly the same or a little lower than the temperatures of the stove-part that is considered.

The area size of the different stove parts are given in table 7.10.

The calculations indicated above, were carried out for a cold as well as a hot stove. They are tabulated in table 7.11.

The unaccounted for heat losses comprise of two parts, sensible heat carried away by the chimney gases and the CO-formation, due to incomplete combustion. These could not be estimated because the gas analysis apparatus was not available at the time of this work.

The heat storage in the stove seems to be the major heat loss component. The percentages may be a little high, but as was pointed out earlier a part of the stored heat (approximately 20 %) is regained.

The expected differences in efficiency of a hot and a cold stove, only taking into account the difference in the amount of heat needed to reach the operational temperature is for high power outputs 4 percentage points, for medium power outputs 10 percentage points and 20 percentage points for low power outputs.

Table 7.11. The global heat balance in percentages of the heat input.

		Cold stove			Hot stove		
heat output (kW)		7.8	5.8	3.9	10.4	6.7	3.0
heat gain of the pans	%	27	29	29	28	30	30
heat loss of the top plate							
conv.	%	1.4	1.4	2.5	1	1.4	2.3
rad	%	0.3	0.3	0.6	0.2	0.4	0.6
heat loss of the walls							
conv.	%	8.5	6.3	7.4	6.1	6.7	11.7
rad	%	7.7	7.7	8.4	9.8	11.6	13.4
heat loss of a 1 m chimney							
conv.	%	2.0	1.7	1.7	2.0	1.7	1.7
rad	%	0.4	0.3	0.2	0.4	0.3	0.2
heat storage	%	28	32	39	24	22	19
total heat output	%	75.5	78.7	88.8	71.5	74.1	78.9
unaccounted for heat losses	%	24.5	21.3	11.2	28.5	25.9	21.1

7.7. CONCLUSIONS AND RECOMMANDATIONS

The performance of this stove in present configuration is reasonably good, though there are serious starting problems with a cold stove.

The power output ranges from 11.7 kW to 2.5 kW.

The efficiency of the stove varies between 25 and 31 %.

At low power outputs the efficiency is 5 percentage points higher than the efficiency at high power outputs.

The efficiency of the stove increases by increasing the chimney height from 1 m to 2 m. The efficiency gain of the second pan is the result of a better convective heat transfer, because of higher flue gas velocities. A probably better combustion sees to the efficiency gain of the first pan.

The introduction of the "light" door appears to reduce the flow-resistance of the stove, and thus provide a better efficiency.

The starting problems of the stove can probably be diminished by reducing the heat capacity and the flow resistance of the stove. The flow resistance can, among others be reduced easily by lifting the chimney entrance, or adjusting the baffles.

The tests on this stove done so far are insufficient to get a complete picture of the performance and efficiency of a heavy stove. They need to be supplemented by tests combined with gas analyses to be able to check on combustion.

List of symbols

P	: power output	(kW)
t_t	: total theoretical calculated duration of the experiment	(min)
t_{b_1}	: time it takes before the first pan boils	(min)
t_{b_2}	: time it takes before the second pan boils.	(min)
	In case the water does not reach the boiling temperature, the maximum temperature that is reached during the experiment is given in $^{\circ}\text{C}$.	
t_{ba_1}	: time the water in the first pan keeps on boiling after the theoretical calculated end of the experiment.	(min)
η_{1H}	: The efficiency of the first pan in the heating-up period (the period before the water boils).	(%)
η_1	: average efficiency of the first pan	(%)
η_2	: average efficiency of the second pan	(%)
η_t	: average total efficiency	(%)
T_i	: initial temperature of the stove (H = hot or C = cold)	
d.p.	: damper position	(% opening)
Δt	: time in between two charges	(min)
m_{s_1}	: evaporated mass of water out of the first pan	(g)
m_{s_2}	: evaporated mass of water out of the second pan	(g)
Δm_f	: the amount of wood used per charge	(kg)
m_f	: the total amount of wood used in the experiment	(kg)
λ	: excess air factor	

APPENDIX 7.1. Summary of experimental results

Run no.	T _i stove (°C)	T _i pan (°C)	d _p (%)	chimney height (m)	door type	P (KW)	t _{ba1} (min)	t _{b1} (min)	t _{b2} (min)	tη _{1h} (%)	η ₁ (%)	η ₂ (%)	η _t (%)	ms ₁ (g)	ms ₂ (g)	Δt (min)	t _t (min)	m _f (kg)	m _{ft} (kg)
22	23	23.5	100	1	H	11.7	740	19	80	12.0	22.0	3.8	25.8	3740	210	8	80	0.3	3.0
16	20	20.5	100	2	H	11.7	-	14	36	17.0	19.2	7.8	27.0	5000	1580	8	96	0.3	3.6
17	50	19	100	1	L	11.7	-	16	46	14.9	20.3	6.2	26.5	4290	800	8	80	0.3	3.0
* 5	17	18	100	1	H	10.4	-	45	92.5°C	6.1	12.4	5.8	18.2	2340	710	9	90	0.3	3.0
6	80	20	100	1	H	10.4	50	20	50	13.4	20.1	7.1	27.2	4210	970	9	90	0.3	3.0
1	19	10	100	1	H	7.8	40	23	62	15.9	21.4	6.2	27.6	4540	740	12	120	0.3	3.0
2	55	-	100	1	H	6.7	30	23	80	18.9	22.0	7.3	29.3	4140	830	14	126	0.3	2.7
3	24	19	100	1	H	5.8	40	38	101	18.1	24.7	6.2	30.9	4750	590	16	144	0.3	2.7
18	16	17.5	100	2	H	5.8	-	22	68	21.9	23.8	8.7	32.5	3340	740	16	112	0.3	2.1
19	40	13	100	1	L	5.8	-	23	78	20.9	25.4	7.3	32.7	3580	450	16	112	0.3	2.1
* 7	16	15	90	1	H	4.9	10	43	116	13.7	18.8	5.8	24.6	2010	90	19	116	0.3	1.8
8	16	18	80	1	H	4.9	-	27	95	22.4	20.5	7.8	28.3	2270	370	19	116	0.3	1.8
** 23	20	18	70	1	H	3.9	-	31	103	23.1	25.0	6.6	31.6	2370	80	24	120	0.3	1.5
9	70	18	60	1	H	3.9	-	33	103	21.7	23.3	7.6	30.9	2130	190	24	120	0.3	1.5
13	17	18	60	1	H	3.9	0	34	92.5°C	22.2	23.4	6.5	29.9	2140	100	24	120	0.3	1.5
** 10	17	18	50	1	H	3.9	0	37	93°C	19.8	20.0	6.8	26.8	1750	80	24	120	0.3	1.5
** 11	60	16	40	1	H	3.0	0	40	88°C	24.4	22.3	8.4	30.7	1430	50	31	124	0.3	1.2
12	17	16	30	1	H	2.5	-	45	62°C	24.8	24.0	5.9	29.9	1000	10	37	111	0.3	0.9
14	18	18	30	1	H	2.5	7	54	49.5°C	26.1	19.8	4.0	23.8	700	10	37	111	0.3	0.9
15	20	19	30	2	H	2.5	-	52	64.6°C	21.5	21.6	6.3	27.9	840	40	37	111	0.3	0.9
21	40	17	30	1	L	2.5	-	47	61.5°C	23.8	21.5	7.2	28.7	820	20	37	111	0.3	0.9

* experiment with starting problems

H : heavy door type

** chimney heated for at least 50 minutes. The calculated efficiencies are corrected for the extra heat input.

L : light door type.

8. SOME IMPLICATIONS OF RESULTS

by

K. Krishna Prasad

Eindhoven University of Technology,

Eindhoven, The Netherlands.

As the title suggests, we will in this chapter try and look between the lines of numbers that adorn the previous chapters. To cite the motto of a famous text on numerical analysis, "The Purpose of Computing is Insight, Not Numbers" [Hamming, 1973]. We will extend this motto a little further. The purpose of doing an experiment or carrying out a computational exercise is primarily to provide insight into the phenomena one is dealing with, not merely to generate a set of numbers.

The theoretical and experimental work of Paul Bussmann provide a few interesting results. Consider first the influence of power output. Increasing the power output does not influence the maximum temperature in the system, but simply the flame height. What this means is that more air is required for completion of combustion and the entrainment process from the surroundings takes a longer distance to provide this air. The flame height is shown to vary according to

$$H \propto P^{\frac{2}{5}}$$

Experiments show that by and large that power output from a fuel bed is essentially controlled by its diameter. Thus

$$P \propto D^2.$$

In other words,

$$H \propto D^{4/5}$$

This is very nearly the relation suggested in the wood stove compendium [De Lepeleire et al, 1981]. This has far reaching implications on the performance of a given design of a three stone fire.

We can illustrate the situation by the following example. Consider a three stone fire with a diameter and height of D_1 and H_1 respec-

tively. Note that we locate the pan at the height H_1 . The configuration is capable of delivering a power output of P_1 . Now we wish to operate the system at a power output of P_2 , smaller than P_1 .

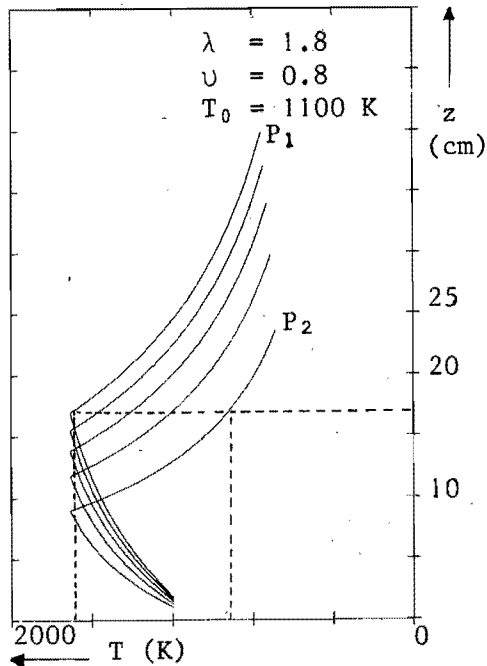


Fig. 8.1.

As illustrated in fig. 8.1 (which is the same as fig. 2.4.a) the gas temperature at the pan location drastically reduces from nearly 1400°C to 650°C . Thus the driving power for convective heat transfer (assuming a pan temperature of 100°C) reduces from 1300 to 550°C . In other words one could expect as much as a halving of convective heat transfer to the pan under these conditions. However since reduction in power output implies a reduction in fuel bed diameter which results in increased radiant heat transfer. Thus the loss in convective heat transfer is partially compensated. One could in general expect a reduction in efficiency of operation with decreased power output. In a subsequent report some calculations on heat transfer will be presented in support (or otherwise!) of these assertions.

Considering the crudeness of the model, a natural question to ask is: How good are these theoretical estimates in practice? Piet Visser's experiments (1980) suggesting the existence of an optimum height of the pan from the fuel bed partially supports this theory. However it is unlikely that the sharp peak predicted by the model will be observed in a real fire. In fact the measurements of Cox and Chitty (1980) suggest a flat temperature curve between $\frac{1}{2}$ to full flame height.

This means that the reduction in convective heat transfer will not be as drastic as the model predicts. Some empirical adjustments to the model is necessary to bring it into line with reality.

We next turn to the experiments of Piet Visser. These show the dramatic impact of shielding on an open fire. The reason for this can be seen by examining fig. 8.1. Due to dilution by entrained air, the temperature of burned gases drop by about 1000°C over a height of about 20 cm. This dilution is suppressed by shielding thus increasing the convective heat transfer to the sides of the pan which from nearly $\frac{3}{4}$ of the total pan area. It is gratifying to note that this simple design provides the highest efficiency (over 50 %) among nearly 400 experiments done by the group over very different types of stoves. Such a design permits the use of ceramic shields coupled with metal combustion chambers that facilitate air control. Moreover because of simplicity of design, it is conceivable that a family could afford to possess 2 or 3 stoves to cater to different power needs of diverse cooking requirements. Finally, it seems worthwhile making two other observations. Firstly, the possibilities of improved performance do not necessarily lie in complex designs incorporating chimneys, baffles and multiple pan configurations but organizing for a modest amount of air control, shielding and some ingenuity in dimensioning of the stove. Secondly, the immediate task of developing a stove that performs better one does not necessarily have to involve elaborate instrumentation. It can be adequately substituted by the twin virtues of systematic approach and patience.

Next we consider the work of Jan Delsing on cylindrical combustion chambers. Such combustion chambers can not operate with deep fuel beds. This was suspected during the tests on the Family Cooker [Siecken and Nieuwvelt, 1981]. Air holes in such systems need to be proportioned rather carefully to obtain anything like an acceptable performance. More interesting is the set of results obtained by varying the distance between the grate and the pan bottom.

If we restrict ourselves to the experiments 17 to 24 in table 4.2., the efficiency increases from 24.7 to 31.6 %. To get a feel about the reasons for these increases, certain radiant heat transfer calculations were performed (table 4.4). These show that the radiant heat transfer increased by nearly 75 % over the height range, but the convective heat transfer remained more or less same within $\pm 5\%$ of a mean value. The latter can be attributed to the flatness of gas temperature profile on top of the fuel bed mentioned earlier. With a little extra calculation, it can be shown that the side walls contribute to the total radiant heat transfer to the extent of 43 % at a distance of 27 cm and 25 % at a distance of 16 cm. However the absolute value of radiant heat transfer delivered from the side walls stays more or less constant around 115 W independent of the configuration.

The conclusion is that for chimneyless designs, the combustion chamber volumes need to be picked on the basis of maximizing radiant transfer. This is the jam that provides the extra bonus. Of course too shallow combustion chambers result in poor combustion as experiment 25 suggests.

Finally, a few comments are called for on the nature of the calculations presented in table 4.4. The radiant heat transfer is estimated on the assumption that a third of the heat content of the fuel is given out as radiation. This is derived from the proximate analysis of the fuel which gives 20 % by weight as the fixed carbon which is assumed to burn in the fuel bed. The heat liberated by this combustion is really distributed among four constituents: (i) sensible heat carried away by the combustion products; (ii) Unburned carbon monoxide in the products leaving the fuel bed; (iii) loss from the wall around the bed; and (iiii) radiant heat transfer from the bed. It is difficult to estimate these quantities with any degree of reliability; but, it is sufficient to state that the radiant power from the fuel bed is considerably smaller than the one assumed in table 4.4. It is probably closer to 1/5th than 1/3rd of the fuel heat content. This change does not however invalidate the qualitative picture presented earlier.

The experiments on fuel bed behaviour clearly show the influence of grates on the performance of stoves. Grates generally permit larger power densities (W/cm^2) than fires operated without them. More experiments are required to delineate their behaviour in greater detail.

We now turn to the experiments on the Nouna stove. Claus et al. provide a wealth of information on the stove. We shall satisfy ourselves here with just three observations. The first one concerns the difficulties one encounters in chimney designs. Higher chimney draft by way of either increasing the damper opening or increasing the chimney draft invariably decreases the efficiency. The first pan is the one that suffers most. This should be attributed to the twin effects of dilution by excess air (and hence lower maximum temperature) and the excessive draft causing the hot gases to be swept away from the first pan. In fact the original design did not provide the door, which was inserted by the TNO. When this door is removed, the efficiencies drop still further. The second observation concerns the enormous amount of heat accumulated in the stove body - this can be as large as 40 %. While a small proportion of this heat can be recovered, one is left wondering whether the user has the need for it and if so the discipline to recoup this heat. Finally, the second pan absorbs so little heat that the question of extra cost involved in providing for it needs to be carefully evaluated.

The experimental stove tested in its basic configuration by Marlies Knoll does perform better than the Nouna stove. A distinctive feature of the work is that it establishes a procedure to obtain a power output range of about 5 in wood burning systems. The increased draft by increasing the chimney height does increase the efficiency in this case. However with the configuration tested, there are severe starting problems and excessive tar deposition. It is too premature to make any general comments about the possible configuration changes that will result in higher performance from the heavy stoves.

REFERENCES

Hamming, R.W., (1962)

"Numerical Methods for Scientists and Engineers", Mc Graw-Hill, Tokyo.

Cox, G. and Chitty, R., (1980)

"A study of the deterministic properties of unbounded fire plumes", in "Combustion and Flame", 39, pp 191.

Visser, P., (1980)

"The three stones open fire", in "Some performance tests on open fires and the family cooker", Krishna Prasad, K., (ed), Eindhoven University of Technology, Eindhoven

Sielcken, M.O. and Nieuwvelt, C.J., (1981)

"Woodburning tests on the family cooker", in "A study on the performance of two metal stoves". Krishna Prasad, K., (ed), Eindhoven University of Technology, Eindhoven

De Leppeleire, G.J., Krishna Prasad, K.,

Verhaart, P., Visser, P. (1981)

"A woodstove compendium", Eindhoven University of Technology, Eindhoven